

Auditory streaming emerges from fast excitation and slow delayed inhibition*

Andrea Ferrario[†] and James Rankin[†]

Abstract. In the auditory streaming paradigm alternating identical sequences of pure tones can be perceived as a single galloping rhythm (integration) or as two sequences with separated low and high tones (segregation). Although studied for decades, the neural mechanisms underlining this perceptual grouping of sound remains a mystery. With the aim of identifying a plausible minimal neural circuit that captures this phenomenon, we investigate a firing rate model consisting of two periodically forced neural populations coupled by fast direct excitation and slow delayed inhibition. By analyzing the model in a non-smooth, slow-fast regime we analytically prove the existence of a rich repertoire of dynamical states and of their parameter dependent transitions. We impose plausible parameter restrictions and link all states with perceptual interpretations based on the detection of threshold crossings. Regions of stimulus parameters occupied by states linked with each percept matches those found in behavioral experiments. Our model suggests that slow inhibition masks the perception of subsequent tones during segregation (forward masking), while fast excitation enables integration for large pitch differences between the two tones.

Key words. Auditory streaming, slow delayed inhibition, fast excitation, periodic forcing

1. Introduction. Understanding how our perceptual system can encode multiple objects simultaneously is an important challenge in sensory neuroscience. In a busy room we can separate out a single voice of interest from other voices and ambient sounds (the so-called *cocktail party problem*) [10, 5]. Yet if someone calls our name from across the room it is immediately salient [43]. Whilst focusing on one sound source we simultaneously process background sound beyond our attentional focus.

Theories of feature discrimination developed with mathematical models are based on evidence that different neurons respond to different stimulus features (e.g. visual orientation [30, 4, 29, 7, 48]). In the auditory system there is a topographic representation of sound frequency (tonotopy) in primary auditory cortex (ACx): a gradient of locations preferentially responding to frequencies from low to high [53, 15]. However, the auditory system's ability to segregate objects that overlap or are interleaved in time (like melodies or voices) cannot be explained solely in terms of feature separation. Understanding the role of temporal neural mechanisms in perceptual segregation presents an interesting modeling challenge because the same neural populations represent different percepts through temporal encoding.

1.1. Auditory streaming and auditory cortex. In the auditory system sequences of sounds (streams) that are close in feature space and interleaved in time lead to multiple perceptual interpretations. The so-called auditory streaming paradigm [60, 5] consists of interleaved sequences of tones A and B, separated by a difference in tone frequency df and repeating in an ABABAB... pattern (Figure 1A). This can be perceived as one stream integrated into an alternating rhythm (Integrated in Figure 1B) or as two segregated streams (Segregated in

*

Funding: EPSRC Reference EP/R03124X/1

[†]Department of Mathematics, College of Engineering, Mathematics & Physical Sciences, University of Exeter, Exeter, UK (A.A.Ferrario@exeter.ac.uk).

Figure 2B). When the feature difference df is small we hear integrated and when df is large we hear segregated, but at an intermediate range, which also depends on presentation rate PR , both percepts are possible (Figure 1C). In this region of (df, PR) -parameter space bistability occurs and perception switches between integrated and segregated every 2–15 s [47]. The curve separating between integration and bistability percept is called the fission boundary, while the curve separating bistability and segregation is called coherence boundary [60] (Figure 1C).

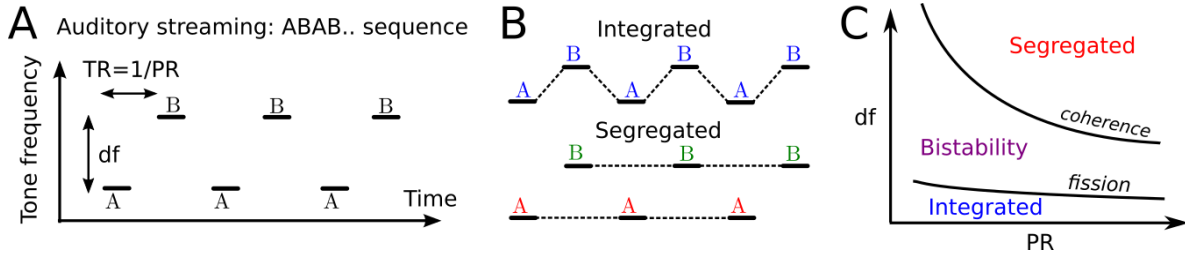


Figure 1. The auditory streaming paradigm (A) Auditory stimuli consist of interleaved higher pitch A and lower pitch B pure tones with duration TD , pitch difference df and time difference between tone onsets TR (the repetition time; $PR=1/TR$ is the repetition rate). (B) The stimulus may be perceived as either an integrated ABAB stream or as two separate streams A-A- and -B-B-. (C) Sketch of the perceptual regions when varying PR and df (Van Noorden diagram), redrawn after [60]. Bistability corresponds to the perception of temporal switches between integration and segregation. The curves in the (PR, df) space separating integration from bistability and bistability from segregation are called fission and coherence boundaries.

We assume that neural activity encoding different perceptual interpretations is represented at an earlier stage than the competition driving bistability. This study aims to explain the first process, which involves the simultaneous temporal encoding of the different perceptual choices. Figure 2A shows our proposal for the encoding of auditory streaming. We follow the hypothesis proposed by [44], where primary and secondary ACx encode respectively perception of the rhythm and the pitch. In our proposed framework the processing of auditory stimuli occurs firstly in primary ACx, which projects to secondary ACx. The various rhythms occurring in the auditory streaming paradigm arise via threshold-crossing detection in the activity of neural populations in secondary ACx. The process underlying bistability is likely resolved downstream of early auditory cortex [49] and will not be addressed in this study.

1.2. Existing models of auditory streaming. These have been inspired by evidence for feature separation shown in neural recordings in primary auditory cortex (A1) [27, 26]. Neurons responding primarily to the A or to the B tones are in adjacent locations spatially separated along A1's tonotopic axis. A continuous tonotopic feature space (a neural field) with a downstream perceptual classification process was presented in [1, 57, 58, 49]. The so-called neuromechanistic model [50] proposed the encoding of percepts based on discrete, tonotopically organised units interacting through plausible neural mechanisms. In general modellers have sidestepped the issue of the temporal encoding of the perceptual interpretations by focusing on a feature representation. However, the entrainment of intrinsic oscillations to inputs was considered in [63], albeit using a highly redundant spatio-temporal array of oscillators. Recently, a parsimonious neural oscillator framework was considered in [45] but without ad-

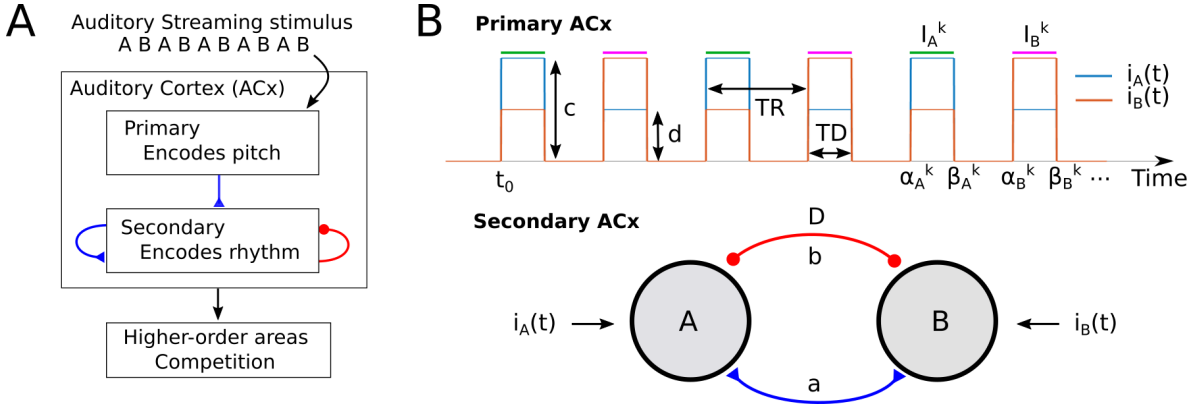


Figure 2. (A) Proposed modelling framework of the auditory streaming paradigm. Stimuli (see Figure 1A) are processed in primary ACx. Secondary ACs receives inputs from primary areas and has recurrent excitatory and inhibitory connections. Primary and secondary areas encode respectively pitch and rhythm perception [44], while high-order cortical areas may encode the focus of attention of and spontaneous switching between the percepts (bistability). (B) ACx circuit model considered here. Primary ACx responses at A and B tonotopic locations are modelled by square-wave inputs i_A and i_B respectively (top traces), which depend on the tone duration (TD) and on the time difference between successive tones' onsets (TR - repetition time, the presetation rate is $PR=1/TR$). Parameter c and d represent respectively the amplitude of i_A during each A(B) tone interval $I_A^k = [\alpha_A^k, \beta_A^k]$ ($I_B^k = [\alpha_B^k, \beta_B^k]$) and the amplitude of i_B during I_B^k (I_A^k). Bottom: sketch of the model circuit: two populations have mutually excitatory and delayed inhibitory connections with strengths a and b respectively, and local with primary tonotopic inputs i_A and i_B . Inhibition is delayed of the amount D .

dressing how the same perceptual interpretations are represented over a wide range of PR (5-20 Hz). Temporal forward masking results in weaker responses to similar-featured sounds that are close in time (like auditory streaming at high PR), but this ubiquitous feature of the auditory system [42] has generally been overlooked in previous models.

1.3. Theoretical framework. The cortical encoding of sensory information involves subpopulations of tens of thousands to millions of neurons that are suitably represented by a coarse-grained variables representing e.g. the mean firing rate of the population. The Wilson-Cowan equations [68] describes the firing rates of neural populations, and they are widely used in small networks with excitatory and inhibitory coupling, intrinsic synaptic dynamics including neural adaptation and a nonlinear gain function [38, 56, 13]. This framework (and related voltage or conductance based formulations) have been widely used to study decision making [65], working memory, perceptual competition in the visual [66, 67, 21, 61] and in the auditory system [50]. The wide range of temporal scales in neural interactions often leads to timescale separation. In slow-fast regimes these models can generate complex temporal patterns. Mathematical approaches to studying these models often make use of idealizations like a discontinuous (Heaviside) gain function due to its analytical tractability. For example, theoretical tools have been applied to study limit cycle solutions in gene regulatory networks of arbitrary dimension and with multiple thresholds for the Heaviside gain functions [24].

Timescale separation is a common feature of models at the single cell level [51, 31], and in populations of neurons [23]. Slow-fast analysis including singular perturbation theory has

been instrumental in revealing the dynamical mechanisms behind spiking and bursting [31, 19] and in explaining complex dynamics in population models of neural competition [13, 12]. Extensions of these methods have been applied to systems with delays [37] and in a non-smooth setting [59], including networks capable of intrinsically generating patterns of rhythmic behaviors (so-called central pattern generators, CPGs), such as locomotion, breathing, sleep [39]. Rubin and Terman [54] used slow-fast analysis to study different circuits with excitatory and inhibitory architectures similar to the one studied here. They found that fast mutual inhibitory neurons generate robust anti-phase oscillations, and that in-phase oscillation can be a stable pattern only if the connections are delayed.

The importance of delayed inhibition (modelled with ODE slow variables) for the generation of in-phase oscillations has been shown in spiking models of the tadpole CPG [25]. Delays in small neural circuits modelled using DDE equations — as will be used here — can lead to many interesting phenomena [2] including inhibition-induced Hopf oscillations, oscillator death, multistability and switching between oscillatory solutions [9, 20]. Two key features of our study are that (1) units are not intrinsically oscillating and (2) we consider periodic forcing to the units driving the oscillations. Periodically forced systems with timescale separation have been explored in models of perceptual competition [61, 32], but not in the presence of delays. Periodic solutions in autonomous delay differential equations with Heaviside and monotonic gain functions have been studied analytically in a recent work [36].

1.4. Neural population model. We present a mathematical model for the encoding of different perceptual interpretations of the auditory streaming paradigm. We consider a periodically-driven competition network of two localised Wilson-Cowan units (Figure 2A) with lumped excitation and inhibition generalised to include dynamics via inhibitory synaptic variables. The units A and B are driven by a stereotyped input signals i_A and i_B representative of neural responses in primary auditory cortex [27] at tonotopic locations that preferentially respond to A and to B tones (Figure 2B). The model is described by the following system of delay differential equations:

$$(1.1) \quad \begin{aligned} \tau \dot{u}_A(t) &= -u_A(t) + H(au_B(t) - bs_B(t - D) + ci_A(t - t_0)), \\ \tau \dot{u}_B(t) &= -u_B(t) + H(au_A(t) - bs_A(t - D) + ci_B(t - t_0)), \\ \dot{s}_A(t) &= H(u_A(t))(1 - s_A(t))/\tau - s_A(t)/\tau_i, \\ \dot{s}_B(t) &= H(u_B(t))(1 - s_B(t))/\tau - s_B(t)/\tau_i, \end{aligned}$$

where the units u_A and u_B represent the average firing rate of two neural populations encoding sequences of tone (sound) inputs with timescale τ . The Heaviside gain function with activity-threshold $\theta \in (0, 1)$: $\{H(x) = 1 \text{ if } x \geq \theta \text{ and } 0 \text{ otherwise}\}$ is frequently used in firing rate and neuronal field models [13, 11, 6] (we later relax this assumption to consider a smooth gain function in our analysis). Mutual coupling through direct fast excitation has strength $a \geq 0$. The delayed, slowly-decaying inhibition has timescale τ_i , strength $b \geq 0$ and delay D (Figure 2A). The synaptic variables s_A and s_B describe the time-evolution of the inhibitory dynamics. Typically we will assume τ_i to be a slow variable and τ to be fast. This slow-fast regime and the choice of a Heaviside gain function allows for the derivation of analytical conditions for the existence and stability of biologically relevant network states (asymptotically stable solutions).

1.5. Outline. We provide detailed analysis of periodic solutions locked to interleaved periodic inputs. We first assess the model’s symmetry, a feature that has important implications on periodic solutions [21, 22]. We then separate the full model (1.1) into slow and fast subsystems using singular perturbation theory and we use this to define a classification of states in the intervals during which tones are active (*active tone intervals*). We formulate binary matricial representations for different groups of states (*matricial form*). For moderate delays the matricial form enables us to (1) determine the rich repertoire of all 1:1 locked states, (2) derive their existence conditions and (3) rule out which states are impossible. We extend this analysis for short delays by assuming that inhibitory strengths are weaker than inputs.

A unique feature of this study is that we rigorously define the existence conditions of all 1:1 locked states in dependence on parameters with biophysical interpretations. For example, inputs include key parameters influencing perception, such as the tone durations, the rate of presentation and the tone pitch difference. We propose a framework linking biologically relevant percepts and classes of model states based on the number of threshold crossings. Remarkably each class occupies a qualitatively similar region of key parameters as its perceptual equivalent in behavioural experiments. Throughout Sections 4–7 we assume a Heaviside gain function and sufficiently small τ , posing the system in the slow-fast regime. In Section 8 we use numerical simulations to extend our results to a smooth gain function with reduced time-scale separation and show that equivalent dynamic states occur with similar regions of stability. Our analyses results in a number of useful predictions as outlined in the Discussion.

2. Model Inputs. Following our proposal for auditory streaming perception we model primary ACx inputs to secondary areas as time-dependent, periodic functions $i_A(t-t_0)$ and $i_B(t-t_0)$ time shifted by the input onset time $t_0 > 0$ (not to be confounded with a delay term) representing the averaged excitatory synaptic currents from primary auditory cortex at A and B tonotopic locations during the repetition of A and B tone streams as illustrated in Fig 2B(top). These functions are defined by:

$$(2.1) \quad \begin{aligned} i_A(t) &= c \sum_{k=0}^{\infty} \chi_{I_A^k}(t) + d \sum_{k=0}^{\infty} \chi_{I_B^k}(t) \\ i_B(t) &= d \sum_{k=0}^{\infty} \chi_{I_A^k}(t) + c \sum_{k=0}^{\infty} \chi_{I_B^k}(t) \end{aligned}$$

Where $c \geq 0$ and $d \geq 0$ represent the input strengths from A (B) tonotopic location respectively to the A (B) unit and to the B (A) unit; χ_I is the standard indicator function over the set I , defined as $\chi_I(t) = 1$ for $t \in I$ and 0 otherwise. The intervals I_A^k and I_B^k represent the intervals when A and B tones are respectively ON, and they are defined $\forall k \geq 1 \in \mathbb{N}$ by

$$I_A^k = [\alpha_k^A, \beta_k^A] = [2kTR, 2kTR+TD], \quad I_B^k = [\alpha_k^B, \beta_k^B] = [(2k+1)TR, (2k+1)TR+TD].$$

To simplify future notation we define $\gamma_k^A = \alpha_k^A + D$ and $\gamma_k^B = \alpha_k^B + D$, and the set of active tone intervals R and its union I :

$$\Phi = \{R \subset \mathbb{R} : R = I_k^A \text{ or } R = I_k^B, \forall k \in \mathbb{N}\} \quad \text{and} \quad I = \bigcup_{R \in \Phi} R.$$

Two important factors influencing auditory streaming [27, 26] are controlled by parameters TD , which represents the duration of tonotopic responses to each tone and PR representing

the repetition frequency of the onsets between successive A and B tones (where $PR=1/TR$ - the interpretation of PR is presented in the Discussion). We consider $PR \in [1, 40]\text{Hz}$, $TR \geq TD$ and $TR \geq D$. These restrictions are typical conditions tested in psychoacoustic experiments. In particular, $TR \geq TD$ guarantees no overlaps between tone inputs, i.e. $I_A^i \cap I_B^j = \emptyset, \forall i, j \in \mathbb{N}$.

We define functions $j_A(t)$ and $j_B(t)$, describing the time evolution of the inputs to the A and B units, respectively:

$$(2.2) \quad \begin{aligned} j_A(t) &= au_B(t) - bs_B(t - D) + i_A(t - t_0) \\ j_B(t) &= au_A(t) - bs_A(t - D) + i_B(t - t_0) \end{aligned}$$

System 1.1 can be decoupled into slow and fast subsystems. The fast subsystem is given by:

$$(2.3) \quad \begin{aligned} u_A(r)' &= -u_A(r) + H(j_A(r)) \\ u_B(r)' &= -u_B(r) + H(j_B(r)) \\ s_A(r)' &= H(u_A(r))(1 - s_A(r)) \\ s_B(r)' &= H(u_B(r))(1 - s_B(r)) \end{aligned}$$

Where $' = d/dr$ is the derivative with respect to the fast scale $r = t/\tau$. The activity of the A (B) unit is determined by the sign of j_A (j_B). Indeed u_A and u_B take a value of 0 or 1, or moves rapidly (on the fast time scale) between these two values. We call A(B) ON if $u_A \sim 1$ and OFF if $u_A \sim 0$. Positive sign changes in j_A (j_B) make u_A (u_B) jump up from 0 to 1, while negative sign changes in j_A (j_B) make u_A (u_B) jump down from 1 to 0. To simplify this notation we define the A (B) unit ON at time t if $j_A > 0$ ($j_B > 0$), and OFF if $j_A < 0$ ($j_B < 0$). Positive sign changes are called OFF to ON transitions (or the unit turning ON), while negative sign changes are called ON to OFF transitions (or the unit turning OFF).

The synaptic variables can act on either the fast or the slow time scales. If the A (B) unit is ON s_A (s_B) jumps to 1 on the fast time scale. Instead, if the A (B) unit is OFF the dynamics of the $s = s_A$ (or $s = s_B$) variable follows the exponential decay of the slow-subsystem:

$$(2.4) \quad \dot{s} = -s/\tau_i$$

Remark 2.1. The previous considerations demonstrate that $s_A(t)$ ($s_B(t)$) is a monotonically decreasing in time, except for when the A (B) unit makes an OFF to ON transition.

Remark 2.2 (\mathbb{Z}_2 symmetry). We now show that the model is symmetric under a transformation swapping the A and B indices in the system's variables and by applying the time shift TR to the active tone input functions. To do so, let us rewrite system 1.1 in the general form of a non-autonomous dynamical system

$$\dot{v}(t) = z(v(t), i_A(t), i_B(t)), \quad v = (u_A, u_B, s_A, s_B)$$

Now consider the map κ whose action swaps the A and B indices of all variables, defined as

$$\kappa : v = (u_A, u_B, s_A, s_B, i_A, i_B) \mapsto (u_B, u_A, s_B, s_A, i_B, i_A)$$

Since $i_A(t+TR) = i_B(t)$ and $i_B(t+TR) = i_A(t)$, $\forall t \in \mathbb{R}$, we have

$$\kappa(z(v(t), i_A(t), i_B(t))) = z(\kappa(v(t+TR), i_B(t+TR), i_A(t+TR)))$$

Which proves the model to be symmetric under transformation κ time shifted by TR . Given that no other symmetric transformation other than κ and the identity exist, the system is \mathbb{Z}_2 -equivariant. Thus, given a periodic solution $v(t)$ with period T , its κ -conjugate cycle $\kappa(v(t+TR))$ must also be a solution with equal period (asymmetric cycle), except in the case that $v(t) = \kappa(v(t))$, $\forall t \in [0, T]$ (symmetric cycle). Asymmetric cycles always exist in pairs: the cycle and its conjugate. We note that in-phase and anti-phase limit cycles with period $2TR$ are both symmetric cycles.

Remark 2.3 (Constraining model parameters). Assuming τ sufficiently small and a Heaviside gain function H , system 1.1 with no inputs ($i_A = i_B = 0$) has two possible equilibrium points: a quiescent state $P = (0, 0, 0, 0)$ and an active state $Q = (1, 1, 1, 1)$. If the difference between excitatory and inhibitory strengths $a - b \geq \theta$, then both P and Q exist, and any trajectory of the non-autonomous system is trivially determined by input strength c :

- If $c < \theta$: any trajectory starting from the basin of attraction of P (or Q) quickly converges to P (Q), assuming $\tau < t_0$, and remains at this equilibrium.
- If $c \geq \theta$: any trajectory converges to Q . Indeed, if an orbit is in the basin of P , the synaptic variables monotonically decrease until one (both) turn ON, converge to Q and remain at this equilibrium.

To avoid these unrealistic scenarios we assume the following conditions:

$$\begin{aligned} (U_1) \quad & a - b < \theta \\ (U_2) \quad & c \geq \theta \end{aligned}$$

Condition (U_1) guarantees that the point $P = (0, 0, 0, 0)$, representing a quiescent state, is the only equilibrium of system 1.1 with no inputs ($i_A = i_B = 0$). Condition (U_2) guarantees inputs to be “strong enough” to turn ON the A (B) unit at the onset time of the A (B) tone in the absence of inhibition ($b = 0$).

3. Fast dynamics. In this section we analyze the units’ dynamics for the fast subsystem 2.3, starting from times $t \in I$ (i.e. for times during one of the active tone intervals). WLOG from the definition of I we assume that $t \in I_k^A$. The analysis below can easily be extended for $t \in I_k^B$ by swapping the parameters c and d . On the fast time scale the A and B unit satisfy the subsystem:

$$(3.1) \quad \begin{aligned} u'_A &= -u_A + H(au_B - b\tilde{s}_B + c) \\ u'_B &= -u_B + H(au_A - b\tilde{s}_A + d) \end{aligned}$$

Where $\tilde{s}_A = s_A(t-D)$ and $\tilde{s}_B = s_B(t-D)$. System 3.1 has the following four equilibrium points:

1. $(0, 0) \leftrightarrow c < b\tilde{s}_B + \theta$ and $d < b\tilde{s}_A + \theta$
2. $(1, 0) \leftrightarrow c \geq b\tilde{s}_B + \theta$ and $a + d < b\tilde{s}_A + \theta$
3. $(0, 1) \leftrightarrow a + c < b\tilde{s}_B + \theta$ and $d \geq b\tilde{s}_A + \theta$
4. $(1, 1) \leftrightarrow a + c \geq b\tilde{s}_B + \theta$ and $a + d \geq b\tilde{s}_A + \theta$

The full system 1.1 may jump between these equilibria due to the slow decay of the synaptic variables or when $s_A(t-D)$ and $s_B(t-D)$ jumps up to 1.

3.1. Basins of attraction. From the above inequalities we note that points $(1, 0)$ and $(0, 1)$ cannot coexist with any other equilibrium and thus have trivial basins of attraction. However, $(0, 0)$ and $(1, 1)$ may coexist under the following conditions:

$$(3.2) \quad \begin{aligned} b\tilde{s}_B + \theta - a &\leq c < b\tilde{s}_B + \theta \\ b\tilde{s}_A + \theta - a &\leq d < b\tilde{s}_A + \theta \end{aligned}$$

Thus we must have $a > 0$, i.e. when the excitation is not absent in the model. To study the basin of attraction for these two equilibria, we consider the vector field of system 3.1. For convenience we introduce the following quantities:

$$\begin{aligned} s_1 &= (b\tilde{s}_A - c + \theta)/a \\ s_2 &= (b\tilde{s}_B - d + \theta)/a \end{aligned}$$

Conditions 3.2 hold if and only if $0 < s_k \leq 1$, for $k = 1, 2$. Thus we can rewrite system 3.1 as:

$$(3.3) \quad \begin{aligned} u'_A &= -u_A + H(a(u_B - s_2)) \\ u'_B &= -u_B + H(a(u_A - s_1)) \end{aligned}$$

Since H is the Heaviside function a can be removed. Figure 3 shows the example basins of attraction for parameter values for which $(0, 0)$ and $(1, 1)$ coexist (black circles). The u_A - and u_B -nullclines are shown in blue and red, respectively. We simulated model 3.3 starting from several initial conditions, covering the phase space. Simulated trajectories converge either to $(0, 0)$ (green) and $(1, 1)$ (purple) and show the subdivision in the basin of attraction.

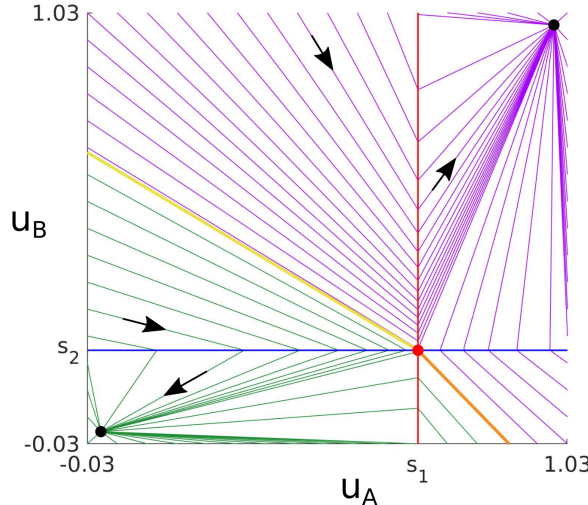


Figure 3. Phase portrait and basin of attraction for system 3.3 with $s_1 = 0.7$ and $s_2 = 0.4$. Purple and green lines show orbits converge to $(1, 1)$ and $(0, 0)$, respectively (black circles). Black arrows indicate example direction of the direction of convergence. The u_A - and u_B -nullclines are shown in blue and red, respectively. Yellow and orange lines show the separatrices of the degenerate saddle point (s_1, s_2) (red circle).

There is a degenerate fixed point (s_1, s_2) (red dot), where separatrices (yellow and orange lines) originate. These lines divide the phase plane into regions of attraction for two fixed

points and they are given by:

$$\begin{cases} (u_A - 1)s_2/(s_1 - 1) & \text{if } u_A \leq s_1 \\ u_A(s_2 - 1)/s_1 + 1 & \text{otherwise} \end{cases}$$

We prove that these curves define the separatrices by showing the convergence of orbits from initial conditions (u_A^0, u_B^0) in the top left corner in Figure 3 to $(1, 1)$ (purple trajectories in Figure 3). A similar proof holds for initial conditions in other regions of the phase-space and for convergence to $(0, 0)$. Points (u_A^0, u_B^0) in the top left corner belong to the set:

$$\Omega_L = \{(u_A, u_B) : u_A < s_1 \text{ and } u_B > (u_A - 1)s_2/(s_1 - 1)\}$$

Since $\Omega_L \subset [0, u_A] \times [u_B, 1]$, system 3.3 becomes:

$$\begin{aligned} u'_A &= 1 - u_A \\ u'_B &= -u_B \end{aligned}$$

Consider an orbit starting from $(u_A^0, u_B^0) \in \Omega_L$. Since $u'_A > 0$ the orbit will move towards the right until it reaches the vertical line $u_A = s_1$. The trajectory follows the same equations at all times t , since:

$$u_B(t) = u_B^0 \frac{u_A - 1}{u_A^0 - 1} > s_2 \frac{u_A - 1}{s_1 - 1} > s_2$$

Where the last inequality holds because $s_1 > u_A$. Thus, any trajectory ends on the top-right corner defined by:

$$\Omega_R = \{(u_A, u_B) : u_A \geq s_1 \text{ and } u_B \geq s_2\}$$

After the orbit reaches the curve $u_A = s_1$, $(u_A, u_B) \in \Omega_R$ it follows the system:

$$\begin{aligned} u'_A &= 1 - u_A \\ u'_B &= 1 - u_B \end{aligned}$$

Since $u'_A > 0$ and $u'_B > 0$ the trajectory continues to satisfy these equations and will converge to $(1, 1)$. Thus both units turn ON simultaneously.

Similar results hold for the Sigmoidal case (see Supplementary Material 11.1).

3.2. Differential convergence to $(1, 1)$. We study the differential rate of convergence of the variables u_A and u_B for parameter values where $(1, 1)$ is the only stable equilibrium, for an orbit starting from the initial point $(0, 0)$. We will use the results below to classify of states of system 1.1.

For simplicity we consider the case $t \in I_A^k$, as in system 3.1. Similar considerations hold in the case $t \in I_B^k$. Obviously, $(0, 0)$ cannot be an equilibrium point, thus at least one of the two conditions in (1) of 3 must not be met. The rate of convergence to $(1, 1)$ can be subdivided in three cases, depending on the system's parameters:

1. If $c - b\tilde{s}_B \geq \theta$ and $d - b\tilde{s}_A \geq \theta$ both units turn ON simultaneously. Indeed, the fast subsystem reduces to:

$$\begin{aligned} u'_A &= 1 - u_A \\ u'_B &= 1 - u_B \end{aligned}$$

Since both units follow the same dynamic equations. If the orbit starts from $(0, 0)$, both units have the same exponential rate of convergence to equilibrium $(1, 1)$.

2. If $c - b\tilde{s}_B \geq \theta$, $d - b\tilde{s}_B < \theta$ and $a + d - b\tilde{s}_A \geq \theta$ the A OFF to ON transition of the A unit precedes the OFF to ON transition of the B unit by some small delay δ ($\sim \tau$) determined below. We show that there is a differential rate convergence for the two units on the fast time scale. From $d - b\tilde{s}_B < \theta$ and $a + d - b\tilde{s}_A \geq \theta$ we have that $\exists u^* \in (0, 1]$ for which:

$$(3.4) \quad au_* + d - b\tilde{s}_A = \theta$$

From condition $c - b\tilde{s}_B \geq \theta$ the fast subsystem reduces to:

$$\begin{aligned} u'_A &= 1 - u_A \\ u'_B &= -u_B + H(au_A - b\tilde{s}_A + d) \stackrel{\text{def}}{=} -u_B + \eta(u_A) \end{aligned}$$

Thus, the dynamics of u_A is independent of u_B . Consider an orbit starting $(0, 0)$ at $r = 0$. From the first equation $u_A(r)$ tends to 1 exponentially as $r \rightarrow \infty$, reaching a point u^* defined in 3.4 at time $r^* = \log[(1 - u^*)^{-1}]$. For $r < r^*$ we have $u_A(r) < u^*$, which yields $\eta(u_A(r)) = 0$. Since the orbit starts from $u_B = 0$, it must remain constant and equal to zero $\forall r < r^*$. For $r \geq r^*$, $\eta(u_A(r)) = 1$ and $u_A(r) \rightarrow 1$ following the same dynamics as u_A at time $r = 0$. On the time scale $t = \tau r$ of system 1.1, the A unit precedes the B unit in converging to 1 precisely after an infinitesimal delay

$$(3.5) \quad \delta = \tau \log[(1 - u^*)^{-1}].$$

3. The case $d - b\tilde{s}_A \geq \theta$, $c - b\tilde{s}_A < \theta$ and $a + c - b\tilde{s}_B \geq \theta$ is analogous to the previous under the transformation replacing u_A with u_B . Thus the B OFF to ON transition precedes the A OFF to ON transition of the B unit with a delay δ .

3.3. fast dynamics for $t \in \mathbb{R} - I$. So far in this section we have analysed the possible dynamics in I . The analysis for $t \in \mathbb{R} - I$ follows analogously by posing $c = d = 0$ into system 3.1. In this case $(0, 0)$ is an equilibrium for any set of parameter values and delayed synaptic quantities \tilde{s}_A and \tilde{s}_B . Instead $(1, 1)$ is an equilibrium if and only if

$$a - b\tilde{s}_A \geq \theta \quad \text{and} \quad a - b\tilde{s}_B \geq \theta.$$

4. Dynamics in the intervals with no inputs ($\mathbb{R} - I$). In this Section we show the possible dynamics of the units during the time intervals when inputs are OFF and some implications applied to the synaptic variables' dynamics during the active tone intervals.

Theorem 4.1 (dynamics in $\mathbb{R} - I$). *For any $t \geq t_0 \in \mathbb{R} - I$:*

1. *If A or B is OFF at time t, both units are OFF in $(t, t^*]$, where t^* is:*

$$t^* = \min_{s \in I} \{s > t\}$$

2. *If A or B is ON at time t, both units are ON in $[t_*, t]$, where t_* is:*

$$t_* = \max_{s \in I} \{s < t\}$$

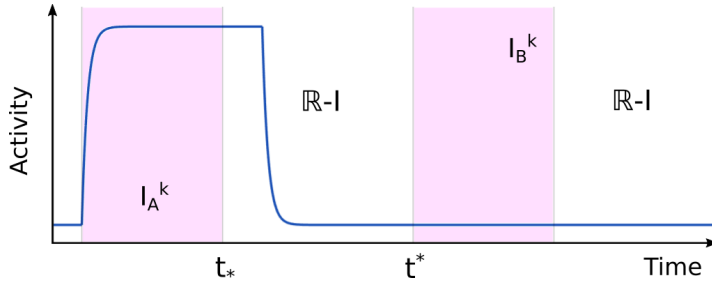


Figure 4. Illustration of Theorem 4.1 showing one unit's dynamics (blue) during one 2TR period. Active tone intervals I_A^k and I_B^k are shown in purple; $t^* = \min_{s \in I} \{s > t\}$ and $t_* = \max_{s \in I} \{s < t\}$.

Proof. We begin by proving 1. Due to Section 3.3 the fast subsystem 3.1 with no inputs ($c = d = 0$) has only two possible equilibrium points at any time in $[t_*, t^*]$: $P = (0, 0)$ and $Q = (1, 1)$. At time t_* , if Q is not an equilibrium or (u_A, u_B) is in the basin of attraction of P the system instantaneously converges to P (i.e. both units are/turn OFF). Since P is an equilibrium at any time in $\mathbb{R}-I$ the units remain OFF throughout $[t_*, t^*] \subset \mathbb{R}-I$, which proves the theorem. Next, assume that Q is also an equilibrium and that (u_A, u_B) instantaneously converges to Q at time t_* (i.e. both units are/turn ON at time t^*). By hypothesis of point 1. one unit is OFF at time t . By continuity there must be a turning OFF time in $\tilde{t} \in [t_*, t]$. This can occur only if Q is not an equilibrium at time \tilde{t} , due to the dynamics of the slow variables. Thus since P is an equilibrium at any time in $\mathbb{R}-I$ both units turn OFF at time \tilde{t} and remain OFF in $(t, t^*] \subset [\tilde{t}, t^*]$. This concludes the proof of 1.

We prove 2. by contradiction. Suppose there $\exists \tilde{t} \in [t_*, t]$ when one unit is OFF. From 1. we have both units OFF in $(\tilde{t}, t^*]$. This is absurd given that one unit is ON at time $t \in (\tilde{t}, t^*]$. ■

Remark 4.2. One important consequence of Theorem 4.1 is that no unit can turn ON at any time $t \in \mathbb{R}-I$. Indeed, if one unit is OFF at time t , point 1. implies that it is OFF in $(t, t^*]$. The only possibility is that the units turn OFF during this interval (see Figure 4).

Definition 4.3 (LONG and SHORT states). We define any state of system 1.1:

- *LONG* if $\exists t \geq t_0 \in \mathbb{R}-I$ such that both units are ON
- *SHORT* if $\forall t \geq t_0 \in \mathbb{R}-I$ both units are OFF

Remark 4.4. Due to Theorem 4.1 units can either be both ON, both OFF, or both making an ON to OFF transition in $\mathbb{R}-I$. Thus, definition 4.3 identifies all possible states in the system. The names LONG and SHORT have been chosen to classify such states based on their activity outside the active phases of A and B tones.

Theorem 4.1 implies the following two lemmas under the assumption $TD + D < TR$, which will be useful in the analysis of possible network states.

Lemma 4.5 (synaptic decay). If $TD + D < TR$ the delayed synaptic variables $s_A(t-D)$ and $s_B(t-D)$ are monotonically decreasing in L , $\forall L \in \Gamma$, where

$$\Gamma = \{L \subset \mathbb{R} : L = [\alpha_k^A, \gamma_k^A] \text{ or } L = [\alpha_k^B, \gamma_k^B], \exists k \in \mathbb{N}\}.$$

Proof. From Remark 2.1 the synaptic variable s_A (s_B) is monotonically decreasing except for when A (B) turns ON. Due to Theorem 4.1 such an event cannot occur at any time $t \in \mathbb{R}-I$.

Thus, it is sufficient to prove that $t-D \in \mathbb{R}-I$. Without loss of generality (WLOG) consider $L = [\alpha_k^A, \gamma_k^A] = [2kTR, 2kTR+D]$ and $t \in L$, which implies:

$$2kTR-D \leq t-D \leq 2kTR$$

The condition $TD+D < TR$ implies:

$$2kTR-D \geq (2(k-1)+1)TR+TD = \beta_{k-1}^B \implies \beta_{k-1}^B \leq t-D \leq \alpha_k^A \implies t-D \in \mathbb{R}-I$$

This completes the proof. ■

Lemma 4.6 (no saturated states). *If $TD+D < TR$ both units are OFF $\forall t \in J$, where:*

$$J = \bigcup_{k \in \mathbb{N}} (\alpha_k^A + TD + D, \alpha_k^B] \cup (\alpha_k^B + TD + D, \alpha_{k+1}^A]$$

Proof. We proof the theorem for the interval $J_k^A = (\alpha_k^A + TD + D, \alpha_k^B]$. The extension to the other intervals is analogous. By contradiction suppose $\exists \bar{t} \in J_k^A$ either unit, say A, is ON. Since $TD+D < TR$ we have that $\bar{t} \in \mathbb{R}-I$. We can thus apply Theorem 4.1, which implies both units being ON in $[t_*, \bar{t})$, where $t_* = \alpha_k^A + TD$. Thus, at time $p_* = t_* + D \in [t_*, \bar{t})$ the delayed synaptic variables jump up to 1 following the fast system 2.3. From this and condition (U_2) we have

$$a - bs_A(p_* - D) \sim a - b < \theta \quad \text{and} \quad a - bs_B(p_* - D) \sim a - b < \theta.$$

This leads (1,1) to be the only stable equilibrium at time p^* , which is absurd since A is ON at this time. ■

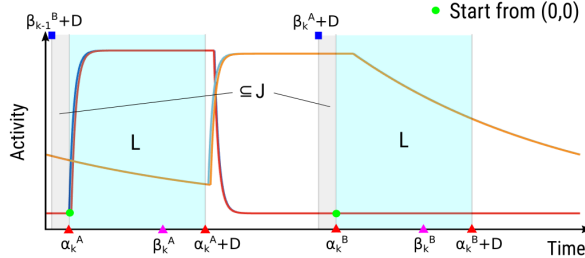


Figure 5. Illustration of the claim of the lemmas 4.5 and 4.6 showing the dynamics of the A and B units in each interval $L \subset \Gamma$ and J defined in these lemmas during one period $2TR$. The dynamics of the u_A (u_B) is shown in blue (red); the delayed synaptic variable $s_A(t-D)$ ($s_B(t-D)$) is shown in light blue (orange).

5. Dynamics during the active tone intervals. In this section we study the dynamics during the active tone intervals $R \in \Phi$ under the conditions $D > TD$ and $TD+D < TR$. We begin by presenting the following lemma that follows from Theorem 4.1.

Lemma 5.1 (single OFF to ON transition). *Consider an active tone interval $R = [\alpha, \beta] \in \Phi$, and let A (B) be ON at a time $\bar{t} \in R$, then*

- (1) A (B) is ON $\forall t \geq \bar{t}$, $t \in R$
- (2) $\exists! t_A^* (t_B^*) \in R$ when A (B) turns ON
- (3) $s_A(t-D)$ ($s_B(t-D)$) is decreasing for $t \in [\alpha, t_A^* + D]$ ($t \in [\alpha, t_B^* + D]$)

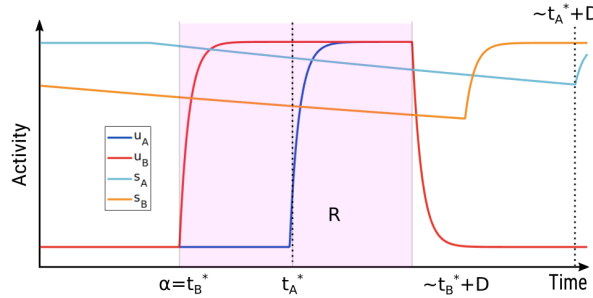


Figure 6. The dynamics of a solution in an interval R , illustrating the quantities in (1–3) of Lemma 5.1 for an active tone interval $R = [\alpha, \beta] \in \Phi$; t_A^* and t_B^* are the turning ON times for A and B , respectively.

The previous Lemma is proven in the Supplementary Material 11.2 and it implies the following Lemma.

Lemma 5.2. *Given any active tone interval $R \in \Phi$ we have:*

1. A (B) turns ON at time $\alpha \Leftrightarrow A$ (B) is ON $\forall t \in (\alpha, \beta]$
2. A (B) is OFF at time $\beta \Leftrightarrow A$ (B) is OFF $\forall t \in R$

Definition 5.3 (MAIN and CONNECT states). *Any state (solution) of system 1.1 is:*

- **MAIN** if $\forall R \in \Phi$, if $\exists t^* \in R$ turning ON time for A or B , then $t^* = \min(R) = \alpha$
- **CONNECT** if $\exists R \in \Phi$ and $\exists t^* \in R$, $t^* > \min(R)$ turning ON time for A or B

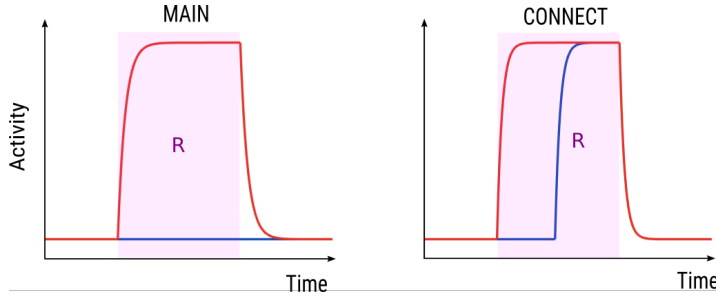


Figure 7. Example of u_A (red) and u_B (blue) for MAIN and CONNECT states in an active tone interval R .

Remark 5.4. Due to Lemma 5.1 each unit may turn ON only once during each interval $R \in \Phi$. Thus the dynamics of MAIN and CONNECT states is determined precisely at the jump up points for the units in R (if these exist). MAIN states are either ON or OFF during any interval $R \in \Phi$, except (possibly) for a negligible interval of length ~ 0 . Indeed due to differential convergence (Section 3.2) one unit may turn ON at α following an infinitesimally small delay $\delta \sim \tau$, where δ is given by equation 3.5. MAIN occupy a larger region of parameter space, compared to CONNECT states (see Remark 6.9).

Remark 5.5. Any state in the network can be classified as MAIN or CONNECT. Indeed, from Lemma 4.6 any state must be OFF in J . Moreover Lemma 5.1 guarantees that each unit may turn ON only once during each active tone interval $R \in \Phi$. Thus we have three possibilities: (1) both units are OFF in R , (2) only one unit turns ON once in R or (3) both

units turn ON in R . Condition (U_1) guarantees that (1) cannot occur $\forall R \in \Phi$, or $(0, 0, 0, 0)$ would be an equilibria.

5.1. Classification of MAIN and CONNECT states - Matricial form. In this section we propose a classification of MAIN and CONNECT states based on their dynamics during each active tone interval $R = [\alpha, \beta]$, $\forall R \in \Phi$. We show that our classification scheme counts 6 distinct MAIN and 5 CONNECT states, and define their existence conditions. For convenience let us define:

$$(5.1) \quad f(s) = \begin{cases} c - bs, & \text{if } R = I_A^k \\ d - bs, & \text{if } R = I_B^k \end{cases}, \quad g(s) = \begin{cases} d - bs, & \text{if } R = I_A^k \\ c - bs, & \text{if } R = I_B^k \end{cases}$$

From Lemma 5.2 the units' dynamics in R is completely determined on the fast time scale at times α and β . Indeed, at time $t = \alpha$ both units must be OFF due to Lemma 4.6 (i.e. any orbit (u_A, u_B) always starts from $(0, 0)$ at time α). Each unit can either turn ON at time α or be OFF at time β , depending on the system's parameters and on the following quantities:

$$\underline{s}_A = s_A(\alpha - D), \quad \bar{s}_A = s_A(\beta - D), \quad \underline{s}_B = s_B(\alpha - D), \quad \bar{s}_B = s_B(\beta - D)$$

From the fixed point analyses presented in the previous section we consider the following three classes of parameter conditions and corresponding MAIN states:

- **Both units turn ON at time α .** This is equivalent to $(1, 1)$ being the only equilibrium for the fast subsystem at time α . Section 3.2 leads to the following cases:

$$\begin{aligned} (M_1) \quad & f(\underline{s}_B) \geq \theta \text{ and } g(\underline{s}_A) \geq \theta \\ (M_2) \quad & g(\underline{s}_A) < \theta, \quad f(\underline{s}_B) \geq \theta \text{ and } a + g(\underline{s}_A) \geq \theta \\ (M_3) \quad & f(\underline{s}_B) < \theta, \quad g(\underline{s}_A) \geq \theta \text{ and } a + f(\underline{s}_B) \geq \theta \end{aligned}$$

In summary, under case M_1 both units instantaneously turn ON at the same time α . For case M_2 (M_3) the B (A) unit turns ON after the A (B) unit following an infinitesimal delay $\delta \sim \tau$. The latter case is the one considered in the analysis of the differential convergence to $(1, 1)$ for orbits starting from $(0, 0)$ (see Section 3.2).

- **One unit turns ON at time α and the other unit is OFF at time β** - this case occurs if and only if one of the following cases hold:

$$\begin{aligned} (M_4) \quad & f(\underline{s}_B) \geq \theta \text{ and } a + g(\bar{s}_A) < \theta \\ (M_5) \quad & g(\underline{s}_A) \geq \theta \text{ and } a + f(\bar{s}_B) < \theta \end{aligned}$$

For case M_4 (M_5) A(B) turns ON at α and B(A) is OFF at β . Indeed we have that $(1, 0)$ ($(0, 1)$) is the only stable equilibria of subsystem at times α and β , and thus $\forall t \in R$ due to Lemma 5.2.

- **A and B are OFF at time β** - which occurs if and only if $(0, 0)$ is the only stable equilibrium of the fast subsystem at time β :

$$(M_6) \quad g(\bar{s}_A) < \theta \text{ and } f(\bar{s}_B) < \theta$$

Overall, the above analysis proves that for a fixed interval $R \in \Phi$ any MAIN state of system 1.1 satisfies only one of the above conditions M_{1-6} , and that all MAIN states satisfying the same condition follow exactly the same dynamics in R . We can therefore define the dynamics of any MAIN state during any interval $R \in \Phi$ as follows.

Definition 5.6 (MAIN classification). We define the set of MAIN states in $R \in \Phi$ as

$$M_R = \{s = s(t) \text{ solutions of 1.1 satisfying one of conditions } M_{1-6} \text{ in } R\}$$

Figure 8 shows an example of a MAIN state satisfying condition M_4 in an interval $R \in \Phi$, where turns ON A turns ON at α and B is OFF $\forall t \in R$.

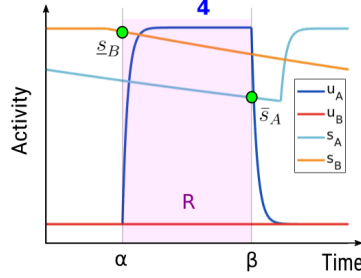


Figure 8. Example dynamics of a MAIN state satisfying condition M_4 in an active tone interval $R \in \Phi$.

The next Theorem shows that the existence conditions of each class of MAIN states in R can equivalently be expressed using a binary matrix $V \in B(2, 2)$, where $B(m, n)$ is the set of m by n binary matrices.

Theorem 5.7. *Let $R \in \Phi$ and M_R be the set of MAIN states in R . There is an injective map*

$$\rho^R: M_R \rightarrow B(2, 2)$$

$$s \mapsto V = \begin{bmatrix} x_A & y_A \\ x_B & y_B \end{bmatrix},$$

with entries defined by

$$x_A = H(f(\underline{s}_B)), \quad x_B = H(g(\underline{s}_A)), \quad y_A = \begin{cases} 1 & \text{if } ax_B + f(\underline{s}_B) \geq \theta \\ 0 & \text{if } ax_B + f(\underline{s}_B) < \theta \end{cases}, \quad y_B = \begin{cases} 1 & \text{if } ax_A + g(\underline{s}_A) \geq \theta \\ 0 & \text{if } ax_A + g(\underline{s}_A) < \theta \end{cases}$$

Moreover:

$$(5.2) \quad \text{Im}(\rho^R) = \Omega \doteq \{V = \rho^R(s) : x_A \leq y_A, x_B \leq y_B, x_A = x_B = 0 \Rightarrow y_A = y_B = 0\}$$

Proof. A necessary condition for ρ^R to be well defined is that y_A and y_B cannot be simultaneously equal to 0 and 1 (i.e. that both inequalities in their definition are not simultaneously satisfied). Due to the decay of the delayed synaptic variables in R (Lemma 5.1) we have $\underline{s}_B \geq \bar{s}_B$. Moreover, since f and g are monotonically increasing, we have

$$(5.3) \quad f(\underline{s}_B) \leq f(\bar{s}_B) \quad \text{and} \quad g(\underline{s}_B) \leq g(\bar{s}_B)$$

Which proves that y_A is exclusively equal to 0 or 1 (analogously for y_B).

Next, we notice that any matrix $V = \rho^R(s)$ satisfies the following:

$$(5.4) \quad x_A \leq y_A, \quad x_B \leq y_B, \quad x_A = x_B = 0 \Rightarrow y_A = y_B = 0$$

We prove the first inequality $x_A \leq y_A$ ($x_B \leq y_B$ is analogous). WLOG we assume $x_A = 1$, and therefore $f(\underline{s}_B) \geq \theta$. Since $a \geq 0$ and $x_B \geq 0$ we have $ax_B + f(\underline{s}_B) \geq f(\underline{s}_B) \geq \theta$, thus implying $y_A = 1$. The final part holds because, given $x_A = x_B = 0$, we have:

$$ax_B + f(\bar{s}_B) \leq f(\underline{s}_B) < \theta, \quad ax_A + g(\bar{s}_A) \leq g(\underline{s}_A) < \theta$$

From conditions 5.3 and 5.4 it is easily checked that each element $s \in M_R$ satisfying condition M_i has one of the following images $\rho^R(s)$:

$$(M_1) \begin{bmatrix} 1 & 1 \\ 1 & 1 \end{bmatrix} \quad (M_2) \begin{bmatrix} 1 & 1 \\ 0 & 1 \end{bmatrix} \quad (M_3) \begin{bmatrix} 0 & 1 \\ 1 & 1 \end{bmatrix} \quad (M_4) \begin{bmatrix} 1 & 1 \\ 0 & 0 \end{bmatrix} \quad (M_5) \begin{bmatrix} 0 & 0 \\ 1 & 1 \end{bmatrix} \quad (M_6) \begin{bmatrix} 0 & 0 \\ 0 & 0 \end{bmatrix}$$

Since any MAIN state has a distinct image, ρ^R is well defined, injective, and $|Im(\rho^R)| = 6$. Given that the total number of matrices $V \in B(2,2)$ satisfying conditions 5.4 are precisely 6 (no other matrix is possible), we must have $Im(\rho^R) = \Omega$ ■

Classification of CONNECT states. We use a similar analysis to define a classification and a matricial form for CONNECT states. For the classification we consider the following cases:

- **A(B) turns ON at time α and B(A) turns ON at time t^* , $\exists t^* \in (\alpha, \beta]$.** These two conditions are equivalent to $(1,0)$ ($(0,1)$) and $(1,1)$ being equilibria for the the fast subsystem at time α and β , respectively. We must note here that the validity of the previous statement is due to $(1,0)$ being in the basin of attraction of $(1,1)$ for any set of parameters (as shown in Figure 3). There are two conditions for which this occurs:

$$(C_1) \quad f(\underline{s}_B) \geq \theta, a + g(\underline{s}_A) < \theta \text{ and } a + g(\bar{s}_A) \geq \theta$$

$$(C_2) \quad g(\underline{s}_A) \geq \theta, a + f(\underline{s}_B) < \theta \text{ and } a + f(\bar{s}_B) \geq \theta$$

C_1 (C_2) describes the case where the B (A) units turn ON within the interval R and the A (B) unit is ON at time α .

- **A(B) is OFF at time β and B(A) turns ON at time t^* , $\exists t^* \in (\alpha, \beta]$.** These two events correspond to $(0,0)$ and $(0,1)$ ($(1,0)$) being equilibria for the the fast subsystem at time α and β , respectively. The following conditions lead to the following cases:

$$(C_3) \quad g(\underline{s}_A) < \theta, g(\bar{s}_A) \geq \theta \text{ and } a + f(\bar{s}_B) < \theta$$

$$(C_4) \quad f(\underline{s}_B) < \theta, f(\bar{s}_B) \geq \theta \text{ and } a + g(\bar{s}_A) < \theta$$

C_3 (C_4) describes the case where the A (B) units is OFF at time β and the B (A) turns ON within R .

- **$\exists t^*, s^* \in (\alpha, \beta]$ times when the A and B unit turns ON.** The conditions leading to this case are different depending on if A turns ON before or after B, that is:

1. A turns ON before B - if $t^* \leq s^*$, $f(\underline{s}_B) < \theta, f(\bar{s}_B) \geq \theta$ and $a + g(\bar{s}_B) \geq \theta$

2. B turns ON before A - if $t^* > s^*$, $g(\underline{s}_A) < \theta, g(\bar{s}_A) \geq \theta$ and $a + f(\bar{s}_A) \geq \theta$

In both cases, $(0,0)$ and $(1,1)$ are equilibria for the fast subsystem respectively for $t < \min\{t^*, s^*\}$ and $t \geq \max\{t^*, s^*\}$. In the first and second cases respectively $(1,0)$ and $(0,1)$ are equilibria for $t \in [t^*, s^*]$ ($t \in [s^*, t^*]$). For simplicity we decide not to distinguish between the cases 1. and 2. and define (C_5) as referring to either condition.

Definition 5.8 (CONNECT classification). We define the set of CONNECT states in $R \in \Phi$

$$C_R = \{s = s(t) \text{ solutions of 1.1 satisfying one of conditions } C_{1-5} \text{ in } R\}$$

Similar to MAIN states, the existence conditions for each CONNECT state in R can equivalently be expressed using a binary matrix $W \in B(2,3)$.

Theorem 5.9. Set $R \in \Phi$ and C_R be the set of CONNECT states in R . There is an injective map:

$$\varphi^R: C_R \rightarrow B(2,3)$$

$$s \mapsto W = \begin{bmatrix} x_A & y_A & z_A \\ x_B & y_B & z_B \end{bmatrix}$$

With entries defined by:

$$(5.5) \quad \begin{aligned} x_A &= H(f(\underline{s}_B)), & y_A &= H(ax_B + f(\underline{s}_B)), & z_A &= H(a + f(\bar{s}_B)) \\ x_B &= H(g(\underline{s}_A)), & y_B &= H(ax_A + g(\underline{s}_A)), & z_B &= H(a + g(\bar{s}_A)) \end{aligned}$$

And we have:

$$Im(\varphi^R) = \Gamma \doteq \{W : x_A \leq y_A \leq z_A, x_B \leq y_B \leq z_B, x_A = x_B = 0 \Rightarrow y_A = y_B = 0, y_A < z_A \text{ or } y_B < z_B\}$$

Proof. We first prove that the entries of any matrix $W = \varphi^R(s)$ satisfy the three conditions in Γ . It is easy to show that, since $a \geq 0$, $f(\underline{s}_A) \leq f(\bar{s}_A)$ and $f(\underline{s}_B) \leq f(\bar{s}_B)$, the entries of any matrix $W = \varphi^R(s)$ defined above satisfy

$$(5.6) \quad x_A \leq y_A \leq z_A \quad x_B \leq y_B \leq z_B.$$

Condition $x_A = x_B = 0 \Rightarrow y_A = y_B = 0$ simply follows from identities 5.5. One can see easily check that any CONNECT state defined by conditions C_i , $\forall i = 1, \dots, 5$ satisfies condition $y_A < z_A$ or $y_B < z_B$.

Using the conditions 5.6 one can easily see that each CONNECT state satisfying one of conditions C_{1-4} has a corresponding image $\varphi^R(s)$ shown below. The case C_5 is treated separately, since both A and B turn ON at times t^* and s^* , respectively.

- If $t^* \leq s^*$ it is clear that $f(s_B(t^*)) = \theta$ and $g(s_A(t^*)) < \theta$. Thus, since s_A and g are respectively decreasing and increasing functions in R , we must have $g(\underline{s}_A) = g(s_A(0)) < g(s_A(t^*)) < \theta$. In addition $a + f(\bar{s}_B) \geq f(\bar{s}_B) \geq \theta$ and $a + g(\bar{s}_B) \geq \theta$.
- If $t^* > s^*$ similar considerations lead to $f(\underline{s}_B) < \theta$. In addition $a + g(\bar{s}_A) \geq g(\bar{s}_A) \geq \theta$ and $a + f(\bar{s}_A) \geq \theta$.

In both cases we thus have $x_A = x_B = 0$ (which leads to $y_A = y_B = 0$) and $z_A = z_B = 1$.

$$(C_1) \begin{bmatrix} 1 & 1 & 1 \\ 0 & 0 & 1 \end{bmatrix} \quad (C_2) \begin{bmatrix} 0 & 0 & 1 \\ 1 & 1 & 1 \end{bmatrix} \quad (C_3) \begin{bmatrix} 0 & 0 & 0 \\ 0 & 0 & 1 \end{bmatrix} \quad (C_4) \begin{bmatrix} 0 & 0 & 1 \\ 0 & 0 & 0 \end{bmatrix} \quad (C_5) \begin{bmatrix} 0 & 0 & 1 \\ 0 & 0 & 1 \end{bmatrix}$$

Since any CONNECT state has a distinct image, φ^R is well defined and injective. It is trivial to prove that $Im(\varphi^R) \subseteq \Gamma$. However, since $|\Gamma| = 6$, we must have $Im(\varphi^R) = \Gamma$. ■

The previous two theorems naturally lead to the definition of the Matricial form of the MAIN and CONNECT states in each interval $R \in \Phi$.

Definition 5.10 (Matricial form). Let $R \in \Phi$ be an active tone interval:

- The matricial form of a MAIN state $s \in M_R$ in R is $V = \rho^R(s)$ defined by 5.2.
- The matricial form of a CONNECT state $s \in C_R$ in R is $W = \varphi^R(s)$ defined by 5.5.

Remark 5.11 (Visualisation via the Matricial form). Given a MAIN state s during an interval $R \in \Phi$ the first and second row vectors of the each matrix $V = \rho^R(s)$ provide an intuitive visualization of the the dynamics of the A and B units respectively. Indeed, given δ as defined in Section 3.2 we may subdivide R into:

$$R = [\alpha, \alpha+\delta] \cup [\alpha+\delta, \beta]$$

The dynamics of the A unit at time α is given by x_A . If $x_A = 1$ the A unit turns ON at this time and is ON $\forall t \in (\alpha, \beta]$. If $x_A = 0$ and $y_A = 1$ the A unit turns ON at time $\alpha + \delta$ and remains ON $\forall t \in (\alpha + \delta, \beta]$. If $y_A = 0$ (which implies $x_A = 0$) A is OFF $\forall t \in R$. Similar considerations hold for the B unit.

Similarly, for any CONNECT state s , the dynamics of the A and B units during an interval $R \in \Phi$ is represented respectively by the first and second row of its matricial representation $W = \varphi^R(s)$. We only show this for the CONNECT state defined by condition C_2 . Similar considerations hold for all the other conditions. Thus assume that the A unit turns ON at time $t^* \in (\alpha, \beta]$ and the B unit turns ON at time α . Given δ as defined in Section 3.2, we may subdivide R into:

$$R = [\alpha, \alpha+\delta] \cup [\alpha+\delta, t^*] \cup [t^*, \beta]$$

From conditions C_2 we have $y_A = 0$ (which implies $x_A = 0$) and $z_A = 1$, thus implying A being OFF during $[\alpha, \alpha+\delta]$ and $[\alpha+\delta, t^*]$, turning ON at time t^* and remaining ON in $[t^*, \beta]$. Since $x_B = 1$ (which implies $y_B = z_B = 1$), the B unit turns ON at time α and remains ON in $[\delta, \beta]$.

Remark 5.12 (Matricial form extension for MAIN states). The previous theorems have shown that each MAIN (CONNECT) state during an interval $R \in \Phi$ can be represented using a 2×2 (2×3) binary matrix. However, MAIN states can also be equivalently represented using the same 2×3 matricial form W defined for CONNECT states in the previous theorem, by replacing the definition of z_A and z_B with

$$z_A = H(ay_B + f(\bar{s}_B)) \quad \text{and} \quad z_B = H(ay_A + g(\bar{s}_A))$$

Indeed, one can check that each existence condition M_{1-6} given in 5.5 defines one of the following 2×3 matrices:

$$(M_1) \begin{bmatrix} 1 & 1 & 1 \\ 1 & 1 & 1 \end{bmatrix} (M_2) \begin{bmatrix} 1 & 1 & 1 \\ 0 & 1 & 1 \end{bmatrix} (M_3) \begin{bmatrix} 0 & 1 & 1 \\ 1 & 1 & 1 \end{bmatrix} (M_4) \begin{bmatrix} 1 & 1 & 1 \\ 0 & 0 & 0 \end{bmatrix} (M_5) \begin{bmatrix} 0 & 0 & 0 \\ 1 & 1 & 1 \end{bmatrix} (M_6) \begin{bmatrix} 0 & 0 & 0 \\ 0 & 0 & 0 \end{bmatrix}$$

Lemma 5.13 (LONG states). A state is LONG if and only if $\exists R = [\alpha, \beta] \in \Phi$ such that

1. A and B turn ON at times t_A^* and $t_B^* \in R$, respectively.
2. $a - bs_A(\beta - D) \geq \theta$ and $a - bs_B(\beta - D) \geq \theta$.

Moreover, both units are ON in $[\beta, t^* + D]$, turn OFF at time $t^* + D$, and are OFF in $(t^* + D, t_{up}]$, where

$$t^* = \min\{t_A^*, t_B^*\} \quad \text{and} \quad t_{up} = \min_{s \in I}\{s > t\}.$$

Proof. We begin by proving the first if and only if (\Leftrightarrow).

(\Rightarrow) Consider a LONG state. By definition one unit is ON at time t , for some $t \geq t_0 \in \mathbb{R} - I$. Thus $t \in T \cup S = (\beta_k^A, \alpha_k^B) \cup (\beta_k^B, \alpha_{k+1}^A)$, for some $k \in \mathbb{N}$ (where $T \cap S = \emptyset$). WLOG suppose

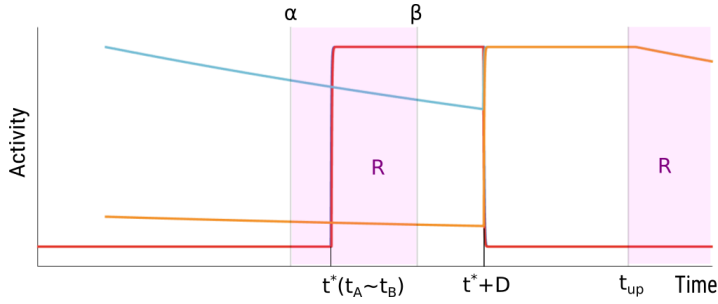


Figure 9. Example dynamics of a LONG state showing quantities used in Lemma 5.13.

$t \in T$. We will prove the claim for $R = [\alpha_k^A, \beta_k^A]$. Theorem 4.1 implies both units being ON in $[\beta, t]$, where $\beta = \beta_k^A$. The application of Lemma 5.1 at time $\bar{t} = \beta \in R$ implies the existence of (unique) OFF to ON transition times $t_A^*, t_B^* \in R$ for the A and B units, respectively, which proves point 1. Since both units are ON in $[\beta, t]$ for $t > \beta$, they are ON at time $\beta + h$, for $h > 0$ arbitrarily small. At this time the inputs are OFF ($\beta + h \in \mathbb{R} - I$) and the delayed synaptic variables act on the slow time scale (due to point 3. in Lemma 5.1). Therefore $(1, 1)$ must be an equilibrium point for (u_A, u_B) in the fast subsystem with no inputs at time $\beta + h$, and must satisfy the condition given in Section 3.3: $a - bs_A(\beta - D + h) \geq \theta$ and $a - bs_B(\beta - D + h) \geq \theta$. Taking the limit as $h \rightarrow 0$ concludes the first part of the proof.

(\Leftarrow) Point 1 of Lemma 5.1 guarantees both unit being ON at time $t = \beta$. Since $a - bs_B(\beta) \geq \theta$ and $a - bs_A(\beta) \geq \theta$ we have that $(1, 1)$ is a stable fixed point for the fast subsystem 3.1. Moreover, from point 3 of Lemma 5.1 $s_A(t - D)$ and $s_B(t - D)$ are monotonically decreasing for $t \in [\beta, t^* + D]$, where $t^* = \min\{t_A^*, t_B^*\}$. Thus, on the fast time scale, $a - bs_B(t - D) \geq \theta$ and $a - bs_A(t - D) \geq \theta$, which implies that $(1, 1)$ is a stable equilibrium for the system in $[\beta, t^* + D]$. Since $TD < D$, $t^* + D > \beta$. Therefore, there $\exists t \in [\beta, t^* + D] \in \mathbb{R} - I$ where both units are ON, ending this part of the proof.

Lastly we prove the remaining claims of the Lemma. We already proved that both units are ON in $[\beta, t^* + D]$ in (\Leftarrow) above. To prove the remaining claims we assume $t^* = t_A^*$ (a similar proof holds if $t^* = t_B^*$). At time $t = t^* + D$, $s_A(t - D)$ jumps up to 1. Since $a - bs_A(t - D) = a - b < \theta$ due to condition (U₂), $(0, 0)$ is the only equilibrium at time t . Therefore the B units instantaneously turns OFF at time t . For Theorem 4.1, also the A unit turns OFF instantaneously after a small delay $\delta \sim \tau$. Both units are OFF in $[t^* + D + \delta, t_{up}]$. By taking the limit $\tau \rightarrow 0$ we thus have that A and B are OFF in $(t^* + D, t_{up}]$ ■

6. 2TR-periodic states. In this section we study the conditions leading to the existence of 2TR-periodic MAIN and CONNECT states (of both the SHORT and LONG types; see Definition 4.3) under the conditions $D > TD$ and $TD + D < TR$. Under these assumptions, we analytically derive the parameter conditions leading to the existence of all 2TR-periodic states in the system. We will use results from the previous sections to define a matricial representation for such states and numerically confirm that the regions of existence for these states coincide with their region of stability.

Definition 6.1. A state $\psi = \psi(t) = (u_A(t), u_B(t), s_A(t), s_B(t))$ is 2TR-periodic if

$$\psi(t+2TR) = \psi(t), \quad \forall t \geq t_0, t \in \mathbb{R}.$$

We call *SM* and *LM* (*SC* and *LC*) the sets of 2TR-periodic MAIN (CONNECT) states of the *SHORT* and *LONG* type, respectively.

To study these states we can replace the set of active tone intervals I by the following:

$$I = I_1 \cup I_2 = [0, TD] \cup [TR, TR+TD]$$

As shown in the previous section, for any state $\psi \in SM$ the activities of both units during each interval I_i , with $i = 1, 2$, can be represented by a matrix V_i . This matrix uniquely depends on the values of the delayed synaptic variables at times $\alpha_i = (i-1)TR$ and $\beta_i = (i-1)TR+TD$. More precisely, in equations 5.2 we must substitute s_A with s_A^{i-} , \bar{s}_A with s_A^{i+} , s_B with s_B^{i-} and \bar{s}_B with s_B^{i+} in 5.2, where:

$$(6.1) \quad s_A^{i-} = s_A(\alpha_i - D), \quad s_B^{i-} = s_B(\alpha_i - D), \quad s_A^{i+} = s_A(\beta_i - D), \quad s_B^{i+} = s_B(\beta_i - D)$$

6.1. SHORT states. It turns out (see below) that for SHORT MAIN and CONNECT states these values depend on the following quantities:

$$(6.2) \quad N^- = e^{-(TR-TD-D)/\tau_i}, \quad N^+ = e^{-(TR-D)/\tau_i}, \quad M^- = e^{-(2TR-TD-D)/\tau_i}, \quad M^+ = e^{-(2TR-D)/\tau_i}$$

We note that $N^- \geq N^+ \geq M^- \geq M^+$.

Theorem 6.2. There is an injective map:

$$\begin{aligned} \rho: SM &\rightarrow B(2, 4) \\ \psi &\mapsto V = [V_A \mid V_B] = \left[\begin{array}{cc|cc} x_A^1 & y_A^1 & x_A^2 & y_A^2 \\ x_B^1 & y_B^1 & x_B^2 & y_B^2 \end{array} \right] \end{aligned}$$

Where, for $i=1, 2$, V_i are the matricial forms of ψ during the interval I_i defined in 5.2, and:

$$(6.3) \quad s_B^{i\pm} = N^\pm y_B^j + M^\pm (1 - y_B^j) y_B^i, \quad \text{and} \quad s_A^{i\pm} = N^\pm y_A^j + M^\pm (1 - y_A^j) y_A^i, \quad \forall i, j = 1, 2, i \neq j$$

In addition,

$$Im(\rho) = \Omega \stackrel{\text{def}}{=} \{V = [V_1 \mid V_2] : V_1 \in Im(\rho^{I_1}), V_2 \in Im(\rho^{I_2}) \text{ satisfying 1-4 below}\}$$

1. $y_A^1 = y_B^2 = 1 \Rightarrow x_A^1 = x_B^2 \text{ and } y_A^2 = y_B^1 = 1 \Rightarrow x_A^2 = x_B^1$
2. $y_B^1 = y_B^2 \Rightarrow x_A^1 \geq x_A^2 \text{ and } y_A^1 = y_A^2 \Rightarrow x_B^2 \geq x_B^1$
3. $y_A^2 = 1 \Rightarrow x_B^1 \leq r \text{ and } y_B^1 = 1 \Rightarrow x_A^2 \leq r, \text{ for any entry } r \text{ in } V$
4. $y_A^2 = y_B^2, y_A^1 = y_B^1 \Rightarrow x_A^1 \geq x_B^1 \text{ and } x_B^2 \geq x_A^2$

Proof. From Theorem 5.7 it is clear that the map $\rho = \rho(\psi)$ is well defined and injective.

We now prove 6.3 for $i=2, j=1$ and s_B , since all other cases are similar. That is:

$$s_B^{2\pm} = N^\pm y_B^1 + M^\pm (1 - y_B^1) y_B^2$$

Since y_B^1 and y_B^2 are binary, we have three cases to consider:

- Case $y_B^1 = 1$. From Remark 5.11, $y_B^1 = 1$ implies the B unit to be ON at time TD . Since ϕ is SHORT the B unit turns OFF at time TD , and due to Remark 4.1 it remains OFF $\forall t \in (TD, TR]$. Thus the delayed synaptic variable $s_B(t-D)$ is equal ~ 1 at time $TD+D$ and decays (slowly) in the interval I_2 , evolving according to:

$$s_B(t-D) = e^{-(t-TD-D)/\tau_i}, \quad \forall t \in I_2$$

Thus evaluating this function at times $TR \in I_2$ and $TR+TD \in I_2$ yields:

$$s_B^{2-} = s_B(TR-D) = N^- \quad \text{and} \quad s_B^{2+} = s_B(TR+TD-D) = N^+.$$

- Case $y_B^1 = 0$ and $y_B^2 = 1$. With a proof similar to the case above, the second condition ($y_B^2 = 1$) implies the B unit being ON at time $TR+TD$, and being OFF $\forall t \in (TR+TD, 2TR]$. The first condition ($y_B^1 = 0$) implies B being OFF at time TD , and therefore $\forall t \in [0, TD]$, due to Lemma 5.2. Thus, since ψ is $2TR$ -periodic, B must be OFF in $[2TR, 2TR+TD]$. Moreover, since ϕ is SHORT, B is OFF in $(TD, TR] \cup (TR+TD, 2TR) \subset \mathbb{R} - I$. In particular, since ψ is $2TR$ -periodic, B must be OFF also in $(2TR+TD, 3TR) \subset \mathbb{R} - I$. Overall we have that B is ON at time $TR+TD$ and OFF during $(TR+TD, 3TR]$. Thus the delayed synaptic variable $s_B(t-D)$ is equal ~ 1 at time $TD+D$ and decays (slowly) in the interval $T = (TR+TD+D, 3TR+D]$, evolving according to:

$$s_B(t-D) = e^{-(t-TR-TD-D)/\tau_i}, \quad \forall t \in T$$

Since $TD+D < TR$ and $TD < D$ we have $3TR \in T$ and $3TR+TD \in T$. Evaluating $s_B(t-D)$ at these times leads to $s_B(3TR-D) = M^-$ and $s_B(3TR+TD-D) = M^+$. Therefore the $2TR$ periodicity of ψ implies:

$$s_B^{2-} = s_B(TR-D) = M^- \quad \text{and} \quad s_B^{2+} = s_B(TR+TD-D) = M^+.$$

- Case $y_B^1 = 0$ and $y_B^2 = 0$. These conditions imply B being OFF during both $[0, TD]$ and $[TR, TR+TD]$. Moreover it must be OFF also in $[TD, TR] \cup [TR+TD, 2TR] \subset \mathbb{R} - I$ since ϕ is SHORT. Overall, the B unit is thus OFF $\forall t \in [0, 3TR]$. This means that the delayed synaptic variables (s_A, s_B) follow the slow subsystem, which have only one possible periodic solution: the fixed point $(0, 0)$. This leads to $s_B = 0$.

The proof that the entries of $V = \rho(\psi)$ satisfy conditions 1-4 is given in the Supplementary Material 11.3. In particular, the validity of these claims implies $Im(\rho) \subseteq \Omega$. In the next paragraph we will prove that $Im(\rho) = \Omega$. Assume for now that this is true. For each matrix $V \in \Omega$, the definition of the entries in V_1 and V_2 (equations 5.4) give multiple necessary and sufficient conditions for determining the dynamics of the corresponding MAIN state $\psi = \rho^{-1}(V)$ in the intervals I_1 and I_2 , respectively. Due to the model's symmetry (see Remark 2.2), V is the image of either a symmetrical or an asymmetrical state ψ . In the latter case, there exists a matrix $V' \in \Omega$ for a state conjugate to ψ . One can easily show that V' is simply defined given V by swapping the first row of V_1 with the second row of V_2 and the second row of V_1 with the first row of V_2 . Notably, both ψ and ψ' , and thus also V and V' , exist

under the same parameter conditions. The top rows of Table 1 shows all matrices $V \in \Omega$ that are an image of either of a symmetrical state or one of two conjugate states and their corresponding names (1st row). Given that I , AP and ID are the only symmetrical cycles (in-phase and anti-phase), from Remark 2.2 all other states have another existing conjugate cycles that exists under the same conditions.

| - | S | SB | SD | AP | AS | ASD | I | ID | IB |
|------------|--|--|---|---|--|--|---------------------------------------|--|---------------------|
| Matrix | 1100 0000 | 1100 1100 | 1100 0100 | 1100 0011 | 1111 0011 | 1101 0011 | 1111 0000 | 1101 0111 | 1111 1111 |
| Conditions | $C_1 < \theta$ $C_2^+ < \theta$ $C_3^+ < \theta$ | $C_3^+ < \theta$ $C_2^- \geq \theta$ $C_8^- \geq \theta$ | $C_4^- \geq \theta$ $C_2^+ < \theta$ $C_3^+ < \theta$ $C_8^- < \theta$ | $C_2^- \geq \theta$ $C_3^- \geq \theta$ $C_5^+ < \theta$ $C_8^- \geq \theta$ | $C_3^- \geq \theta$ $C_5^+ < \theta$ $C_8^- \geq \theta$ | $C_2^- \geq \theta$ $C_3^- \geq \theta$ $C_5^+ < \theta$ $C_8^- < \theta$ | $C_1 \geq \theta$ $C_6^+ < \theta$ | $C_3^- \geq \theta$ $C_5^- \geq \theta$ $C_7^- < \theta$ | $C_7^- \geq \theta$ |
| Short | — | $C_9 < \theta$ | $C_9 < \theta$ | — | $C_{10} < \theta$ | $C_{10} < \theta$ | — | $C_{10} < \theta$ | $C_{10} < \theta$ |

Table 1
Matricial form and existence conditions of all 2TR-periodic SHORT MAIN states

In the next part we define the conditions for existence of each of the states reported in the third row of Table 1, which are equivalent to the well-definedness conditions of the corresponding matricial form $V \in \Omega$. These conditions depend on the following quantities:

$$(6.4) \quad \begin{aligned} C_1 &= d, & C_2^\pm &= a - bM^\pm + d, & C_3^\pm &= c - bN^\pm, & C_4^\pm &= c - bM^\pm, & C_5^\pm &= a - bN^\pm + d, \\ C_6^\pm &= a - bN^\pm + c, & C_7^\pm &= d - bN^\pm, & C_8^\pm &= d - bM^\pm, & C_9 &= a - bM^+, & C_{10} &= a - bN^+ \end{aligned}$$

One can easily determine conditions for the well-definedness of each matrix $V \in \Omega$ from the definitions of the entries of V_1 and V_2 given in 5.4 and using formulas 6.3. Notably, the latter formulas guarantee that all existence conditions uniquely depend on the system's parameters. When determining these conditions one notices that many of them are redundant, and can be simplified using the following properties: $N^- \geq N^+ \geq M^- \geq M^+$, $d \leq c$ and $a \geq 0$. In the next paragraph, we show one example (AS) and leave the remaining for the reader to prove. All sets of inequalities defining each state is reported in the middle row of Table 1. We note that the set of inequalities defining each state is well-posed, meaning that there is a region of parameter where these inequalities are all satisfied. This effectively proves that for each matrix $V \in \Omega$ there exists a state $\psi = \rho^{-1}(V) \in SM$ whose dynamics during intervals I_1 and I_2 are defined by the entries of V .

We proceed by proving that the conditions of AS in Table 1 are well-defined, that is:

$$(6.5) \quad V_{AS} = \left[\begin{array}{cc|cc} x_A^1 & y_A^1 & x_A^2 & y_A^2 \\ x_B^1 & y_B^1 & x_B^2 & y_B^2 \end{array} \right] = \left[\begin{array}{cc|cc} 1 & 1 & 1 & 1 \\ 0 & 0 & 1 & 1 \end{array} \right] \quad \Leftrightarrow \quad C_3^- \geq \theta, \quad C_5^+ < \theta, \quad C_8^- \geq \theta.$$

From condition (1) in 6.2 we have that

$$x_A^1 = 1 \Rightarrow y_A^1 = 1, \quad x_A^2 = 1 \Rightarrow y_A^2 = 1, \quad x_B^2 = 1 \Rightarrow y_B^2 = 1, \quad y_B^1 = 0 \Rightarrow x_B^1 = 0,$$

This obviously leads to the follow equivalence

$$V_{AS} = \left[\begin{array}{cc|cc} 1 & 1 & 1 & 1 \\ 0 & 0 & 1 & 1 \end{array} \right] \Leftrightarrow x_A^1 = 1, \quad x_B^2 = 1, \quad x_A^2 = 1, \quad y_B^1 = 0.$$

Using the definition of the entries defined in 5.4 and the identities for the synaptic quantities given in equations 6.3 we observe the following:

1. $y_A^1 = 1$ ($y_B^2 = 1$) $\Rightarrow s_A^{2-} = N^-$ ($s_B^{1-} = N^-$), which implies $x_B^2 = x_A^1 = H(c - bN^-)$
2. $y_B^1 = 0$ and $y_B^2 = 1 \Rightarrow s_B^{2-} = M^-$. From this $x_A^2 = H(d - bM^-)$
3. $y_A^2 = 1 \Rightarrow s_A^{1+} = N^+$. This and $y_B^1 = 0$ give $y_B^1 = H(a + d - bN^+)$

Overall, from the cases (1-3) above we obtain

$$x_A^1 = 1, x_B^2 = 1 \Leftrightarrow C_3^- \geq \theta, \quad x_A^2 = 1 \Leftrightarrow C_8^- \geq \theta, \quad y_B^1 = 0 \Leftrightarrow C_5^+ < \theta.$$

This completes the proof for both the claim 6.5 and the Theorem. ■

Remark 6.3 (Conditions C_9 and C_{10}). The middle row of Table 1 shows conditions for determining the dynamics of each state $\psi \in M_1^S$ in the intervals I_1 and I_2 . However, they do not guarantee these states being OFF in $[0, 2TR] - I$ (ie being SHORT). From Lemma 5.13 there are two cases to consider:

1. If both units turn ON during interval I_1 or I_2 one must guarantee that the second condition of Lemma 5.13 is not true for that interval. For each interval $I = [\alpha, \beta] = I_1$ or I_2 during which this occurs, one must impose

$$(6.6) \quad \min\{a - bs_A(\beta - D), a - bs_B(\beta - D)\} < \theta$$

- For states SB and SD in 1 both units turn ON during interval I_1 (I_2 for their conjugate state). Equations 6.3 lead to $s_A(TD - D) = s_B(TD - D) = M^+$. Thus condition $C_9 < 0$ guarantees that inequalities 6.6 are satisfied.
- For states AS and ASD in Table 1 units are both ON during I_2 (I_1 for their conjugate counterpart). To guarantee 6.6 at time $\beta = TR + TD$ one notices that equations 6.3 give $s_A(TR + TD - D) = N^+$ and $s_B(TR + TD - D) = M^+$. Thus, condition $C_{10} < 0$ guarantees that inequalities 6.6 are satisfied.
- For states ID and IB we notice that condition 6.6 is symmetrical on both intervals I_1 and I_2 . Thus we may restrict the study on interval I_1 . Similar to the two previous cases the application of equations 6.3 gives $s_A(TD - D) = s_B(TD - D) = N^+$. Thus we obtain $C_{10} < 0$.

The bottom row of Table 1 contains the additional conditions on C_9 and C_{10} to be applied to each of the states analysed above.

2. If during both intervals I_1 and I_2 at least one unit is OFF the first condition of Lemma 5.13 is not satisfied, thus the state is SHORT with no extra conditions. These considerations hold for S , AP and I .

Remark 6.4 (Table 1). Overall, conditions in the middle and bottom rows of Table 1 complete the existing conditions for all $2TR$ -periodic SHORT MAIN states. Indeed these conditions covers all possible combinations of dynamics in the interval $[0, 2TR]$. The middle

row shows conditions that determine the dynamics within in the intervals I_1 and I_2 . The bottom row shows conditions that guarantee units to be OFF in $[0, 2TR] - I$.

Figure 10A shows time histories for each 2TR-periodic SHORT MAIN states in Table 1. We notice that conditions given in this table allow us to determine the regions where each of these states exists in the parameter space. To visualise 2-dimensional existence regions when varying pairs of model parameters we defined a new parameter $DF \in [0, 1]$ and set $d = cDF$, so that condition $c \geq d$ is guaranteed (DF is a scaling factor for the inputs from tonotopic locations). Figure 10B shows the two dimensional region of existence of states of each of these states at varying DF and input strength c . This enables us to determine how changes in parameters affect the dynamic organisation of the model.

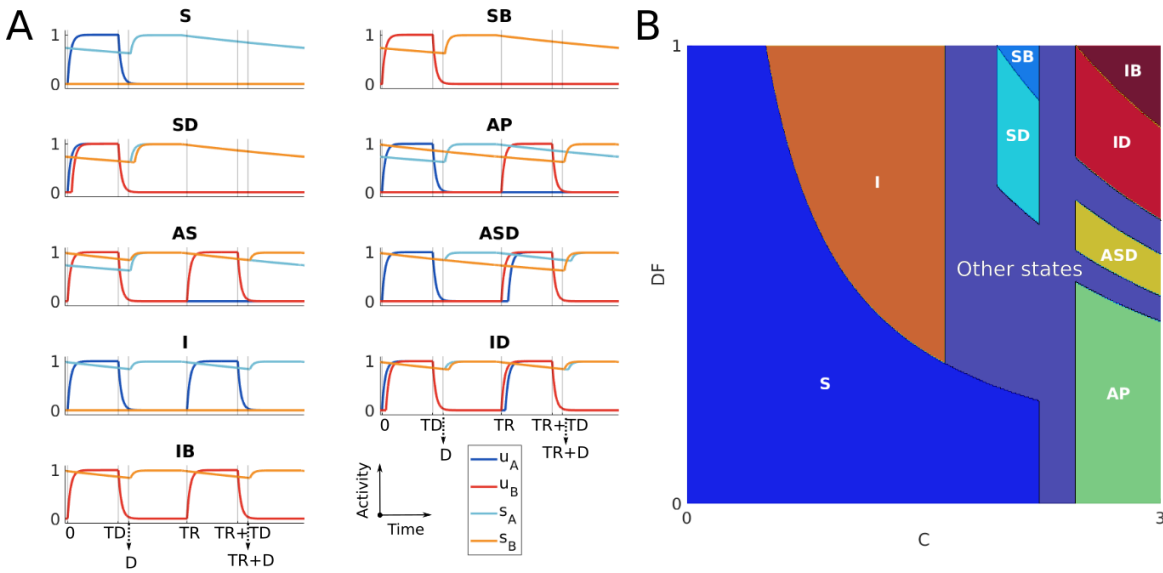


Figure 10. A. Time histories of 2TR-periodic SHORT MAIN states B. Existence regions of states in A. when varying DF and c . Parameters in B are: $\tau_i = 0.4$, $\theta = 0.5$, $TD = 0.03$, $D = 0.03$, $PR = 17\text{Hz}$, $a = 0.6$ and $b = 2$.

Theorem 6.5 (Multistability). *The state I may coexist with SB or SD . Any other pair of 2TR-periodic SHORT MAIN states cannot coexist.*

Proof. The inequalities shown in black in Table 2 report all the existence conditions for MAIN SHORT states from Table 1. Using the properties $a \geq 0$, $N^+ \geq M^+$ and $c \geq d$ on the quantities C_i^\pm defined in 6.4 one can easily show that

$$(6.7) \quad 1) C_2^- \geq C_8^- \quad 2) C_3^+ \geq C_6^+ \quad 3) C_3^- \geq C_7^- \quad 4) C_3^- \geq C_7^- \quad 5) C_5^- \geq C_7^- ,$$

which imply the inequalities reported in blue in Table 2.

Inspecting this tables demonstrates that for each pair of MAIN SHORT states (ψ_1, ψ_2) except (I, SB) and (I, SD) there exist at least one index i for which either (a) $C_i^- < \theta$ for ψ_1

| C | S | SB | SD | AP | AS | ASD | I | ID | IB |
|-----|------------------|---------------------|---------------------|---------------------|---------------------|---------------------|-------------------|---------------------|---------------------|
| 1 | $C_1 < \theta$ | | | | | | $C_1 \geq \theta$ | | |
| 2 | $C_2^+ < \theta$ | $C_2^- \geq \theta$ | $C_2^- \geq \theta$ | $C_2^+ < \theta$ | $C_2^- \geq \theta$ | $C_2^- \geq \theta$ | | | |
| 3 | $C_3^+ < \theta$ | $C_3^+ < \theta$ | $C_3^+ < \theta$ | $C_3^- \geq \theta$ | $C_3^- \geq \theta$ | $C_3^- \geq \theta$ | $C_3^- < \theta$ | $C_3^- \geq \theta$ | $C_3^- \geq \theta$ |
| 4 | | | $C_4^- \geq \theta$ | | | | | | |
| 5 | | | | $C_5^+ < \theta$ | $C_5^+ < \theta$ | $C_5^+ < \theta$ | | $C_5^- \geq \theta$ | $C_5^- \geq \theta$ |
| 6 | | | | | | | $C_6^+ < \theta$ | | |
| 7 | | | | | | | | $C_7^- < \theta$ | $C_7^- \geq \theta$ |
| 8 | | $C_8^- \geq \theta$ | $C_8^- < \theta$ | | $C_8^- \geq \theta$ | $C_8^- < \theta$ | | | |

Table 2

Existence conditions for MAIN SHORT states (black) and of the conditions derived from 6.7 (blue).

(ψ_2) and $C_i^- \geq \theta$ for ψ_1 (ψ_2) or (b) $C_i^+ < \theta$ for ψ_1 (ψ_2) and $C_i^- \geq \theta$ for ψ_1 (ψ_2). Both (a) and (b) lead to conditions that cannot be satisfied simultaneously in the parameter space. This is obvious for case (a). For case (b) this holds because, since $N^- \geq N^+$ and $M^- \geq M^+$, we have $C_i^- \leq C_i^+$, $\forall i = 2, \dots, 8$. Figure 11 shows the stability regions for states I , SB and S at varying c and DF , demonstrating that bistability between the pairs (I, SB) and (I, SD) can occur (note I and SD have a conjugate, hence we talk of *multistability* for this Theorem). ■

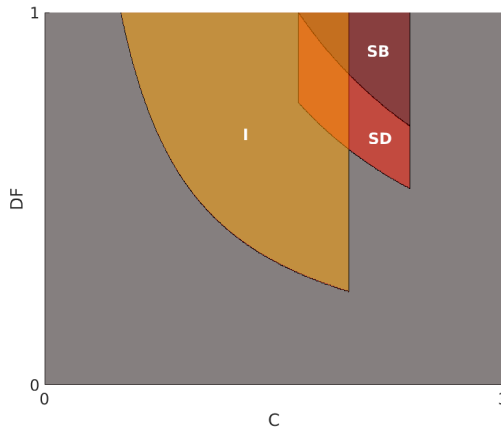


Figure 11. Bistability in the pairs of states (I, SB) and (I, SD) at varying c and DF . Model parameters in B are: $\tau_i = 0.4$, $\theta = 0.5$, $TD = 0.005$, $D = 0.015$, $PR = 5\text{Hz}$, $a = 0.4$ and $b = 3$

A similar analysis for $2TR$ -periodic SHORT CONNECT states can be carried out, as stated in the next theorem.

Theorem 6.6. *There is an injective map:*

$$\varphi: SC \rightarrow B(2, 6)$$

$$\psi \mapsto W = [W_1 \mid W_1] = \begin{bmatrix} x_A^1 & y_A^1 & z_A^1 & x_A^2 & y_A^2 & z_A^2 \\ x_B^1 & y_B^1 & z_B^1 & x_B^2 & y_B^2 & z_B^2 \end{bmatrix}$$

Where, for $i=1, 2$, W_i is the matricial forms of ψ during the interval I_i defined in 5.5, and:

$$(6.8) \quad s_B^{i\pm} = N^\pm z_B^j + M^\pm(1 - z_B^j)z_B^i, \quad \text{and} \quad s_A^{i\pm} = N^\pm z_A^j + M^\pm(1 - z_A^j)z_A^i, \quad \forall i, j=1, 2, i \neq j$$

Let φ^{I_1} (φ^{I_2}) be the map defined in Theorem 5.9 for ψ in I_1 (I_2). Then:

$$Im(\varphi) = \{W = \varphi(\psi), \text{ where } W \text{ is one of the matrices shown in Table 3}\}$$

| ZcS^* | $ZcAP$ | $ZcAS^*$ | ZcI | $ScAS^*$ | $SDcAS^*$ | $ScSD^*$ | $APcAS^*$ | $APcI$ |
|---------------------|---------------------|-------------------|---------------------|---------------------|---------------------|---------------------|---------------------|---------------------|
| 001000 | 001000 | 001001 | 001001 | 001111 | 001111 | 111000 | 111001 | 111001 |
| 001000 | 000001 | 000001 | 001001 | 000001 | 000001 | 001000 | 000111 | 001111 |
| $C_4^- < \theta$ | $C_2^+ < \theta$ | see 11.4 | $C_3^- < \theta$ | $C_3^+ \geq \theta$ | $C_3^- < \theta$ | $C_4^- \geq \theta$ | $C_3^- \geq \theta$ | $C_3^- \geq \theta$ |
| $C_4^+ \geq \theta$ | $C_3^- < \theta$ | | $C_3^+ \geq \theta$ | $C_5^+ < \theta$ | $C_3^+ \geq \theta$ | $C_2^- < \theta$ | $C_5^+ < \theta$ | $C_5^- < \theta$ |
| $C_2^+ \geq \theta$ | $C_3^+ \geq \theta$ | | $C_5^+ \geq \theta$ | $C_8^- \geq \theta$ | $C_5^+ < \theta$ | $C_2^+ \geq \theta$ | $C_2^- < \theta$ | $C_5^+ \geq \theta$ |
| | | | | $C_6^- < \theta$ | $C_8^- \geq \theta$ | $C_3^+ < \theta$ | $C_2^+ \geq \theta$ | |
| | | | | | $C_6^- \geq \theta$ | | | |
| $C_9 < \theta$ | — | $C_{10} < \theta$ | $C_{10} < \theta$ | $C_{10} < \theta$ | $C_{10} < \theta$ | $C_9 < \theta$ | $C_{10} < \theta$ | $C_{10} < \theta$ |

Table 3

Matricial form and existence conditions of 2TR-periodic SHORT CONNECT states. Asymmetrical states in $*$.

The proof of this Theorem is in the Supplementary Material 11.4. The Table 3 shows the names (first row) and the matricial forms (second row) of all possible 2TR-periodic SHORT CONNECT states. Each of these matrices can be used to easily visualise the dynamics of both A and B units in $[0, 2TR]$ (see Remark 5.11). In addition, this Table shows the existence condition for each of these states in the third and fourth rows.

6.2. LONG MAIN states. In this section we analyse the existence conditions for 2TR-periodic LONG MAIN states. To do so we use a similar analysis to the one described in the previous section for SHORT states. The first step is to extend the definition of the matricial forms for SHORT states given in Theorems 6.2 and 6.6 to LONG states. From Theorem 4.3, LONG states can exist only if there exist one active tone interval $R=I_1$ or $R=I_2$ for which two conditions are satisfied. Let us name $R=[\alpha, \beta]$. The conditions are:

1. Both units must be ON at time β
2. $a - bs_A(\beta - D) \geq \theta$ and $a - bs_B(\beta - D) \geq \theta$

We can then extend the definition of the matricial form of MAIN LONG states by including a last column in the matricial form of SHORT MAIN states. More precisely, the matricial form for a state $\psi \in LM$ is the 2×6 binary matrix V defined as

$$V = [V_1 \mid \vec{w}^1 \parallel V_2 \mid \vec{w}^2] = \begin{bmatrix} x_A^1 & y_A^1 & w^1 & x_A^2 & y_A^2 & w^2 \\ x_B^1 & y_B^1 & w^1 & x_B^2 & y_B^2 & w^2 \end{bmatrix}$$

Where V_A and V_B are the same matricial forms defined for MAIN SHORT states, respectively, with entries defined by equations 5.2. Entries of the binary vectors \vec{w}^1 and \vec{w}^2 are defined by

$$(6.9) \quad w^1 = H(ay_A^1 - bs_A^{1+})H(ay_B^1 - bs_B^{1+}) \quad \text{and} \quad w^2 = H(ay_A^2 - bs_A^{2+})H(ay_B^2 - bs_B^{2+}).$$

We remind the reader that $s_A^{1+} = s_A(TD - D)$, $s_B^{1+} = s_B(TD - D)$, $s_A^{2+} = s_A(TR + TD - D)$ and $s_B^{2+} = s_B(TR + TD - D)$. These quantities appear also in the definition of the V_1 and V_2 entries. In the case of LONG MAIN states they depend on both N^\pm and M^\pm defined in equations 6.2 and on the following quantities:

$$(6.10) \quad N_L^- = e^{-(TR-2D)/\tau_i}, \quad N_L^+ = e^{-(TR+TD-2D)/\tau_i}, \quad M_L^- = e^{-(2TR-2D)/\tau_i}, \quad M_L^+ = e^{-(2TR+TD-2D)/\tau_i}.$$

We note that $N_L^+ \geq N^+$, $N_L^- \geq N^-$, $M_L^+ \geq M^+$ and $M_L^- \geq M^-$. Using a similar analysis carried to prove equations 6.3 in Theorem 6.2 one can easily show that:

$$(6.11) \quad \begin{aligned} s_B^{i\pm} &= w^j N_L^\pm + (1-w^j)y_B^j N^\pm + (1-w^j)(1-y_B^j)w_B^i M_L^\pm + (1-w^j)(1-y_B^j)(1-w^i)y_B^i M^\pm \\ s_A^{i\pm} &= w^j N_L^\pm + (1-w^j)y_A^j N^\pm + (1-w^j)(1-y_A^j)w_A^i M_L^\pm + (1-w^j)(1-y_A^j)(1-w^i)y_A^i M^\pm \end{aligned}$$

To analyse LONG MAIN states $\psi \in LM$ we may restrict to the case where the interval R for which properties (1-2) given above are satisfied is $R = I_1$ (the case $R = I_2$ will be analysed using symmetry principles). Properties (1-2) may then be rewritten as (a) both units are ON at time $\beta = TD$, and (b) $a - bs_A^{1+} \geq \theta$ and $a - bs_B^{1+} \geq \theta$. From (a) we have that (1,1) is an equilibrium for the fast subsystem at time TD , which implies that V_1 satisfies one of M_{1-3} during the interval I_1 (see Section 5.1). From (b) we obtain $w^1 = 1$. Before we consider separately each of cases M_{1-3} , we note that the entries of the matricial form of any MAIN LONG state ψ satisfy the properties stated in the next theorem.

Theorem 6.7. *The matricial form V of any LONG MAIN state $\psi \in LM$ satisfies:*

1. $x_A^2 \leq x_B^2$
2. If $w^2 = 1 \Rightarrow x_A^2 = x_B^1, x_B^2 = x_A^1, y_A^2 = y_B^1$ and $y_B^2 = y_A^1$
3. $x_A^2 \leq x_B^1$ and $x_B^2 \leq x_A^1$
4. If $w^2 = y_A^2 = y_B^2 = 0 \Rightarrow x_A^1 \geq x_B^1$
5. $x_A^2 \leq y_A^2$ and $x_B^2 \leq y_B^2$
6. $x_A^2 = x_B^2 = 0 \Rightarrow y_A^2 = y_B^2 = 0$

Proof. Since $w^1 = 1$, from the identities 6.11 we have $s_B^{2-} = s_A^{2-} = N_L^-$, which leads to $x_A^2 = H(d - bN_L^-)$ and $x_B^2 = H(c - bN_L^-)$. Since $d \leq c$, we have (1). Similarly, if $w^2 = 1$, we have $s_B^{1\pm} = s_A^{1\pm} = N_L^\pm$. This implies $x_A^2 = H(d - bN_L^-) = x_B^1$ and $x_B^2 = H(c - bN_L^-) = x_A^1$. Analogously, one can easily show that $y_A^2 = y_B^1$ and $y_B^2 = y_A^1$ using the definition of these entries given in the definitions 5.2. Since $w^1 = 1$ we have that $s_A^{2-} = s_B^{2-} = N_L^- \geq s_A^{1-}$, which proves (3). Under the hypothesis of (4) we have that $s_B^{1\pm} = s_A^{1\pm} = M_L^\pm$. This and $c \geq d$ implies $x_A^1 = H(c - bM_L^-) \geq H(d - bM_L^-) = x_B^1$, proving (4). Since ψ is MAIN, conditions (5-6) derive from Theorem 5.7. \blacksquare

The previous theorem allow us to restrict the number of possible LONG MAIN states. Indeed the possible matricial forms for states satisfying one of condition M_{1-3} on the interval I_1 and satisfying conditions (1-7) are only the ones shown in the top rows of Table 4. These can be divided into:

- The first 5 matrices in Table 4 correspond to the states satisfying M_1 in I_1
- The last 4 matrices in Table 4 correspond to the states satisfying M_2 in I_1
- ψ cannot satisfy M_3 in I_1 since conditions (1-7) lead to no possible matricial forms

Symmetry arguments lead to the obvious symmetrical conjugates for these states, and they complete the case where both units are ON at time $\beta = TR+TD$, and $a-bs_A^{2+} \geq \theta$ and $a-bs_B^{2+} \geq \theta$.

| IL_1 | IL_2^* | $ASDL_1^*$ | ASL^* | SL^* | IDL_1 | IDL_2^* | $ASDL_2^*$ | SDL^* |
|--------|----------|------------|---------|--------|---------|-----------|------------|---------|
| 111111 | 111110 | 111010 | 111000 | 111000 | 111011 | 111010 | 111000 | 111000 |
| 111111 | 111110 | 111110 | 111110 | 111000 | 011111 | 011110 | 011110 | 011000 |

Table 4

Matricial form of the $2TR$ -periodic LONG MAIN states (asymmetrical states in *).

The existence conditions for all existing LONG MAIN states are given in the Supplementary Material 11.5 (summarised in Table 8), including their proof.

Remark 6.8 (Regions of existence of SHORT CONNECT and LONG MAIN states in 2D).

The existence conditions can be visualised as a projection of the parameter space in 2D, similar to Figure 10B for SHORT MAIN states. Figure 12A,C show two examples when varying parameters (c, DF) , and the remaining parameters have been fixed to satisfy $TD < D$ and $TD + D < TR$. Panels A. and C. respectively show the existence regions for SHORT CONNECT and LONG MAIN states. In panel A. SHORT MAIN states are shown in dark blue. Figure 12B,D show example of time histories for the SHORT CONNECT state $APcAS$ and the LONG MAIN state SDL .

Remark 6.9 (CONNECT states). From Figure 12A we note that the union of the regions of existence of all MAIN states is larger than the one of all CONNECT states. In addition SHORT CONNECT states connect branches of SHORT MAIN states, hence why we called them CONNECT. This property is due to the slow decay of the inhibition.

6.2.1. Remaining states. As shown in the Section 6, $2TR$ -periodic states can be SHORT MAIN (SM), SHORT CONNECT (SC), LONG MAIN (LM) or LONG CONNECT (LC) during each interval I_1 and I_2 . We define $X|Y$ the set of states satisfying condition X during I_1 and Y during I_2 , where $X, Y \in \{SM, SC, LM, LC\}$. In Section 6 we have the existence conditions of all possible states in some of these sets. More precisely:

- The analysis of $SM|SM$ is summarized in Table 1
- The analysis of $SC|SM$, $SM|SC$ and $SC|SC$ is summarized in Table 3
- The analysis of $LM|LM$, $SM|LM$ and $LM|SM$ is summarized in Table 4

All the remaining combinations of $X|Y$ set of states are analyzed in the Supplementary Material 11.6. This finally concludes the existence conditions for all $2TR$ -periodic states in the system.

7. Biologically relevant case: $2TR$ periodic states for $D \leq TD$ and $TD+D < TR$. In this section we analyse the case where $D \leq TD$. We assume that

$$(7.1) \quad c - b \geq \theta$$

a condition that allows the A (B) unit to be ON during each A (B) active tone interval I_A^k (I_B^k). Indeed, $\forall t \in I_A^k$, $j_A(t) = ax_B - bs_B(t-D) + c \geq c - b$, where functions j_A and j_B are

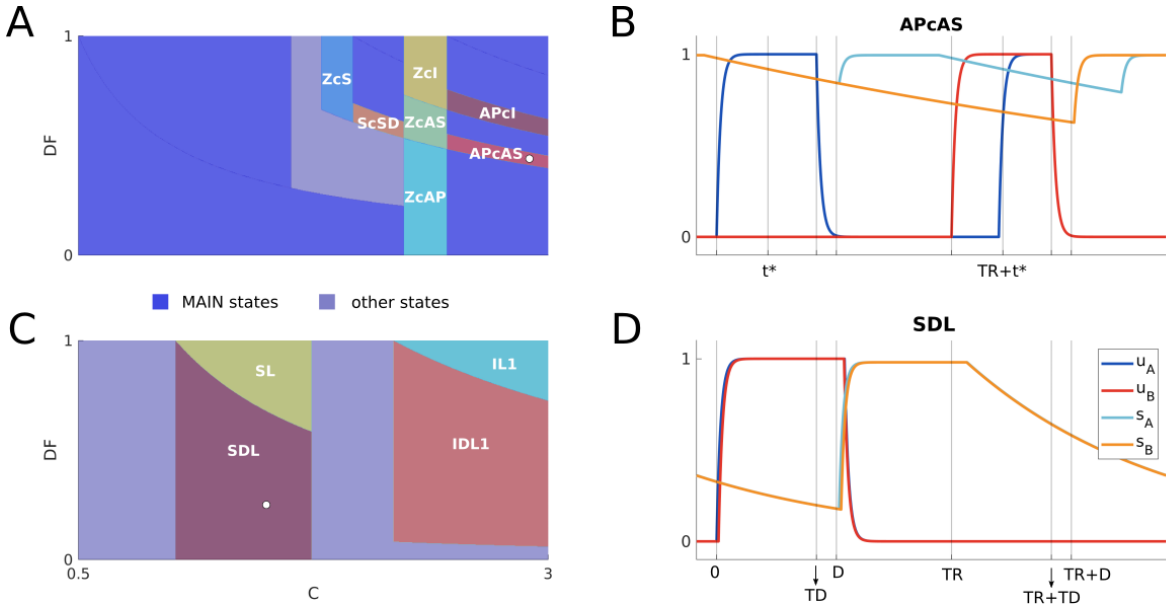


Figure 12. Visualisation of SHORT CONNECT and LONG MAIN states. Panels A. and C. show regions of existence respectively for SHORT CONNECT and LONG MAIN states at varying (c, DF) . SHORT MAIN states in panel A. are shown in dark blue. States that are neither SHORT MAIN, SHORT CONNECT or LONG MAIN are shown in light blue. For the same parameters as in A. and D., panels B. and D. respectively show example time histories for a SHORT CONNECT state (APcAS) and a LONG MAIN state (SDL) with fixed (c, DF) shown by white dots in A. and D. In panel A. the parameters are the same as in Figure 10B. In panel C. the parameters are the same as in A. except for $\tau_i=0.05$ and $a=2$.

by equations 2.2. Thus on the fast time scale, the A unit turns ON instantaneously at time $\alpha_k^A = \min(I_A^k)$ and remains ON $\forall t \in I_A^k$. Analogously the B unit turns ON instantaneously at time β_k^B and remains ON $\forall t \in I_B^k$. This has two important consequences:

1. The delayed synaptic variables $s_A(t-D)$ and $s_B(t-D)$ are constant and equal to b for $t \in [\gamma_k^A, \gamma_k^A + TD]$ and for $t \in [\gamma_k^B, \gamma_k^B + TD]$, respectively. This implies $j_B(t) = a - b + d$ for $t \in [\gamma_k^A, \beta_k^A]$ and $j_A(t) = a - b + d$ for $t \in [\gamma_k^B, \beta_k^B]$.
2. Both units are OFF $\forall t \in \mathbb{R} - I$ (i.e. no LONG states can exist). Indeed since $\beta_k^A \in [\gamma_k^A, \gamma_k^A + TD]$ we have $s_A(t-D) = b$. Thus the total input to the B unit is $j_B(\beta_k^A) = a - b < \theta$ for (U₂). Thus the B unit turns OFF instantaneously at time β_k^A , and it is followed by the A unit due to Section 3.1. Similar considerations hold for time β_k^B after swapping A and B. Since $(0, 0)$ is an equilibrium for the fast subsystem with no input (see Section 3.3), we conclude that both unit are OFF until the next active tone input.

From point 1. the total input to the B unit in $[\gamma_k^A, \beta_k^A] \subset I_A^k$ and to the A unit in $[\gamma_k^B, \beta_k^B] \subset I_B^k$ are constant and equal to $a - b + d$. This and point 2. imply that both units can turn ON only during the intervals $L_A^k = [\alpha_k^A, \gamma_k^A]$ and $L_B^k = [\alpha_k^B, \gamma_k^B]$, leading to the following two possibilities depending on the value of

$$P = a - b + d$$

- If $P \geq \theta$ both units turn ON instantaneously at times α_k^A and α_k^B and remain ON in I_A^k

and I_B^k . Indeed, since the A unit are ON in I_A^k , we have that $j_B(t) = a - bs_A(t-D) + d \geq a - b + d \geq \theta$, $\forall t \in I_A^k$. Analogously we have that $j_A(t) \geq \theta$, $\forall t \in I_B^k$. Given that both units turn OFF instantaneously at times β_k^A and β_k^B the delayed synaptic variables evolve together on the slow time scale on both intervals I_A^k and I_B^k . In particular, when evaluated at times 0 and TR these variables are equal to N^- . This implies that the input to the B unit in I_A^k and the input to the A unit in I_B^k are identical. Therefore only two symmetrical states can exist: I and ID . The difference between these states is the dynamics at the start of each active tone intervals α_k^A and α_k^B on the fast time scale. For I both units turn ON precisely at same time α_k^A and α_k^B , which occurs if and only if $d - bN^- \geq \theta$ ($C_7^- \geq \theta$). If $d - bN^- < \theta$ we have case ID , for which B (A) turns ON a small delay $\delta \sim \tau$ after A (B) in I_A^k (I_B^k).

| I | ID |
|---------------------|------------------|
| $C_7^- \geq \theta$ | $C_7^- < \theta$ |
| $P \geq \theta$ | $P \geq \theta$ |

Table 5

Names and existence conditions MAIN states for $D < TD$ and $TD + D < TR$ and $P \geq \theta$.

- If $P < \theta$ the two units are OFF in $[\gamma_k^A, \beta_k^A]$ and $[\gamma_k^B, \beta_k^B]$ and in $\mathbb{R} - I$ (point 2. above). The dynamics of the B and A units during the intervals L_A^k and L_B^k respectively is yet to be determined. Lemma 4.5 proves that the delayed synaptic variables are monotonically decaying in each of these intervals. We can therefore use the classification of MAIN and LONG states presented in Sections 5.1 by replacing interval I with interval L , where $L = L_A^k$ or $L = L_B^k$. We fix $L = L_A^k$ ($L = L_B^k$). Since A (B) is ON in L due to condition 7.1, MAIN states in L can satisfy only conditions M_1 , M_2 and M_4 (M_1 , M_3 and M_5). By the same reasoning CONNECT states in L can satisfy only condition C_1 (C_2).

Let us now consider $2TR$ -periodic states, and define $L_1 = L_A^1 = [0, D]$ and $L_2 = L_B^1 = [TR, TR + D]$. The matricial form of MAIN states can be extended to a 2×3 binary matrix (see Remark 5.12). Moreover, since A (B) is ON in L_1 (L_2) due to condition 7.1, the matricial form of any $2TR$ -periodic MAIN and CONNECT state can be written as

$$\left[\begin{array}{ccc|ccc} 1 & 1 & 1 & x_A^2 & y_A^2 & z_A^2 \\ x_B^1 & y_B^1 & z_B^1 & 1 & 1 & 1 \end{array} \right]$$

The synaptic quantities defining the entries of the matricial form in L_1 and L_2 are given by

$$(7.2) \quad s_A^{2\pm} = s_B^{1\pm} = N^\pm, \quad s_A^{1\pm} = \begin{cases} R^\pm & \text{if } z_A^2 = 1 \\ M^\pm & \text{otherwise} \end{cases} \quad \text{and} \quad s_B^{2\pm} = \begin{cases} R^\pm & \text{if } z_B^1 = 1 \\ M^\pm & \text{otherwise} \end{cases}$$

Where $R^- = e^{-(TR-2D)/\tau_i}$ and $R^+ = e^{-(TR-D)/\tau_i}$. Quantities M^\pm and N^\pm were defined in equations 6.1. The proof of these identities is in the Supplementary Material 11.7.

By simply applying identities 7.2 to the definition of the entries of the matricial form of MAIN (Theorem 5.7) or CONENCT states (Theorem 5.3) we obtain that

$$z_A^2 = z_B^1 \Rightarrow x_A^2 = x_B^1 \text{ and } y_A^2 = y_B^1$$

This condition reduces the number of possible MAIN and CONNECT states to the ones shown in Table 6. The first 5 states in this table are MAIN and the last two are CONNECT. Using the identities 7.2 on the definition of the entries in each state's matricial form and applying simplifications (i.e. the same analysis carried out in the previous sections) implies the existence conditions of each state shown in the bottom row of Table 6, where we define

$$R_6^- = a - bR^- + d \quad \text{and} \quad R_7^- = d - bR^-.$$

| IS | IDS | AS* | ASD* | AP | APcAS* | AScI |
|---------------------|---------------------|---------------------|---------------------|------------------|---------------------|---------------------|
| 111 111 | 111 011 | 111 000 | 111 000 | 111 000 | 111 000 | 111 001 |
| 111 111 | 011 111 | 111 111 | 011 111 | 000 111 | 001 111 | 001 111 |
| $R_7^- \geq \theta$ | $R_7^- < \theta$ | $C_5^+ < \theta$ | $C_5^+ < \theta$ | $C_2^+ < \theta$ | $C_2^- < \theta$ | $R_6^- < \theta$ |
| $P < \theta$ | $R_6^- \geq \theta$ | $C_8^- \geq \theta$ | $C_8^- < \theta$ | | $C_2^+ \geq \theta$ | $C_5^+ \geq \theta$ |
| | $P < \theta$ | | $C_2^- \geq \theta$ | | | |

Table 6

Matricial forms of MAIN and CONNECT states for $D < TD$ and $TD + D < TR$ and $P \geq \theta$. Asymmetrical states in *.

Figure 13A shows time histories for the states presented in Tables 5 and 6. Since the A(B) unit must be ON during the A(B) active tone interval for property 7.1 we there are no possible other network states apart. Moreover, a proof analogous to the one of Theorem 6.5 demonstrates that all of these states exist in non-overlapping regions of the parameter space (no multistability).

Remark 7.1 (Extension to the case $TD+D \geq TR$). The condition $TD + D < TR$ enabled us to obtain a complete classification of network states via the application of Lemma 4.5 (see Table 5 and Table 6). Each of these states (except for $AScI$) has the same existence conditions given in the two tables also for $TD + D \geq TR$ with two adjustments. More precisely, if $TD + D \geq TR$ and $2D < TR$ we must replace the quantity N^- with unity in the existing condition C_7^- in Table 5. If $2D \geq TR$ (which implies $TD + D \geq TR$) in conditions R_6^- and R_7^- in Table 6. This is valid for all states except for $AScI$, for which we additionally need to impose that the turning ON time t^* for the B unit in $[0, D]$, or equivalently the turning ON time $TR + t^*$ for the A unit in $[TR, TR + D]$, satisfies

$$t^* + D < TR.$$

Where t^* is given by the solution of $a - be^{-(TR-D-t^*)/\tau_i} + d = \theta$. Indeed in the Supplementary Material 11.8 we prove that $AScI$ cannot exist for $t^* + D \geq TR$. We note that, although the network states presented in this section extend to the case $TD + D \geq TR$, other $2TR$ -periodic

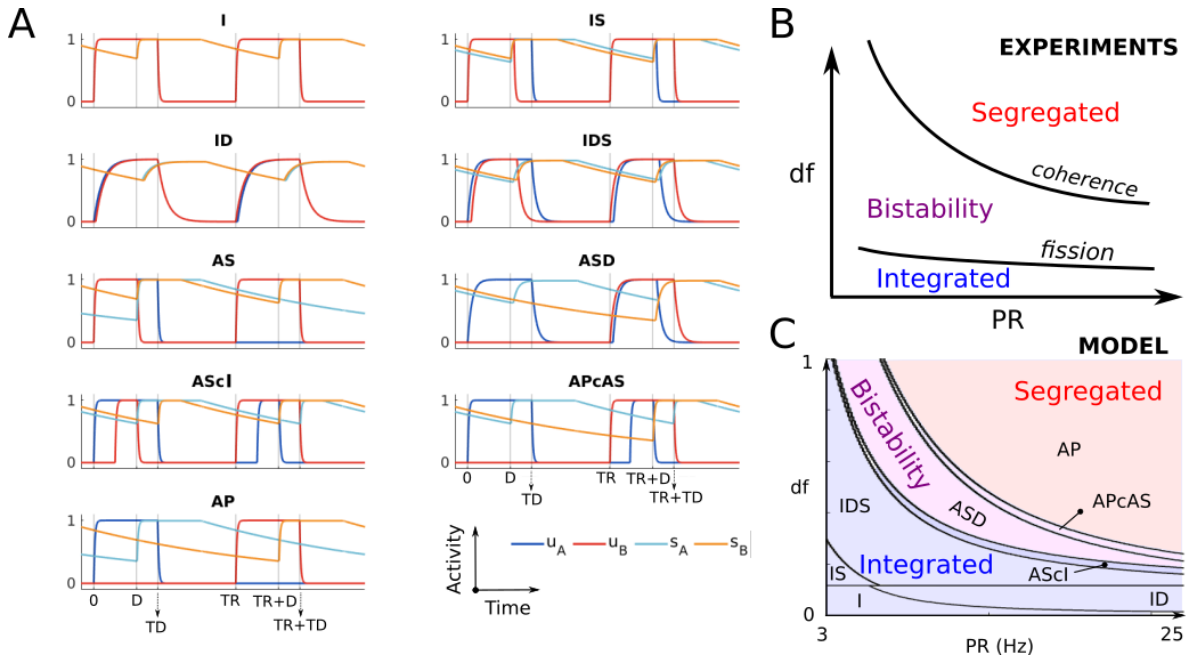


Figure 13. A. Time histories of all 2TR-periodic states for $D < TD$ and $TD+D < TR$. B. Schematic diagram of the experimentally measured perceptual regions when varying PR and df . C. Existence regions of the states in A. at varying PR and df . States corresponding to integration, segregation or bistability interpretations are grouped using blue, red and purple background colours respectively (see Remark 7.2). Model parameters in C are: $\tau_i = 0.2$, $\theta = 0.5$, $TD = 0.03$, $D = 0.01$, $c = 5$, $a = 1$, $b = 2$ and $m = 6$.

states beyond the ones studied here might exist. For example, the transition of $AScI$ at $t^* + D = TR$ leads to the emergence of a 2TR-periodic solution where both units turn ON and OFF multiple times during each active tone interval (not shown). Since the condition $TD+D \geq TR$ is met for high values of PR for which $TR \sim TD$, and it is explored further using computational tools (see Section 8).

7.1. Model states and link with auditory streaming percepts. We now show how states described in the previous section can explain how different percepts emerge for the two-tone auditory streaming stimulus. In our proposed framework rhythms are tracked via threshold detection in the A and B units' activities of 2TR-periodic states. More precisely:

- Integration corresponds to states in which both units respond to (cross threshold during) both tones (I , ID , IS , IDS and $AScI$).
- Segregation corresponds to states in which no unit responds to both tones (AP).
- Bistability corresponds to states in which the A (B) unit responds to both tones the B (A) unit responds to only one tone (AS , ASD and $APcAS$). This interpretation is motivated further in Remark 7.2.

Therefore, all model states presented in the previous section belong to one perceptual class. The changes in the predominance of integrated and segregated percepts in psychoacoustic experiments have been studied using wide ranges of presentation rates PR and pitch differences

df . The cartoon in Figure 13B shows the regions of parameters df and PR where participants are more likely to perceive integration or segregation (van Noorden diagram). The neural responses to two-tone streams explored in various animals (macaque [27, 40], guinea pigs [55]) show that the average spiking activity at A tonotopic locations in the primary auditory cortex decreases non-linearly with df during B tone presentations. In line with these experimental findings we assume that the model parameter d can be scaled by df according to $d=c \cdot (1-df^{1/m})$, where m is a positive integer and df is a unitless parameter in $[0, 1]$ which may be converted to semitone units using the formula $12 \log(1+df)$ for the experimental data shown in Figure 14C.

This allows us to monitor network states in the (df, PR) -plane that are consistent with different perceptual interpretations (percepts) and compare them with the different percepts in the van Noorden diagram. Figure 13C shows regions of existence of model states when fixing all other parameters (as reported in the caption). States classified as integration, segregation and bistability are grouped by blue, red and purple background colours to facilitate the comparison with Figure 13B. Remarkably, the existence regions of states corresponding to integration and segregation qualitatively matches the perceptual organization in the Van Noorden diagram. We note that these regions naturally emerge from the model's properties and are robust to parameter perturbations. Our analytical approach enables us to formulate the coherence and fission boundaries as functions of PR . More precisely, the coherence boundary is the curve $df_{coh}(PR)$ separating states $APcAS$ and AP , while the fission boundary is the curve $df_{fiss}(PR)$ separating states $AScI$ and IDS . From the analysis described in the previous section we can express df as functions of $TR=1/PR$:

$$(7.3) \quad df_{coh}(PR) = [(a - bN^+ + c - \theta)/c]^m \quad \text{and} \quad df_{fiss}(PR) = [(a - bM^+ + c - \theta)/c]^m,$$

where we remind the reader that $N^+ = e^{-(TR-D)/\tau_i}$ and $M^+ = e^{-(2TR-D)/\tau_i}$. We note that these curves do not depend on N^- nor R^- . Therefore, as shown in the Remark 7.1 these curves mark the transition between the same states even at high values of PR for which $TD+D \geq TR$, as confirmed by the computational analysis in Section 8.

Remark 7.2. So far, we have shown that the model predicts the emergence of integration, segregation and bistability in plausible regions of the parameter space. Yet, it currently cannot explain (1) how perception can switch between these two interpretations for fixed df and PR values (i.e. perceptual bistability) and (2) which of the two tone streams is followed during segregation (i.e. A-A- or -B-B). This could be resolved in a competition network model, such as the one proposed by [50]. The selection of which rhythm is being followed by human listeners at a specific moment in time would be resolved by a mutually exclusive selection of either unit: the perception is either integration if a unit responding to both tones is selected or segregation if a unit responding to every other tone is selected. We discuss future directions on this topic in the discussion.

Remark 7.3 (A note on the word bistability). Bistability (as used in Figure 13C) corresponds states that encode both rhythms, due to one unit responding in response to both tones and the other unit responding to only one tone: AS , ASD and $APcAS$. We note that each of these states is asymmetrical and thus they coexist with their conjugate cycles since they have the same existence conditions due to the model's symmetry. One of these pairs of states

corresponds to the A unit responding to both tones with the B unit responding only to B tones. The other corresponds to the B unit responding to both tones with the A unit responding only to A tones. The coexistence between these pairs of states should not to be confounded with our definition of bistability in terms the simultaneous encoding of both rhythms (say ABAB... and A-A-...).

8. Computational analysis under smooth gain and inputs, non slow-fast scales. In this section we use numerical simulations to explore the effect on the existence of network states using continuous rather than piecewise linear, gain function and inputs. Additionally we study the changes in the regions of existence of the states under changes in time scale ratio τ_i/τ up to an order of magnitude. We restrict our study for $D < TD$ and parameters satisfying conditions (U_1) , (U_2) and 7.1. However, we do not impose condition $TD + D < TR$, which allows to make numerical predictions at high PR that were only analysed analytically in the previous section (see Remark 7.1). In summary, we find that a smooth and non slow-fast regime generate similar states which occupy slightly perturbed regions of stability.

We consider a sigmoid gain function $S(x) = [1 + \exp(-\lambda x)]^{-1}$ with fixed slope $\lambda = 30$. We make the inputs continuous using function S by redefining them as

$$\begin{aligned} I_A(t) &= p(t)p(TD-t) + (1 - df^{1/m})q(t)q(TD-t) \\ I_B(t) &= (1 - df^{1/m})p(t)p(TD-t) + q(t)q(TD-t) \end{aligned}$$

Where $p(t) = S(\sin(\pi PR \cdot t))$ and $q(t) = S(-\sin(\pi PR \cdot t))$, so that the first (second) part of these equations $p(t)p(TD-t)$ ($q(t)q(TD-t)$) represents the input during the A (B) tone with duration TD . These new inputs are similar to the discontinuous input but with smooth sigmoidal ramps at the discontinuous jump up and jump down points α_A^k (α_B^k) and β_A^k (β_B^k), respectively, for the A (B) unit shown in Figure 2B.

We classify integration (INT), segregation (SEG) and bistability (BIS) based on counting the number of threshold crossings during one periodic interval $[0, 2TR]$. Let us call n_A (n_B) the number of threshold crossings of the A (B) unit, and $n = n_A + n_B$. Based on the correspondence between states and perception described in the previous section, states for which $n = 4$ ($n = 2$) correspond to integration (segregation) and states for which $n = 3$ correspond to the bistability. We run massive parallel simulations to systematically study the convergence to the $2TR$ -periodic states under changes in df and PR and detect boundaries of transitions between different perceptual interpretations, similar to Figure 13C except for covering a larger range of PR , spanning the interval $[1, 40]$ Hz. We consider a grid of $l \times l$ uniformly spaced parameters PR and df ($l = 98$). For each node we simulate the dynamics for the same initial conditions and simulate the dynamics for sufficiently long times enabling the convergence to a stable $2TR$ -periodic state (see caption of Figure 14 for more details). We note that the selected values of D and TD in these figures lead to the condition $TD + D \geq TR$ for PR s greater than approximately 27Hz. Thus the computations and analytical predictions shown in this figure go beyond the analysis in the previous sections. We compute the total number of threshold crossings during the last period $2TR$. Figure 14A, B and C show the computed value of $n \in \{0, 2, 3, 4\}$ in greyscale under variation of df and PR for different values of parameter τ . Black corresponds to $n = 0$ and the lightest gray to $n = 4$. There are find 5 different regions corresponding to different values of n . Three of these regions (the ones in panel A) correspond

to those found analytically in Figure 13C. Figure 14D shows example time histories of all the states in these five regions when $\tau=0.01$ (parameters PR and df are indicated by white dots in panel B).

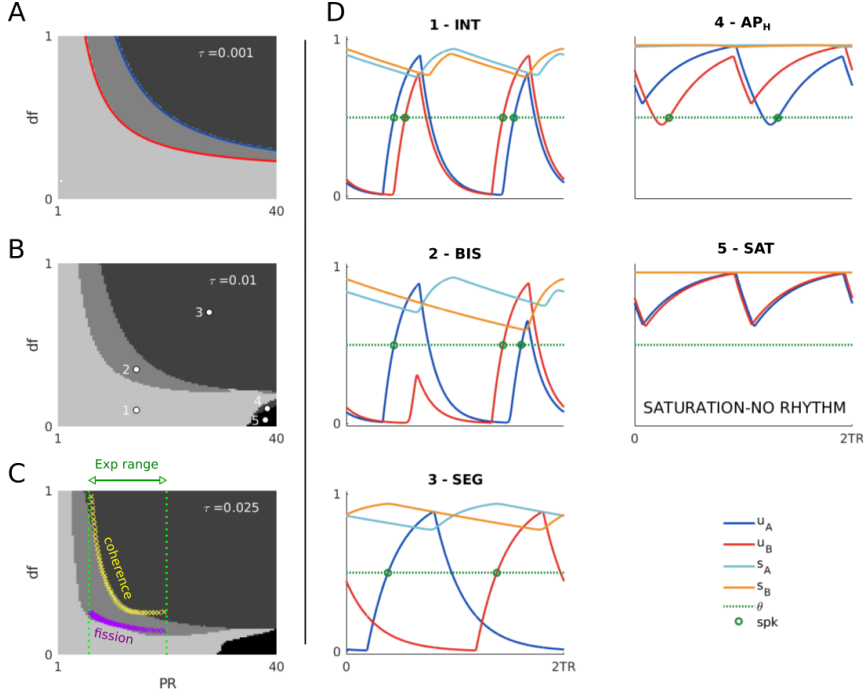


Figure 14. A-C. show the number of threshold crossings for both units (n) in greyscale colormap for simulated trajectories at varying PR and df (uniformly sampled in 96 points) for different values of τ reported in top-right corner of each panel. Black corresponds to $n=0$ and the lightest gray to $n=4$. In A. the blue and red curves correspond to the analytically predicted coherence and fission boundaries defined in equations 7.3. In C. yellow and purple crosses represent respectively the experimentally detected coherence and fission boundaries, data replotted from Figure 2 in [1] (digitalized using the software WebPlotDigitizer [52]). These lines are defined for PRs in $\sim [7, 20]$ Hz, i.e. the typical range considered in psychoacoustic experiments. D. Example of simulated time histories for all possible model states in each of the five regions of panel B. The values of PR and df used in panel 1-5 in panel D are shown by white dots in panel B. Parameters values in all panels are $a=2$, $b=2.8$, $c=5.5$, $D=0.015$, $\theta=0.5$, $TD=0.022$, $\tau_i=0.25$, $\theta=0.5$ and $m=6$. Simulations are performed using the solver `dde23` in Matlab with absolute and relative tolerances set to 10^{-7} . The initial conditions on the interval $[-D, 0]$ are specified as a constant vector function equal to $[1, 0, 1, 0]$.

For low values of τ (panel A.) the system is near the slow-fast regime. The blue and red curves show the analytically predicted coherence and fission boundaries for the Heaviside case under slow-fast regime defined in equations 7.3. These curves closely match the numerically predicted boundaries separating these regimes, showing the validity of the analytical approach also for smooth gain functions and assuming $\tau/\tau_i \ll 1$. We note that the analytical predictions hold for high values of PR for which $TD+D \geq TR$, confirming the results of the previous section. For panel B. and C. τ is increased (in panel C. $\tau/\tau_i \sim 10^{-1}$). All the existing states found in panel A. persist and occupy the largest region of the parameter space, but the predicted fission and coherence boundaries perturb. We notice the existence of the following two new

$2TR$ -periodic states, which appear under the condition $TD + D \geq TR$:

1. AP_H is characterized $n = 2$. The two units oscillate at higher activity levels than the threshold $\sim \theta$. Since $n = 2$ this state may correspond to segregation, but its perceptual relevance is difficult to assess, because it occurs in a small region of the parameter space and at high PRs , which is outside the range tested in psychoacoustic experiments.
2. SAT is characterized by $n=0$ (no threshold crossings) and occupies a relatively large region of the parameter space. The activity of both units is higher than the threshold θ for $t \in [0, 2TR]$ (saturation). This state exists at (a) low dfs and (b) high PRs , greater than 30Hz. Property (a) guarantees that the inputs during both active tones are strong enough to turn ON both units, while property (b) guarantees that that successive active A and B tone intervals occur rapidly. If τ is high, although the units turn OFF between two successive tone intervals, they never cross the threshold θ . This state does not correspond to any percepts studied in the auditory streaming experiments (integration or segregation). However, PR typically ranges between 5 and 20Hz in these experiments. The existence of this state may explain why perceivable isochronal rhythms above ~ 30 Hz are heard as a pure tone in the first (lowest) octave of human hearing. Indeed, when $df = 0$ the model inputs represent the repetition of a single tone (B=A) with frequency PR . According our proposed framework linking percepts to neural states (see previous section) suggests that SAT cannot track any rhythm simply because no unit crosses threshold.

Remarkably the coherence and fission boundaries detected from the network simulations in panel C quantitatively match those from psychoacoustic experiments (yellow and purple crosses in Figure 14C). The selected parameters of the model in the this figure (including τ) have been manually tuned to match the data. We note that the organization of these existence regions is robust to parameter perturbations. Overall, we conclude that the proposed modeling framework is a good candidate for explaining the perceptual organization in the van Noorden diagram and for the perception of isochronal rhythms as pure tones at high frequencies.

9. Discussion. We proposed a minimal firing rate model that aims to clarify the neuro-computational principles underlying the perception of interleaved auditory stimuli. The model consists of a periodically forced system of four delay differential equations representing two neural populations coupled by fast direct excitation and slow delayed inhibition forced by stepwise periodic inputs. The populations' firing rates are encoded by activity variables with a discontinuous gain function that turns these variables on or off. The inhibition dynamics, described by one equation for each population, incorporate fast activation and a slow deactivation timescales. By acting on different timescales excitation and inhibition respectively give rise to regimes of cooperation and competition between the populations, and lead to the rich dynamics explored in this work.

The model was designed to incorporate neural mechanisms commonly found in auditory cortex (ACx). Following [44], we hypothesized that the perception of pitch and rhythm are encoded in primary and secondary ACx, respectively. In the proposed model units represent the activation of neural populations in secondary ACx, whereas inputs to these populations represent tonotopically localised projections from primary ACx (as identified in neuroanatom-

ical tracing experiments [28]). The inputs mimick responses from primary auditory cortex to stimuli consisting of two interleaved A and B tones [27] and they depend on key parameters influencing psychoacoustic perception: the tones' presentation rate (PR), the pitch difference between the two tones (df) and the duration of responses to streaming inputs (TD). The timescale separation between the excitation and the inhibition in the model is consistent with synapses with AMPA and GABA receptors, respectively (widely found in cortex). Delayed inhibition would be affected by several factors including typically slower inhibitory activation times (vs excitation), indirect connections via interneurons and propagation times between the spatially separated A and B populations. Rather than try to model each of these features explicitly we opted for a single fixed delay term D .

We used analytical and computational tools to investigate periodic solutions 1:1 locked to the inputs (1:1 locked states) and their dependence on parameters influencing auditory perception. By posing the model in the slow-fast regime we used singular perturbation theory to describe the dynamics and to propose a classification of these states. For the analytical study we assumed that $TD+D < 1/PR$, a condition ensuring the inhibition activated during the active tone intervals does not affect activity at successive tone intervals. We separated the analysis into two cases: $D \geq TD$ (intermediate delays) and $D < TD$ (short delays). For intermediate delays the inhibition decays monotonically during each tone interval. For short delays we assumed that the primary tonotopic inputs to the local populations are stronger than the inhibition. These restrictions enabled us to define a binary matricial representation for the 1:1 locked states. This tool was used to formulate the existence conditions for all existing states and rule out others that are impossible, thus giving a complete description of all 1:1 locked states in the model and their dependence on parameters.

The condition $TD+D < 1/PR$ assumed in our analytical approach is relevant for studying the correspondence between the model states and the psychoacoustic streaming experiments. The factors that may play a role in generating delayed inhibition discussed above would most likely lead to short or moderate delays, for which the condition $TD+D < 1/PR$ is guaranteed for the value of PR s and TD s typically considered in psychoacoustic experiments ($PR \in [5, 20]\text{Hz}$ and $TD \in [10, 30]\text{ms}$ - the interpretation of TD is discussed further in "Predictions" below). We proposed a correspondence between classes of 1:1 locked states and the different percepts arising during auditory streaming based on threshold crossing of the units' responses. More precisely, ABAB integrated ("galloping") percepts correspond to states where both units respond to every tone and segregated A-A- or -B-B percepts correspond to states in which both units respond to only one tone. Lastly, bistability corresponds to states in which one unit responds to every tone and the other unit responds to every other tone. This interpretation of bistability can explain how both integrated and segregated rhythms may be perceived simultaneously, as reported in some behavioral studies [17, 18], but it cannot explain the dynamic alternation between these two percepts (see the section "Future work" below). This classification of states enabled us to compare their existence regions with those occupied by their corresponding percepts when varying df and PR in experiments (van Noorden diagram). Remarkably, a qualitatively similar organization of these regions emerges naturally from the model's properties and is robust to parameter perturbations. We performed this analysis by imposing short delays, but similar results hold for moderate delays (not shown).

Finally, we carried out numerical analysis with a smooth gain function, smooth inputs and

different levels of timescale separation both to confirm the validity of the analytical approach and to investigate the case $TD+D \geq 1/PR$, which was only partially studied analytically. We selected parameter values that fit the experimental data from the van Noorden diagram and found that the analytical predictions closely match the numerical analysis under the slow-fast regime. Furthermore, all the numerically detected states correspond to the ones analytically derived, even at large PRs when $TD+D \geq 1/PR$. Reducing the timescale separation shifts the regions of existence of the perceptually relevant states and produces a qualitatively close match the van Noorden diagram [1]. Moreover, this case leads to the emergence of new solutions, such as a high activity state occurring at high PRs and low df . Interestingly, the emergence of this state could explain how the perception of repeated tones is heard as single pure tone in the first (lowest) octave of human hearing, rather than a rhythm 30Hz (discussed below). The case $TD+D \geq 1/PR$ may lead to the existence of 1:1 phase locked states in which the units turn ON and OFF multiple times in the active tone intervals due to non-monotonically decaying synaptic variables. However, as these did not exist at parameter values giving a match to the van Noorden diagram, we left their analysis as beyond the scope of this work.

9.1. Models of neural competition. In this work we proposed a network motif with realistic physiological parameter constraints that produces dynamic states consistent with the perceptual interpretations of the auditory streaming paradigm. The model addresses the formation of percepts but not switching between them, so-called auditory perceptual bistability [46, 50]. Future work will address auditory bistability where the present description acts as a front-end to a competition network (one can think of the present study as a reformulation of the pre-competition stages of the model from [50]). Perceptual bistability (e.g. in like binocular rivalry) is the focus of many theoretical studies that feature mechanisms and dynamical states similar to those reported here. We note a key distinction here: the units are associated with tonotopic locations of the A and B tones, not with percepts as typically the case in other models. Firing rate models similar to ours are widely used assuming fixed inputs, mutual inhibition (often assumed instantaneous), and a slow adaptation process that drives slow-fast oscillations [38, 67, 56, 13]. Periodic inputs associated with specific experimental paradigms have been considered in several models [66, 32, 61, 16]. In common with the present study, [32] used square-wave inputs and a Heaviside gain function, revealing in-phase oscillations, anti-phase oscillations and other complex states reminiscent of those presented here.

9.2. Models of auditory streaming. The auditory streaming paradigm has been the focus of a wealth of electrophysiological and imaging studies in recent decades. However, it has received far less attention from modelers when compared with visual paradigms. Many existing models of auditory streaming have used signal-processing frameworks without a link to neural computations (recent reviews: [57, 58, 49]). In contrast our study is based on a biologically plausible network with biophysically constrained and biologically meaningful parameters. Simplifications (like the Heaviside gain function) provide the tractability to perform a detailed analysis of all states relevant to perceptual interpretations and find their existence conditions. Despite the model's apparent simplicity (4 DDEs) it produces a rich repertoire of dynamical 1:1 locked to the inputs that can all be linked to perceptual interpretations. Our model is a departure from (purely) feature-based models because it incorporates a combination of mechanisms acting at timescales close to the interval between tones. By contrast, [1]

considers neural dynamics only on a fast time scale (less than TR). Further, [50] considers slow adaptation ($\tau > 1$ s) to drive perceptual alternations, assumes instantaneous inhibition and slow NMDA-excitation, a combination that precludes forward masking as reported in [27].

A central hypothesis underpinning our model is that network states associated with different perceptual interpretations of the stimulus are generated before entering into competition that produces perceptual bistability (an idea put forward in [41] with a purely algorithmic implementation). Here the network states are emergent from a combination of neural mechanisms: mutual fast, direct excitation and mutual slow acting, delayed inhibition. In contrast with [50] our model is sensitive to the temporal structure of the stimulus present in our stereotypical description of inputs to the model from primary auditory cortex and over the full range of stimulus presentation rate PR. Furthermore, when physiological constraints are applied to the model, all the dynamical states correspond to possible perceptual interpretations.

9.3. Predictions. In van Noorden's original work on the auditory streaming paradigm boundaries for df were identified: the so-called temporal coherence boundary below which only the integrated state is possible and the so-called fission boundary above which only the segregated state is possible. We were able to derive exact expressions for these boundaries and so can explore how biophysically meaningful parameters determine the location of these behaviorally important boundaries in the (df, PR) -plane. Furthermore, we were able to show that segregation relies on slow acting, delayed inhibition, which performs forward masking. Whilst the locus for this GABA-like inhibition cannot yet be specified, we predict that its disruption, e.g. pharmacologically or with optogenetics, would promote the integrated percept.

One of challenges in developing a model that reproduces the van Noorden organization is to explain how a neural network produce an integrated-like state at very large df -values (found at low PR). The responses of neurons in primary auditory cortex show no tonotopic region of overlap in this parameter range (A-location neurons exclusively respond to A tones). We have shown that fast excitation is a mechanism through which this is possible. Similarly disrupting AMPA excitation is predicted to preclude the integrated state at large df -values.

Some model parameters control inputs properties (i.e. TD , TR , input strengths), while others internal neural processes (i.e. connection strengths, the delay D , time constants). The first set of parameters can be tested in psychcoacoustic experiments by changing features of the sound inputs, and the model could be used to readily predict the effect of such changes on rhythmic perception. We used this approach to validate and tune the model by finding a good fit to the data in the van Nordean diagram. Yet, the role of parameter TD was not investigated. In this respect it is important to note that in our model TD represents the durations of the primary auditory cortical responses to each tone's input (active tone durations), rather than the duration of the presentation of the tones (tone durations). This choice is supported by recordings of the average firing responses at tonotopic locations in the Macaque's primary locations used to model the inputs [27]. By analyzing these data we found that $\sim 80\%$ of the responses to both tones are periodically localized within a small time window starting shortly after the onset of each active tone. This time window is approximately constant across different tone intervals, tone durations, PR and df (unpublished results). Importantly, the active tone duration is less than the tone duration for all combinations of input parameters analyzed in these experiments and it is always less than ~ 30 ms.

We identified a region of parameter space at large PR for which network responses are saturated (no threshold crossings). This network state would be consistent with rapidly repeating discrete sound events at rates above 30Hz sounding like a low-frequency tone (20Hz is typically quoted as the lowest frequency for human hearing). At presentation rates above 30Hz we predict a transition from hearing a modulated low-frequency tone to, as df is increased, hearing two fast segregated streams.

9.4. Future work. Here we reported the study of $2TR$ -periodic states for two different input and delay parameter regimes. There is a rich set of dynamical behaviors to be found if the scope is extended to higher periods (such as multiples of $2TR$). Whilst beyond the scope of the current work, we have found period doubled and cycle skipping solutions that exist in smaller regions of parameter space than $2TR$ -periodic states. These appear to accumulate in cascades with increasing period but in regions of parameter space that are not biophysically relevant, and may be reported in later work.

The present model address the formation of network states representative of the integrated and segregated percepts in a tonotopically organised, non-primary area auditory cortex (i.e. a secondary auditory area in the belt or parabelt regions of auditory cortex). This is supported by evidence for specific non-primary belt and parabelt regions encoding temporal features (i.e. rhythmicity) only present in sound envelope rather stimulus features (i.e. content like pitch) as in primary auditory cortex [44]. The resolution of competition between these states is not considered at present. Imaging studies implement a network of brain areas (e.g. frontal and parietal) extending beyond auditory cortex for streaming [14, 33, 34, 35], some of which are implicated in perceptual bistability more generally [62, 64, 69]. The model could be extended to consider perceptual competition and bistability by incorporating a competition stage further downstream (in the same spirit as [50]).

Our findings rely on fast excitation and slow-acting delayed inhibition. However, we suspect that the proposed architecture is not unique in being able to produce similar dynamic states and the van Noorden diagram. The implementation of globally excitatory inputs ($i_A(t)$ and $i_B(t)$ drive both the A and B units) rather than mutual fast-excitation is expected to produce similar results, which should be explored in future work.

10. Conclusion. The present work addresses an important issue in the formulation of models of auditory streaming: how interleaved sequences of tones are integrated or segregated through a combination of feature-based and temporal mechanisms. Here the feature of tone frequency is incorporated with input-strength dependence stereotyped directly from neural recordings in primary auditory cortex. Timing mechanisms are introduced via excitatory and inhibitory interactions at different timescales including delays. Next steps include the extension the model with a competition stage to capture the dynamics of perceptual bistability [46, 50]. An extended framework would provide the ideal setting to explore perceptual entrainment through the periodic [8] or stochastic [3] modulation of a parameter like df .

Acknowledgments. The authors thank Pete Ashwin and Jan Sieber for valuable feedback on earlier versions of this manuscript.

REFERENCES

- [1] F. ALMONTE, V. JIRSA, E. LARGE, AND B. TULLER, *Integration and segregation in auditory streaming*, *Physica D*, 212 (2005), pp. 137–159.
- [2] P. ASHWIN, S. COOMBES, AND R. NICKS, *Mathematical frameworks for oscillatory network dynamics in neuroscience*, *The Journal of Mathematical Neuroscience*, 6 (2016), p. 2.
- [3] D. H. BAKER AND B. RICHARD, *Dynamic properties of internal noise probed by modulating binocular rivalry*, *PLoS Comput Biol*, 15 (2019), pp. 1–18, <https://doi.org/10.1371/journal.pcbi.1007071>.
- [4] R. BEN-YISHAI, R. BAR-OR, AND H. SOMPOLINSKY, *Theory of orientation tuning in visual cortex*, *Proceedings of the National Academy of Sciences*, 92 (1995), p. 3844.
- [5] J. K. BIZLEY AND Y. E. COHEN, *The what, where and how of auditory-object perception*, *Nat Rev Neurosci*, 14 (2013), pp. 693–707.
- [6] P. C. BRESSLOFF, *Spatiotemporal dynamics of continuum neural fields*, *Journal of Physics A: Mathematical and Theoretical*, 45 (2011), p. 033001.
- [7] P. C. BRESSLOFF, J. D. COWAN, M. GOLUBITSKY, P. J. THOMAS, AND M. C. WIENER, *Geometric visual hallucinations, Euclidean symmetry and the functional architecture of striate cortex*, *Philosophical Transactions of the Royal Society of London. Series B: Biological Sciences*, 356 (2001), pp. 299–330, <https://doi.org/10.1098/rstb.2000.0769>.
- [8] Á. BYRNE, J. RINZEL, AND J. RANKIN, *Auditory streaming and bistability paradigm extended to a dynamic environment*, *Hearing Res*, 383 (2019), p. 107807.
- [9] S. A. CAMPBELL, *Time delays in neural systems*, in *Handbook of brain connectivity*, Springer, 2007, pp. 65–90.
- [10] E. C. CHERRY, *Some experiments on the recognition of speech, with one and with two ears*, *The Journal of the acoustical society of America*, 25 (1953), pp. 975–979.
- [11] S. COOMBES, P. BEIM GRABEN, R. POTTHAST, AND J. WRIGHT, *Neural fields: theory and applications*, Springer, 2014.
- [12] R. CURTU, *Singular hopf bifurcations and mixed-mode oscillations in a two-cell inhibitory neural network*, *Physica D*, 239 (2010), pp. 504–514.
- [13] R. CURTU, A. SHPIRO, N. RUBIN, AND J. RINZEL, *Mechanisms for frequency control in neuronal competition models*, *SIAM journal on applied dynamical systems*, 7 (2008), pp. 609–649.
- [14] R. CUSACK, *The intraparietal sulcus and perceptual organization*, *J Cognit Neurosci*, 17 (2005), pp. 641–651.
- [15] S. DA COSTA, W. VAN DER ZWAAG, J. P. MARQUES, R. S. FRACKOWIAK, S. CLARKE, AND M. SAENZ, *Human primary auditory cortex follows the shape of heschl's gyrus*, *The Journal of Neuroscience*, 31 (2011), pp. 14067–14075.
- [16] F. DARKI AND J. RANKIN, *Methods to assess binocular rivalry with periodic stimuli*, *The Journal of Mathematical Neuroscience*, (2020).
- [17] S. L. DENHAM, A. BENDIXEN, R. MILL, D. TÓTH, T. WENNEKERS, M. COATH, T. BÖHM, O. SZALARDY, AND I. WINKLER, *Characterising switching behaviour in perceptual multi-stability*, *J Neurosci Methods*, 210 (2012), pp. 79–92.
- [18] S. L. DENHAM, T. BOHM, A. BENDIXEN, O. SZALÁRDY, Z. KOCSIS, R. MILL, AND I. WINKLER, *Stable individual characteristics in the perception of multiple embedded patterns in multistable auditory stimuli*, *Front Neurosci*, 8 (2014), pp. 1–15.
- [19] M. DESROCHES, A. GUILLAMON, E. PONCE, R. PROHENS, S. RODRIGUES, AND A. E. TERUEL, *Canards, folded nodes, and mixed-mode oscillations in piecewise-linear slow-fast systems*, *SIAM review*, 58 (2016), pp. 653–691.
- [20] M. DHAMALA, V. K. JIRSA, AND M. DING, *Enhancement of neural synchrony by time delay*, *Physical review letters*, 92 (2004), p. 074104.
- [21] C. DIEKMAN, M. GOLUBITSKY, T. McMILLEN, AND Y. WANG, *Reduction and dynamics of a generalized rivalry network with two learned patterns*, *SIAM Journal on Applied Dynamical Systems*, 11 (2012), pp. 1270–1309.
- [22] C. O. DIEKMAN AND M. GOLUBITSKY, *Network symmetry and binocular rivalry experiments*, *The Journal of Mathematical Neuroscience (JMN)*, 4 (2014), pp. 1–29.
- [23] G. B. ERMENTROUT AND D. H. TERMAN, *Mathematical foundations of neuroscience*, vol. 35, Springer Science & Business Media, 2010.
- [24] E. FARCOL AND J.-L. GOUZÉ, *Limit cycles in piecewise-affine gene network models with multiple inter-*

action loops, International Journal of Control, 41 (2010), pp. 119–130.

[25] A. FERRARIO, R. MERRISON-HORT, S. R. SOFFE, W.-C. LI, AND R. BORISYUK, *Bifurcations of limit cycles in a reduced model of the *xenopus* tadpole central pattern generator*, The Journal of Mathematical Neuroscience, 8 (2018), p. 10.

[26] Y. FISHMAN, D. RESER, J. AREZZO, AND M. STEINSCHNEIDER, *Neural correlates of auditory stream segregation in primary auditory cortex of the awake monkey*, Hear Res, 151 (2001), pp. 167–187.

[27] Y. I. FISHMAN, J. C. AREZZO, AND M. STEINSCHNEIDER, *Auditory stream segregation in monkey auditory cortex: effects of frequency separation, presentation rate, and tone duration*, The Journal of the Acoustical Society of America, 116 (2004), pp. 1656–1670.

[28] T. A. HACKETT, L. A. DE LA MOTHE, C. R. CAMALIER, A. FALCHIER, P. LAKATOS, Y. KAJIKAWA, AND C. E. SCHROEDER, *Feedforward and feedback projections of caudal belt and parabelt areas of auditory cortex: refining the hierarchical model*, Frontiers in neuroscience, 8 (2014), p. 72.

[29] D. HANSEL AND H. SOMPOLINSKY, *Methods in neuronal modeling: From ions to networks*, MIT Press, 1998, ch. 13 Modeling feature selectivity in local cortical circuits, pp. 499–567.

[30] D. H. HUBEL AND T. N. WIESEL, *Receptive fields, binocular interaction and functional architecture in the cat's visual cortex*, The Journal of physiology, 160 (1962), pp. 106–154.

[31] E. M. IZHIKEVICH, *Dynamical Systems in Neuroscience*, MIT Press, 2007.

[32] S. JAYASURIYA AND Z. P. KILPATRICK, *Effects of time-dependent stimuli in a competitive neural network model of perceptual rivalry*, B Math Biol, 74 (2012), pp. 1396–1426.

[33] R. KANAI, B. BAHRAMI, AND G. REES, *Human parietal cortex structure predicts individual differences in perceptual rivalry*, Curr Biol, 20 (2010), pp. 1626–1630.

[34] M. KASHINO AND H. KONDO, *Functional brain networks underlying perceptual switching: auditory streamlining and verbal transformations*, Philos T Roy Soc B, 367 (2012), pp. 977–987.

[35] H. M. KONDO, D. PRESSNITZER, Y. SHIMADA, T. KOCHIYAMA, AND M. KASHINO, *Inhibition-excitation balance in the parietal cortex modulates volitional control for auditory and visual multistability*, Scientific reports, 8 (2018), p. 14548.

[36] T. KRISZTIN, M. POLNER, AND G. VAS, *Periodic solutions and hydra effect for delay differential equations with nonincreasing feedback*, Qualitative Theory of Dynamical Systems, 16 (2017), pp. 269–292.

[37] M. KRUPA AND J. D. TOUBOUL, *Canard explosion in delay differential equations*, Journal of Dynamics and Differential Equations, 28 (2016), pp. 471–491.

[38] C. LAING AND C. CHOW, *A spiking neuron model for binocular rivalry*, Journal of computational neuroscience, 12 (2002), pp. 39–53.

[39] E. MARDER AND R. L. CALABRESE, *Principles of rhythmic motor pattern generation*, Physiological reviews, 76 (1996), pp. 687–717.

[40] C. MICHEYL, B. TIAN, R. CARLYON, AND J. RAUSCHECKER, *Perceptual organization of tone sequences in the auditory cortex of awake macaques*, Neuron, 48 (2005), pp. 139–148.

[41] R. MILL, T. BÖHM, A. BENDIXEN, I. WINKLER, AND S. DENHAM, *Modelling the emergence and dynamics of perceptual organisation in auditory streaming*, PLoS Comput Biol, 9 (2013), p. e1002925.

[42] B. C. MOORE, *An introduction to the psychology of hearing*, Brill, 2012.

[43] N. MORAY, *Attention in dichotic listening: Affective cues and the influence of instructions*, Quarterly journal of experimental psychology, 11 (1959), pp. 56–60.

[44] G. MUSACCHIA, E. W. LARGE, AND C. E. SCHROEDER, *Thalamocortical mechanisms for integrating musical tone and rhythm*, Hearing research, 308 (2014), pp. 50–59.

[45] A. PÉREZ-CERVERA, P. ASHWIN, G. HUGUET, T. M. SEARA, AND J. RANKIN, *The uncoupling limit of identical hopf bifurcations with an application to perceptual bistability*, The Journal of Mathematical Neuroscience, 9 (2019), p. 7.

[46] D. PRESSNITZER AND J. HUPÉ, *Temporal dynamics of auditory and visual bistability reveal common principles of perceptual organization*, Curr Biol, 16 (2006), pp. 1351–1357.

[47] D. PRESSNITZER, M. SAYLES, C. MICHEYL, AND I. WINTER, *Perceptual organization of sound begins in the auditory periphery*, Curr Biol, 18 (2008), pp. 1124–1128.

[48] J. RANKIN AND F. CHAVANE, *Neural field model to reconcile structure with function in primary visual cortex*, PLoS computational biology, 13 (2017), p. e1005821.

[49] J. RANKIN AND J. RINZEL, *Computational models of auditory perception from feature extraction to stream segregation and behavior*, Curr Opin Neurobiol, 58 (2019), pp. 46–53.

[50] J. RANKIN, E. SUSSMAN, AND J. RINZEL, *Neuromechanistic model of auditory bistability*, PLoS computational biology, 11 (2015).

[51] J. RINZEL AND G. ERMENTROUT, *Analysis of neural excitability and oscillations*, in Methods in neuronal modeling, MIT Press, 1998.

[52] A. ROHATGI, *Webplotdigitizer*, 2017. last accessed on 23/06/2020.

[53] G. L. ROMANI, S. J. WILLIAMSON, AND L. KAUFMAN, *Tonotopic organization of the human auditory cortex*, Science, 216 (1982), pp. 1339–1340.

[54] J. RUBIN AND D. TERMAN, *Geometric analysis of population rhythms in synaptically coupled neuronal networks*, Neural computation, 12 (2000), pp. 597–645.

[55] C. SCHOLES, A. R. PALMER, AND C. J. SUMNER, *Stream segregation in the anesthetized auditory cortex*, Hearing research, 328 (2015), pp. 48–58.

[56] A. SHIPIRO, R. CURTU, J. RINZEL, AND N. RUBIN, *Dynamical characteristics common to neuronal competition models*, J Neurophysiol, 97 (2007), pp. 462–473.

[57] J. S. SNYDER AND M. ELHILALI, *Recent advances in exploring the neural underpinnings of auditory scene perception*, Ann. N.Y. Acad. Sci., (2017).

[58] B. T. SZABÓ, S. L. DENHAM, AND I. WINKLER, *Computational Models of Auditory Scene Analysis: A Review*, Front Neurosci, 10 (2016).

[59] M. A. TEIXEIRA AND P. R. DA SILVA, *Regularization and singular perturbation techniques for non-smooth systems*, Physica D: Nonlinear Phenomena, 241 (2012), pp. 1948–1955.

[60] L. VAN NOORDEN, *Temporal coherence in the perception of tone sequences*, PhD Thesis, Eindhoven University, 1975.

[61] S. VATTIKUTI, P. THANGARAJ, H. W. XIE, S. J. GOTTS, A. MARTIN, AND C. C. CHOW, *Canonical cortical circuit model explains rivalry, intermittent rivalry, and rivalry memory*, PLoS Comput Biol, 12 (2016), p. e1004903.

[62] M. VERNET, A.-K. BREM, F. FARZAN, AND A. PASCUAL-LEONE, *Synchronous and opposite roles of the parietal and prefrontal cortices in bistable perception: A double-coil tms–eeg study*, Cortex, 64 (2015), pp. 78–88.

[63] D. WANG AND P. CHANG, *An oscillatory correlation model of auditory streaming*, Cogn Neurodynamics, 2 (2008), pp. 7–19.

[64] M. WANG, D. ARTEAGA, AND B. J. HE, *Brain mechanisms for simple perception and bistable perception*, Proceedings of the National Academy of Sciences, 110 (2013), pp. E3350–E3359, <https://doi.org/10.1073/pnas.1221945110>.

[65] X.-J. WANG, *Probabilistic decision making by slow reverberation in cortical circuits*, Neuron, 36 (2002), pp. 955–968.

[66] H. WILSON, *Computational evidence for a rivalry hierarchy in vision*, Proc Natl Acad Sci USA, 100 (2003), pp. 14499–14503.

[67] H. WILSON, *Minimal physiological conditions for binocular rivalry and rivalry memory*, Vision Res, 47 (2007), pp. 2741–2750.

[68] H. R. WILSON AND J. D. COWAN, *Excitatory and Inhibitory Interactions in Localized Populations of Model Neurons*, Biophys J, 12 (1972), pp. 1–24, [https://doi.org/10.1016/S0006-3495\(72\)86068-5](https://doi.org/10.1016/S0006-3495(72)86068-5).

[69] N. ZARETSKAYA, A. THIELSCHER, N. K. LOGOTHETIS, AND A. BARTELS, *Disrupting parietal function prolongs dominance durations in binocular rivalry*, Curr Biol, 20 (2010), pp. 2106–2111.

11. Supplementary Material.

11.1. Basins of attraction for the fast subsystem with Sigmoid gain. Here we numerically analyze the units' fast dynamics after replacing the Heaviside function H with a Sigmoid gain function with threshold 0 and slope λ for parameter values for which points $(0, 0)$ and $(1, 1)$ coexist and compare with the results presented in Remark 3.1 for the Heaviside gain. We consider the following system:

$$(11.1) \quad \begin{aligned} u'_A &= -u_A + S(a(u_B - s_2)) \\ u'_B &= -u_B + S(a(u_A - s_1)) \end{aligned}$$

Parameter a acts as a multiplicative factor on the slope λ . Figure 15 shows qualitatively similar phase portrait and the basins of attraction between the case with the Heaviside and Sigmoid gains (slope $\lambda=20$ and $a=1$). The stable equilibrium points $(0, 0)$ and $(1, 1)$ (black circles), the u_A - and u_B -nullclines (blue and red) and the saddle-separatrices (yellow and orange curves) discussed in Remark 3.1 for the Heaviside case persist and are slightly shift in the Sigmoid case. Furthermore, the degenerate (s_1, s_2) saddle for the Heaviside case becomes a standard saddle point and slightly deviates from (s_1, s_2) (red circles). The equilibria for the Sigmoidal case were detected numerically with Newton's method. Saddle separatrices (yellow and orange curves) were also found numerically via backward integration from an initial point near the saddle, in the unstable direction of the eigenvector.

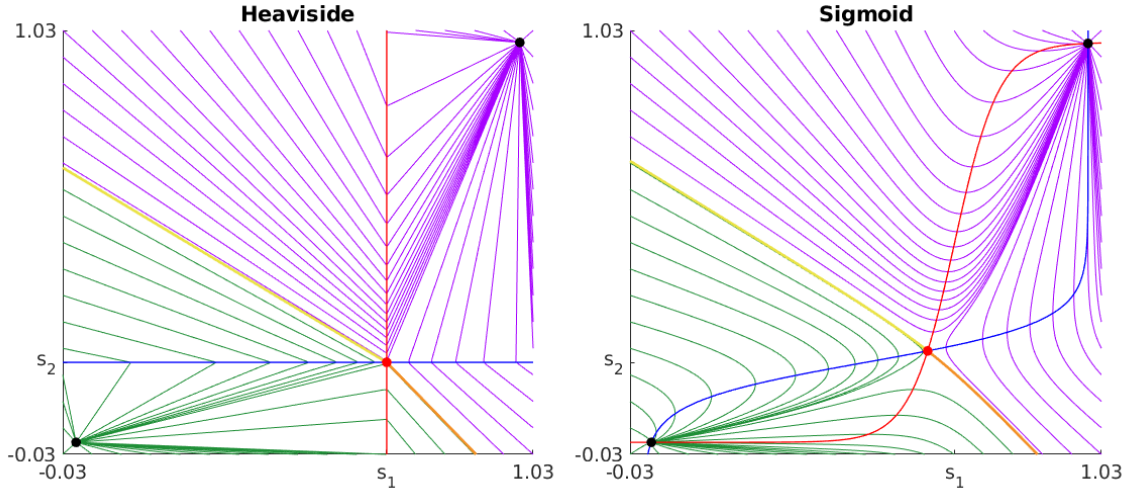


Figure 15. Phase portrait and basin of attraction for system 3.3 with $s_1 = 0.7$ and $s_2 = 0.4$ with gain function given by a Heaviside (left) or a Sigmoid with slope $\lambda=20$ and $a=1$ (right). The left panel is redrawn from Figure 3. Purple and green lines show orbits converge to $(1, 1)$ and $(0, 0)$, respectively in the Heaviside case, or to equilibria $\sim (1, 1)$ and $\sim (0, 0)$ in the Sigmoid case (black circles). The u_A - and u_B -nullclines are shown in blue and red, respectively. Yellow and orange lines show the saddle-separatrices of the point (s_1, s_2) (red circle). Point (s_1, s_2) is a degenerate saddle for the Heaviside case and a standard saddle for the Sigmoid case.

11.2. Single OFF to ON transition Lemma. Here we prove the following Lemma, that derives from Lemma 4.5 and Lemma 4.6.

Lemma 11.1 (single OFF to ON transition). *Let $D > TD$ and $TD + D < TR$ and consider an active tone interval $R = [\alpha, \beta] \in \Phi$. Let A (B) be ON at a time $\bar{t} \in R$, then*

- (1) *A (B) is ON $\forall t \geq \bar{t}$, $t \in R$*
- (2) *$\exists! t_A^* (t_B^*) \in R$ when A (B) turns ON*
- (3) *$s_A(t-D) (s_B(t-D))$ is decreasing for $t \in [\alpha, t_A^*+D] (t \in [\alpha, t_B^*+D])$*

Proof. We prove this Lemma for the A unit and for the interval $R = I_k^A$, i.e. we assume that $\alpha = \alpha_k^A$ and $\beta = \beta_k^A$, where $R = [\alpha, \beta]$. The extension to the other intervals and for the B unit is analogous. Let us call $\gamma = \gamma_k^A$. Since $TD + D < TR$ we can apply Lemma 4.5, which implies $s_A(t-D)$ and $s_B(t-D)$ to be monotonically decreasing in $[\alpha, \gamma]$. Moreover, since $D > TD$ we have that $R \subseteq [\alpha, \gamma]$. Thus the delayed synaptic variables are monotonically decreasing in R .

We now prove (1). On the fast time scale (u_A, u_B) follow the fast subsystem 3.1 at time \bar{t} and may converge to one of the four equilibria described in 3. However, since A is ON at time \bar{t} trajectories converge to either (1, 0) or (1, 1).

In the first case (convergence to (1, 0)) we have

$$c \geq bs_B(\bar{t}-D) + \theta.$$

Due to the decay of the synaptic variables, the same inequality holds $\forall t \geq \bar{t} \in R$. This condition is guaranteed only for the two equilibrium points (1, 0) and (1, 1). Therefore any orbit either remains fixed at (1, 0) or undergo a transition to (1, 1).

In the second case (convergence to (1, 1)) we have

$$a+c \geq bs_B(\bar{t}-D) + \theta$$

$$a+d \geq bs_A(\bar{t}-D) + \theta.$$

Due to the decay of the synaptic variables these inequalities hold $\forall t \geq \bar{t} \in R$. Therefore (1, 1) remains an equilibrium at such times. In both cases (convergence to (1, 0) or (1, 1)) the A unit is ON $\forall t \geq \bar{t} \in R$, proving (1).

We now prove (2). Lemma 4.6 implies that A is OFF for some $t < \alpha$. Suppose that A is ON at time \bar{t} . For continuity, there $\exists t_A^* \in R$ when the A unit undergoes an OFF to ON transition, thus proving the first claim. The uniqueness of t_A^* follows by contradiction. Suppose the existence of two distinct OFF to ON transition times $p^*, q^* \in R$ for the A unit. We can assume that $p^* < q^*$. Since A turns ON at time q^* , there $\exists r^* \in R$ with $p^* < r^* < q^*$ such that A is OFF at time r^* . The fact that A turns ON at time p^* and is OFF at time $r^* > p^*$ contradicts (1).

Lastly we prove (3) for $s_A(t-D)$. Since $[\alpha, t_A^*+D]$ is the union of closed intervals R and $[\beta, t_A^*+D]$, proving that $s_A(t-D)$ is monotonically decreasing in each of these subintervals would suffice. We previously proved that $s_A(t-D)$ is monotonically decreasing in R . Thus, we are left to prove that the same property holds in $[\beta, t_A^*+D]$.

Due to Remark 2.1 we have to prove that A cannot turn ON at any time in the interval $[\beta-D, t_A^*]$. Due to point (2) of the current lemma the turning ON time t_A^* for A exists

and is unique in the interval R . Therefore A does not turn ON in $[\alpha, t_A^*]$. Moreover since $D < TR$ we have $\beta - D = \beta_k^A - D > \alpha_{k-1}^B$, which leads to $[\beta - D, \alpha] \subset \mathbb{R} - I$. From Lemma 4.2 we have that A cannot turn ON in $[\beta - D, \alpha]$. Thus we have that A cannot turn ON in $[\beta - D, \alpha] \cup [\alpha, t_A^*] = [\beta - D, t_A^*]$, which yields the desired result. \blacksquare

11.3. Proof of the remaining claims of Theorem 6.2.

We restate Theorem 6.2 for clarity.

Theorem 11.2. *There is an injective map:*

$$\rho: SM \rightarrow B(2, 4)$$

$$\psi \mapsto V = [V_A \mid V_B] = \begin{bmatrix} x_A^1 & y_A^1 & x_A^2 & y_A^2 \\ x_B^1 & y_B^1 & x_B^2 & y_B^2 \end{bmatrix}$$

Where, for $i=1, 2$, V_i are the matricial forms of ψ during the interval I_i defined in 5.2, and:

$$(11.2) \quad s_B^{i\pm} = N^\pm y_B^j + M^\pm(1 - y_B^j)y_B^i, \quad \text{and} \quad s_A^{i\pm} = N^\pm y_A^j + M^\pm(1 - y_A^j)y_A^i, \quad \forall i, j=1, 2, i \neq j$$

In addition,

$$Im(\rho) = \Omega \stackrel{\text{def}}{=} \{V = [V_1 \mid V_2] : V_1 \in Im(\rho^{I_1}), V_2 \in Im(\rho^{I_2}) \text{ satisfying 1-4 below}\}$$

1. $y_A^1 = y_B^2 = 1 \Rightarrow x_A^1 = x_B^2$ and $y_A^2 = y_B^1 = 1 \Rightarrow x_A^2 = x_B^1$
2. $y_B^1 = y_B^2 \Rightarrow x_A^1 \geq x_A^2$ and $y_A^1 = y_A^2 \Rightarrow x_B^2 \geq x_B^1$
3. $y_A^2 = 1 \Rightarrow x_B^1 \leq r$ and $y_B^1 = 1 \Rightarrow x_A^2 \leq r$, for any entry r in V
4. $y_A^2 = y_B^2, y_A^1 = y_B^1 \Rightarrow x_A^1 \geq x_B^1$ and $x_B^2 \geq x_A^2$

Proof. The proof of all the claims in this theorem is given in the proof of Theorem 6.2 in the main text, except for conditions 1–4 above. We now show that the entries of $V = \rho(\psi)$ satisfy conditions 1–4, which proves that $Im(\rho) \subseteq \Omega$. We only prove one of the two statements for points 1,2 and 3. The proof of second statements is analogous. We recall that, given the definition of function f and g given in 5.1, the 1st and 3rd columns of V are defined by:

$$x_A^1 = H(c - bs_B^{1-}), \quad x_B^1 = H(d - bs_A^{1-}), \quad x_A^2 = H(d - bs_B^{2-}), \quad x_B^2 = H(c - bs_A^{2-})$$

1. Given the x_A^1 and x_B^2 equations above, we need to prove $s_B^{1-} = s_A^{2-}$. Assuming $y_A^1 = y_B^2 = 1$, from equations 11.2 we have:

$$s_B^{1-} = N^- y_B^2 + M^- (1 - y_B^2) y_B^1 = N^- = N^- y_A^1 + M^- (1 - y_A^1) y_A^2 = s_A^{2-}$$

2. If $y_B^1 = y_B^2$ simple substitutions in 11.2 lead to $s_B^{1-} = s_B^{2-}$. Since $c \geq d$ we have:

$$x_A^1 = H(c - bs_B^{1-}) = H(c - bs_B^{2-}) \geq H(d - bs_B^{2-}) = x_A^2$$

3. Substituting $y_A^2 = 1$ in the formula for s_A^{1-} in 11.2 implies $s_A^{1-} = N^-$ and $s_B^{i-}, s_A^{i-} \leq N^- = s_A^{1-}, \forall i=1, 2$. The latter inequalities and $c \geq d$ imply

$$x_B^1 \leq x_B^i, \quad x_B^1 \leq x_A^i, \quad \forall i=1, 2,$$

since V_1 and V_2 are matricial forms of ψ in I_1 and I_2 , respectively, their entries satisfy the first line of system 5.4, which imply $x_B^i \leq y_B^i$ and $x_A^i \leq y_A^i, \forall i=1, 2$. This proves that $x_B^1 \leq y_B^i$ and $x_B^1 \leq y_A^i, \forall i=1, 2$, and concludes the proof.

4. If $y_A^2 = y_B^2$ and $y_A^1 = y_B^1$, simple substitutions in 11.2 lead to $s_B^{1-} = s_A^{1-}$ and $s_B^{2-} = s_A^{2-}$. These equalities, together with $c \geq d$ imply:

$$x_A^1 = H(c - bs_B^{1-}) \geq H(d - bs_A^{1-}) = x_B^1 \quad \text{and} \quad x_B^2 = H(c - bs_A^{2-}) \geq H(d - bs_B^{2-}) = x_A^2$$

11.4. Analysis of 2TR-periodic SHORT CONNECT states.

Theorem 11.3. *There is an injective map:*

$$\varphi: SC \rightarrow B(2, 6)$$

$$\psi \mapsto W = [W_1 \mid W_1] = \begin{bmatrix} x_A^1 & y_A^1 & z_A^1 & x_A^2 & y_A^2 & z_A^2 \\ x_B^1 & y_B^1 & z_B^1 & x_B^2 & y_B^2 & z_B^2 \end{bmatrix}$$

Where, for $i = 1, 2$, W_i is the matricial forms of ψ during the interval I_i defined in 5.5, and:

$$(11.3) \quad s_B^{i\pm} = N^\pm z_B^j + M^\pm(1 - z_B^j)z_B^i, \quad \text{and} \quad s_A^{i\pm} = N^\pm z_A^j + M^\pm(1 - z_A^j)z_A^i, \quad \forall i, j = 1, 2, i \neq j$$

In addition, let φ^{I_1} (φ^{I_2}) be the map defined in Theorem 5.9 for ψ in I_1 (I_2). Then:

$$Im(\varphi) = \Gamma_{2TR} \doteq \{W = [W_1 \mid W_2] : W_1 \in Im(\varphi^{I_1}), W_2 \in Im(\varphi^{I_2}) \text{ satisfy conditions 1-11}\}$$

1. (a) $z_A^i \geq y_A^i \geq x_A^i$ and (b) $z_B^i \geq y_B^i \geq x_B^i$, for $i = 1, 2$
2. (a) If $x_A^i = x_B^i = 0 \Rightarrow y_A^i = y_B^i = 0$, for $i = 1, 2$
3. (a) If $z_A^1 = z_B^2 = 1 \Rightarrow x_A^1 = x_B^2$ and (b) if $z_A^2 = z_B^1 = 1 \Rightarrow x_A^2 = x_B^1$
4. (a) If $z_B^1 = z_A^2 \Rightarrow x_A^1 \geq x_A^2$ and (b) if $z_A^1 = z_B^2 \Rightarrow x_B^2 \geq x_A^1$
5. (a) If $z_A^2 = 1 \Rightarrow x_B^1 \leq r$ and (b) if $z_B^1 = 1 \Rightarrow x_A^2 \leq r$, for any entry r in V
6. If $z_A^2 = z_B^2$ and $z_A^1 = z_B^1 \Rightarrow x_A^1 \geq x_B^1$ and $x_B^2 \geq x_A^2$
7. If $z_A^1 > y_A^1$ or $z_A^2 > y_A^2$ or $z_B^1 > y_B^1$ or $z_B^2 > y_B^2$
8. (a) $z_A^1 \neq 0$ or $z_A^2 \neq 0$ and (b) $z_B^1 \neq 0$ or $z_B^2 \neq 0$
9. (a) $z_A^1 = z_B^1 = 1, y_A^2 = y_B^2 \Rightarrow z_B^2 \geq z_A^2$ and (b) $z_A^2 = z_B^2 = 1, y_A^1 = y_B^1 \Rightarrow z_A^1 \geq z_B^1$
10. $z_A^2 = 1, z_B^1 = 1 \Rightarrow z_B^2 = 1$
11. $z_A^1 = z_B^2, z_B^1 = z_A^2, x_A^1 = x_B^2 \Rightarrow y_A^2 = y_B^1$

Proof. By definition, for each state $\psi \in SC$ at least one unit turns ON at some time $t^* \in (0, TD] \cup (TR, TR+TD]$. This means that ψ may be MAIN during interval I_1 (I_2) and CONNECT during interval I_2 (I_1), or CONNECT during both intervals I_1 and I_2 . In the latter scenario Theorem 5.3 implies that ψ has a 2 by 3 matricial form W_1 (W_2) defined during interval I_1 (I_2). If ψ is MAIN during I_1 (I_2), Remark 5.12 guarantees that ψ can still be represented during interval I_1 by the same matricial form of CONNECT states given in Theorem 5.3. These considerations guarantee that the transformation given in Theorem 5.3 can be applied to both intervals I_1 and I_2 , thus proving that the map φ is well-defined and injective.

We skip the proof of the identities 11.3, since it is analogous the one given in the proof of identities 6.3 of Theorem 6.2. We now prove that each matrix $W \in Im(\varphi)$ satisfies conditions 11.3. For conditions 1-5 and 8-9 we prove only conditions (a) since the (b) ones are analogous. The proof of the first two conditions follows trivially from the definition of the entries of W . We thus prove the other conditions below

3. $z_A^1 = z_B^2 = 1 \Rightarrow s_A^{2-} = s_B^{1-} = N^- \Rightarrow x_B^1 = x_A^1 = H(c - bN^-)$
4. $z_B^1 = z_B^2 \Rightarrow s_B^{1-} = s_B^{2-} \Rightarrow x_A^1 = H(c - bs_B^{1-}) \geq H(d - bs_B^{2-}) = x_A^2$
5. Since $z_A^1 = 1 \Rightarrow s_A^{1-} = N^-$. Therefore, $x_B^1 = H(d - N^-)$. Any entry r of V is either $H(c - s_A^{i\pm})$, $H(d - s_A^{i\pm})$, $H(c - s_B^{i\pm})$ or $H(d - s_B^{i\pm})$, for some $i = 1, 2$. Since $s_A^{i\pm}, s_B^{i\pm} \leq N^-$ and $d \leq c$, we must have that $r \geq H(d - N^-) = z_A^1$
6. Given $z_A^2 = z_B^2$ and $z_A^1 = z_B^1$ and $c \geq d$ we have that

$$x_A = H(c - bN^- z_B^2 - bM^- (1 - z_B^2) z_B^1) \geq H(d - bN^- z_A^2 - bM^- (1 - z_A^2) z_A^1) = x_B$$

7. By definition, for any CONNECT state s at least one must turn ON within the interval $I = I_1$ or $I = I_2$ (or both). If $I = I_1$, from Theorem 5.9 we have that the matricial form $W_1 \in \Gamma$. In particular, it must satisfy $y_A^1 < z_A^1$ or $y_B^1 < z_B^1$. Similarly, if $I = I_2$, then $W_2 \in \Gamma$ and $y_A^2 < z_A^2$ or $y_B^2 < z_B^2$
8. By contradiction suppose there exist a CONNECT state s such that $z_A^i = 0$, for $i = 1, 2$. This leads to $s_A^{i\pm} = 0$ and to $x_A^i = y_A^i = 0$ (from 1). Thus, since we hypothesise $c \geq \theta$ then $x_B^2 = H(c) = 1$, which guarantees $z_B^2 = y_B^2 = 1$ (again from 1). Since $z_A = 0$ we also have that $x_A^1 = 0$. This leads to $x_B^2 = y_B^2 = z_B^2 = H(d)$. This leads to the matricial form

$$\left[\begin{array}{ccc|ccc} 0 & 0 & 0 & 0 & 0 & 0 \\ H(d) & H(d) & H(d) & 1 & 1 & 1 \end{array} \right]$$

Since $y_A^i = z_A^i$ or $y_B^i = z_B^i$ for $i = 1, 2$, we have $W_1 \notin \text{Im}(\varphi^{I_1})$ and $W_2 \notin \text{Im}(\varphi^{I_2})$, which is absurd.

9. Given $z_A^1 = z_B^1 = 1$ we have $s_A^{1+} = s_B^{1+} = N^+$. Since $y_A^2 = y_B^2$ and $d \leq c$ we have that $z_B^2 = H(ay_A^2 - bN^+ + c) \geq H(ay_B^2 - bN^+ + d) = z_A^2$
10. If $y_B^2 = 1$ from (1) we have $z_B^2 = 1$, which proves the claim. Thus we can assume that $y_B^2 = 0$. Condition $z_B^1 = 1$ implies $s_B^{2+} = N^+$. This identity and $y_B^2 = 0$ implies that $z_A^2 = H(d - bN^+)$. Thus from the hypothesis $z_A^2 = 1$ we have $d - bN^+ \geq \theta$. Moreover, since $d \leq c$, $ay_B^2 \geq 0$, and $s_A^{2+} \leq N^+$ we must have $z_B^2 = H(ay_B^2 + c - bs_A^{2+}) \geq H(d - bN^+) = 1$
11. Given $z_A^1 = z_B^2$, $z_B^1 = z_A^2$, $x_A^1 = x_B^2$ it obviously follows that

$$y_B^2 = H(ax_B^2 - bN^- z_B^1 - bM^- (1 - z_B^1) z_B^2 + d) = H(ax_A^1 - bN^- z_A^2 - bM^- (1 - z_A^2) z_A^1 + d) = y_A^1$$

Next, we algorithmically find all matrices in Γ_{2TR} . We proceed by generating all 2 by 6 binary matrices matrices $W = [W_1 \mid W_2]$ with entries satysfying conditions 1-11. In total, we find that $|\Gamma_{2TR}| = 15$, thus implying $|\text{Im}(\varphi)| \leq 15$.

Due to the model's symmetry, for any matrix $W = \varphi(\psi)$ of an asymmetrical state ψ there exist a matrix $W' \in \Gamma_{2TR}$ image of the state ψ' conjugate to ψ , and this matrix is defined by swapping the first row of W_1 with the second row of W_2 and the second row of W_1 with the first row of W_2 . Notably, both ψ and ψ' , and thus also W and W' , exist under the same parameter conditions. The top rows of Table 1 shows all matrices $V \in \Omega$ that are an image of either of a symmetrical state or one of two conjugate states and their corresponding names (1st row).

The analysis of existence conditions for SHORT CONNECT states is slightly more involved than the one done in Theorem 6.2 for SHORT MAIN states. The reason is that for the

| ZcS^* | $ZcAP$ | $ZcAS^*$ | ZcI | $ScAS^*$ | $SDcAS^*$ | $ScSD^*$ | $APcAS^*$ | $APcI$ |
|---------------------|---------------------|-------------------|---------------------|---------------------|---------------------|---------------------|---------------------|---------------------|
| 001000 | 001000 | 001001 | 001001 | 001111 | 001111 | 111000 | 111001 | 111001 |
| 001000 | 000001 | 000001 | 001001 | 000001 | 000011 | 001000 | 000111 | 001111 |
| $C_4^- < \theta$ | $C_2^+ < \theta$ | see 11.4 | $C_3^- < \theta$ | $C_3^+ \geq \theta$ | $C_3^- < \theta$ | $C_4^- \geq \theta$ | $C_3^- \geq \theta$ | $C_3^- \geq \theta$ |
| $C_4^+ \geq \theta$ | $C_3^- < \theta$ | | $C_3^+ \geq \theta$ | $C_5^+ < \theta$ | $C_3^+ \geq \theta$ | $C_2^- < \theta$ | $C_5^+ < \theta$ | $C_5^- < \theta$ |
| $C_2^+ \geq \theta$ | $C_3^+ \geq \theta$ | | $C_5^+ \geq \theta$ | $C_8^- \geq \theta$ | $C_5^+ < \theta$ | $C_2^+ \geq \theta$ | $C_2^- < \theta$ | $C_5^+ \geq \theta$ |
| | | | | $C_6^- < \theta$ | $C_8^- \geq \theta$ | $C_3^+ < \theta$ | $C_2^+ \geq \theta$ | |
| | | | | | $C_6^- \geq \theta$ | | | |
| $C_9 < \theta$ | — | $C_{10} < \theta$ | $C_{10} < \theta$ | $C_{10} < \theta$ | $C_{10} < \theta$ | $C_9 < \theta$ | $C_{10} < \theta$ | $C_{10} < \theta$ |

Table 7

Matricial form and existence conditions of 2TR-periodic SHORT CONNECT states. Asymmetrical states in *.

well-definedness conditions for the entries of each SHORT MAIN state's matricial form are necessary and sufficient for determining the dynamics of each state in I_1 and I_2 . In the case of CONNECT states, this property is not valid. Therefore, we analyse each of the remaining 15 matrices given in Table 3 separately using conditions C_{1-5} and M_{1-6} . Similar to the proof of formulas 6.3 of Theorem 6.2, one may show that that variables $s_A(t-D)$ and $s_B(t-D)$ of any SHORT CONNECT states are monotonically decreasing and depend on functions

$$N(t) = e^{(-TR-D-t)/\tau_i} \quad \text{and} \quad M(t) = e^{(-2TR-D-t)/\tau_i}.$$

More precisely, these variables satisfy the following $\forall t \in I_1 \cup I_2$:

$$s_B(t-D) = N(t)z_B^j + M(t)(1-z_B^j)z_B^i, \quad \text{and} \quad s_A(t-D) = N(t)z_A^j + M(t)(1-z_A^j)z_A^i, \quad \forall i, j = 1, 2, i \neq j.$$

Obviously, this is an extension of the proof of 11.3, since these quantities can be obtained by evaluating the equations above at time $t=0, TD, TR$ and $TR+TD$. Using these identities we now prove that the existence conditions for each state shown in the third row of Table 3.

1. **ZcS** - This state is CONNECT during interval I_1 (satisfying condition C_5) and MAIN during interval I_2 (satisfying condition M_6). Since $z_A^1 = z_B^1 = 1$ and $z_A^2 = z_B^2 = 0$ we have

$$s_A(t-D) = s_B(t-D) = M(t), \quad \forall t \in I_1 \quad \text{and} \quad s_A(t-D) = s_B(t-D) = N(t), \quad \forall t \in I_2.$$

In particular, evaluating these equations at time $t=0, TD, TR$ and $TR+TD$ we obtain

$$s_A^{1\pm} = s_B^{1\pm} = M^\pm \quad \text{and} \quad s_A^{2\pm} = s_B^{2\pm} = N^\pm.$$

Condition C_5 on the interval I_1 requires that A(B) turns ON at the (unique) times $t^*(s^*)$ in $(0, TD]$. It must be that $t^* \leq s^*$. Indeed, on the contrary suppose that B turns ON at time $s^* < t^*$. Thus we must have $d - bs_A(s^* - D) = \theta$ (i.e. point $(0, 1)$ is an equilibrium for the fast subsystem at time s^*) and $c - bs_B(s^* - D) < \theta$ (i.e. point $(1, 0)$ is not an equilibrium for the fast subsystem at time s^*). This is absurd because

$c \geq d$ and $s_A(s^* - D) = s_B(s^* - D) = M(s^*)$. Thus necessary and sufficient existence conditions for ZcS are given by conditions C_5 under the case $t^* \leq s^*$, which are

$$C_4^- = c - bM^- < \theta, \quad C_4^+ = c - bM^+ \geq \theta \quad \text{and} \quad C_2^+ = a - bM^+ + d \geq \theta.$$

Lastly we need to ensure that ZcS satisfies condition M_6 on the interval I_1 . More precisely, these conditions are $c - bN^+ < \theta$ and $d - bN^+ < \theta$. We notice that, since $N^+ \geq M^-$, both of these conditions automatically hold due to $C_4^- = c - bM^- < \theta$.

2. **ZcAP** - This state is CONNECT for both intervals I_1 (satisfying condition C_4) and I_2 (satisfying condition C_3). Since $z_A^1 = z_B^2 = 1$ and $z_A^2 = z_B^1 = 0$ we have $s_B^{1\pm} = s_A^{2\pm} = N^\pm$ and $s_A^{1\pm} = s_B^{2\pm} = M^\pm$. Thus from the conditions given in C_3 we have that

$$C_3^- = c - bN^- < \theta, \quad C_3^+ = c - bN^+ \geq \theta, \quad C_2^+ = a - bM^+ + d < \theta.$$

3. **ZcI** - This state is CONNECT for both intervals I_1 (satisfying condition C_5) and I_2 (satisfying condition C_5). Conditions $z_A^1 = z_B^1 = z_A^2 = z_B^2 = 1$ lead to

$$s_A(t - D) = s_B(t - D) = N(t) \quad \forall t \in I_1 \cup I_2.$$

In particular, evaluating these equations at time $t = 0, TD, TR$ and $TR + TD$ we obtain $s_A^{1\pm} = s_B^{1\pm} = s_A^{2\pm} = s_B^{2\pm} = N^\pm$. Since the synaptic variables evolve equally on both intervals and due to the model's symmetry (see 2.2) it must be that A and B turn ON at the same time t^* during intervals I_1 and I_2 respectively, and B and A turn ON at the same time s^* during intervals I_1 and I_2 respectively (applying condition C_5 on both intervals). Similar considerations made for the case ZcS lead to $t^* \leq s^*$. Thus the existence conditions for ZcAP are given by conditions C_5 under the case $t^* \leq s^*$, and they are

$$C_3^- = c - bN^- < \theta, \quad C_3^+ = c - bN^+ \geq \theta, \quad C_5^+ = a - bN^+ + d \geq \theta.$$

4. **ScAS** - This state is CONNECT for both intervals I_1 (satisfying condition C_4) and I_2 (satisfying condition C_1). Since $z_A^1 = z_A^2 = z_B^2 = 1$ and $z_B^1 = 0$ we have $s_A^{1\pm} = s_A^{2\pm} = s_B^{1\pm} = N^\pm$ and $s_B^{2\pm} = M^\pm$. Condition C_4 on interval I_1 leads to (1) $c - bN^- < \theta$, (2) $c - bN^+ \geq \theta$ and (3) $a - bN^+ + d < \theta$. Condition C_1 on interval I_2 lead to (4) $d - bM^- \geq \theta$, (5) $a - bN^- + c < \theta$ and (6) $a - bN^+ + c \geq \theta$. Conditions (1) and (6) can be discarded because they derive respectively from conditions (5) and (2) (using the properties $N^- \geq N^+$ and $a \geq 0$). Thus, the remaining conditions are

$$C_3^+ = c - bN^+ \geq \theta, \quad C_5^+ = a - bN^+ + d < \theta, \quad C_8^- = d - bM^- \geq \theta \quad \text{and} \quad C_6^- = a - bN^- + c < \theta.$$

5. **SDcAS** - This state is CONNECT for interval I_1 (satisfying condition C_4) and MAIN for interval I_2 (satisfying condition M_2). Like in the case of ScAS, since $z_A^1 = z_A^2 = z_B^2 = 1$ and $z_B^1 = 0$ we have $s_A^{1\pm} = s_A^{2\pm} = s_B^{1\pm} = N^\pm$ and $s_B^{2\pm} = M^\pm$. Condition C_4 on the interval I_1 implies conditions (1-3) in ScAS. Condition M_2 on interval I_2 implies (4) $d - bM^- \geq \theta$, (5) $c - bN^- < \theta$ and (6) $a - bN^- + c \geq \theta$. Obviously, condition (1) can be discarded because it is the same as (5), and the remaining conditions thus are

$$C_3^- = c - bN^- < \theta, \quad C_3^+ = c - bN^+ \geq \theta, \quad C_5^+ = a - bN^+ + d < \theta, \quad C_8^- = d - bM^- \geq \theta, \quad C_6^- = a - bN^- + c \geq \theta. \blacksquare$$

6. **ScSD** - This state is CONNECT for interval I_1 (satisfying condition C_1) and MAIN for interval I_2 (satisfying condition M_6). As in case ZcS we have $s_A^{1\pm} = s_B^{1\pm} = M^\pm$ and $s_A^{2\pm} = s_B^{2\pm} = N^\pm$. Condition C_1 on interval I_1 leads to $c - bM^- \geq \theta$, $a - bM^- + d < \theta$ and $a - bM^+ + d \geq \theta$. Condition M_6 on interval I_2 implies (1) $d - bN^+ < \theta$ and (2) $c - bN^+ < \theta$. Obviously, since $d \leq c$, (2) implies (1), and thus (1) can be discarded. The remaining conditions are

$$C_4^- = c - bM^- \geq \theta, \quad C_2^- = a - bM^- + d < \theta, \quad C_2^+ = a - bM^+ + d \geq \theta, \quad C_3^+ = c - bN^+ < \theta.$$

7. **APcAS** - This state is CONNECT for interval I_1 (satisfying condition M_5) and MAIN for interval I_2 (satisfying condition C_2). Similarly to the case ScAS we have that $s_A^{1\pm} = s_A^{2\pm} = s_B^{1\pm} = N^\pm$ and $s_B^{2\pm} = M^\pm$. Condition M_5 on interval I_1 leads to $c - bN^- \geq \theta$ and $a - bN^+ + d < \theta$. Condition C_2 on interval I_2 leads to $c - bN^- \geq \theta$ (again), $a - bM^- + d < \theta$ and $a - bM^+ + d \geq \theta$. In summary these conditions are

$$C_3^- = c - bN^- \geq \theta, \quad C_5^+ = a - bN^+ + d < \theta, \quad C_2^- = a - bM^- + d < \theta, \quad C_2^+ = a - bM^+ + d \geq \theta.$$

8. **APcINT** - This state is CONNECT for both intervals I_1 and I_2 , satisfying condition C_1 and C_2 respectively. As for ZcI, conditions $z_A^1 = z_B^1 = z_A^2 = z_B^2 = 1$ lead to

$$s_A(t-D) = s_B(t-D) = N(t) \quad \forall t \in I_1 \cup I_2.$$

Thus we obtain $s_A^{1\pm} = s_B^{1\pm} = s_A^{2\pm} = s_B^{2\pm} = N^\pm$. Moreover, since the synaptic variables evolve equally on both intervals and due to the model's symmetry it must be that A and B turn ON at the same time t^* during intervals I_1 and I_2 respectively (applying conditions C_{1-2} on I_{1-2}). Moreover conditions C_1 and C_2 are equal and lead to $C_3^- = c - bN^- \geq \theta$, $C_5^- = a - bN^- + d < \theta$ and $C_5^+ = a - bN^+ + d \geq \theta$.

9. **ZcAS** - Showing the existence conditions for this state is the most involved case. This state is CONNECT for both intervals I_1 (satisfying condition C_4) and I_2 (satisfying condition C_5). Since $z_A^1 = z_A^2 = z_B^2 = 1$ and $z_B^1 = 0$ we have

$$s_A(t-D) = N(t) \quad \text{and} \quad s_B(t-D) = M(t), \quad \forall t \in I_2.$$

In particular, evaluating these equations at time $t=0, TD, TR$ and $TR+TD$ we obtain $s_A^{1\pm} = s_A^{2\pm} = s_B^{1\pm} = N^\pm$ and $s_B^{2\pm} = M^\pm$. For condition C_5 on I_2 we have that B and A turn ON at times t^* and s^* in $(TR, TR+TD]$, respectively. We have two cases to consider:

- Case $t^* < s^*$. From the evolution of the synaptic variables and since they are monotonically decaying we may express existence conditions as follows:

$$(P_1) \quad \exists t^* \in (TR, TR+TD] : c - bN(t^*) = \theta \Leftrightarrow C_3^- = c - bN^- < \theta \text{ and } C_3^+ = c - bN^+ \geq \theta.$$

$$(P_2) \quad \forall s \in (0, t^*) : d - bM(s) < \theta \Leftrightarrow d - bM(t^*) < \theta$$

$$(P_3) \quad \exists s^* \in (t^*, TR+TD] : a - bM(s^*) + d \geq \theta \Leftrightarrow C_2^+ = a - bM^+ + d \geq \theta$$

Where (P1) guarantees that B turns ON at t^* , (P2) that A is OFF $\forall s \leq t^*, s \in I_2$ and (P3) that A turns ON at time s^* . Thus (P2) guarantees $s^* > t^*$. From (P1) we have that

$$t^* = N^{-1}((c - \theta)/b) = \tau_i \log((c - \theta)/b) + (TR - D)$$

By substituting this identity in (P2) and we obtain that $d - bM(t^*) < \theta$ if and only if $K = c - (d - \theta)e^{TR/\tau_i} > \theta$. Lastly we need to guarantee conditions C_4 on I_1 . Two conditions are $C_3^- = c - bN^- < \theta$ and $C_3^+ = c - bN^+ \geq \theta$, which are equivalent to case (P1). The second condition is that $C_5^+ = a - bN^+ + d < \theta$.

- Case $t^* \geq s^*$. Similar to the previous case we can formulate the following conditions:

$$(Q_1) \exists s^* \in (TR, TR + TD] : d - bM(s^*) = \theta \Leftrightarrow C_8^- = d - bM^- < \theta \text{ and } C_8^+ = d - bM^+ \geq \theta$$

$$(Q_2) \exists t^* \in (s^* - TR, TD] : c - bN(t^*) = \theta \Leftrightarrow c - bN(s^*) < \theta \text{ and } C_3^+ = c - bN^+ \geq \theta$$

Where (Q1) guarantees that A turns ON at $s^* \in (TR, TR + TD]$ and (Q2) that it turns ON at time t^* , where $t^* - TR \geq s^*$ (ie one of conditions C_4 on I_1). From (Q1) we have that

$$s^* = N^{-1}((d - \theta)/b) = \tau_i \log((d - \theta)/b) + (2TR - D),$$

Thus the first condition in (Q2) is equivalent to $K \leq \theta$. Condition $C_3^+ \geq \theta$ and $a \geq 0$ imply $a + c - bN^+ \geq \theta$, thus completing conditions C_2 on I_2 . Analogously to the previous case, the last condition to be ensured is $C_5^+ = a - bN^+ + d < \theta$.

Thus, in summary, the conditions for both cases are:

$$(11.4) \quad \begin{cases} C_3^- < \theta, C_3^+ \geq \theta, C_2^+ \geq \theta, C_5^+ < \theta, & \text{if } K > \theta \\ C_8^- < \theta, C_8^+ \geq \theta, C_3^+ \geq \theta, C_5^+ < \theta, & \text{if } K \leq \theta. \end{cases}$$

This completes the proof of the existence conditions for ZcAS.

Notably, we numerically simulated each state that corresponds to a matrix in Γ_{2TR} , thus proving that these conditions can be satisfied in a non-empty region of parameters. This proves that $Im(\rho) = \Gamma_{2TR}$. \blacksquare

11.5. Analysis of 2TR-periodic MAIN LONG states. Here prove the conditions for the MAIN LONG states summarized in Table 8.

| IL_1 | IL_2^* | $ASDL_1^*$ | ASL^* | SL^* | IDL_1 | IDL_2^* | $ASDL_2^*$ | SDL^* |
|----------------------|---------------------|----------------------|----------------------|---------------------|----------------------|----------------------|----------------------|---------------------|
| 111111 | 111110 | 111010 | 111000 | 111000 | 111011 | 111010 | 111000 | 111000 |
| 111111 | 111110 | 111110 | 111110 | 111000 | 011111 | 011110 | 011110 | 011000 |
| $D_7^- \geq \theta$ | $D_7^- \geq \theta$ | $D_7^- < \theta$ | $D_3^+ \geq 0$ | $D_3^+ < \theta$ | $D_3^- \geq \theta$ | $D_3^- \geq \theta$ | $D_3^- \geq \theta$ | $D_4^- \geq \theta$ |
| | | $D_5^- \geq \theta$ | $D_5^+ < \theta$ | $D_8^- \geq \theta$ | $D_7^- < \theta$ | $C_7^- < \theta$ | $D_5^- \geq \theta$ | $D_8^- < \theta$ |
| | | $D_3^- \geq \theta$ | $D_8^- \geq \theta$ | | $D_5^- \geq \theta$ | $D_5^- \geq \theta$ | $D_8^- < \theta$ | $D_2^- \geq \theta$ |
| | | | | | | | $D_2^- \geq \theta$ | $D_3^+ < \theta$ |
| $D_{10} \geq \theta$ | $D_{10} < \theta$ | $D_{10} < \theta$ | $C_{10} \geq \theta$ | $D_9 \geq \theta$ | $D_{10} \geq \theta$ | $D_{10} < \theta$ | $C_{10} \geq \theta$ | $D_9 \geq \theta$ |
| | | $C_{10} \geq \theta$ | | | | $C_{10} \geq \theta$ | | |

Table 8

Matricial form and existence conditions of 2TR-periodic LONG MAIN states (asymmetrical states in *).

We now prove that the existence conditions shown in the middle row of Table 8 using equations 6.11. For simplicity we write the following conditions using the analogue version

of quantities 6.4 in the case of LONG states.

$$(11.5) \quad \begin{aligned} D_2^\pm &= a - bM_L^\pm + d, & D_3^\pm &= c - bN_L^\pm, & D_4^\pm &= c - bM_L^\pm, & D_5^\pm &= a - bN_L^\pm + d, \\ D_6^\pm &= a - bN_L^\pm + c, & D_7^\pm &= d - bN_L^\pm, & D_8^\pm &= d - bM_L^\pm, & D_9 &= a - bM_L^+ & D_{10} &= a - bN_L^+ \end{aligned}$$

Next, we prove the existence conditions for each state separately.

- *IL*₁ - This state satisfies conditions M_1 during both intervals I_1 and I_2 . Due to the symmetry of the matricial form conditions M_1 are equal to conditions M_2 . Since $w^2 = 1$ we have that $s_A^{1\pm} = s_B^{1\pm} = N_L^\pm$. From this, conditions M_1 on interval I_1 are $c - bN_L^- \geq \theta$ and $D_7^- = d - bN_L^- \geq \theta$. Since $c \geq d$, the condition $D_7^- \geq \theta$ is sufficient to imply $c - bN_L^- \geq \theta$. Since $y_A^1 = y_B^1 = 1$, the identity $w^1 = H(a - bN_L^+) = 1$ implies $D_{10} \geq \theta$.
- *IL*₂ - Analogously to the previous case, this state satisfies conditions M_1 during both intervals I_1 and I_2 . Since $w^1 = 1$, $w^2 = 0$ and $y_A^2 = y_B^2 = 1$ we have $s_A^{1\pm} = s_B^{1\pm} = N^\pm$ and $s_A^{2\pm} = s_B^{2\pm} = N_L^\pm$. Since $c \geq d$ and $N_L^- \geq N^-$, conditions M_1 during both intervals I_1 and I_2 are simplified to obtain $D_7^- = d - bN_L^- \geq \theta$. In addition, $w^1 = 1$ and $w^2 = 0$ are equivalent to $D_{10} < \theta$ and $C_{10} \geq \theta$.
- *ASDL*₁ - We notice that the same arguments used for *IL*₂ lead to $D_{10} < \theta$ and $C_{10} \geq \theta$, and to $s_A^{1\pm} = s_B^{1\pm} = N^\pm$ and $s_A^{2\pm} = s_B^{2\pm} = N_L^\pm$. This state satisfies conditions M_1 during interval I_1 and M_3 during interval I_2 . The first set of conditions (M_1) lead to $C_7^- = d - bN^- \geq \theta$ (which implies also the second condition in M_1 , ie $c - bN^+ \geq \theta$). The second set of conditions (M_3) lead to $D_7^- = d - N_L^- < \theta$, $D_5^- = a + d - N_L^- \geq \theta$ and $D_3^- = c - N_L^- \geq \theta$.
- *ASL* - This state satisfies conditions M_1 during interval I_1 and M_5 during interval I_2 . Since $w^1 = 1$ we have that $s_A^{2\pm} = s_B^{2\pm} = N_L^\pm$. Since $w^2 = 1$, $y_A^2 = 0$ and $y_B^2 = 1$ we have that $s_A^{1\pm} = N^\pm$ and $s_B^{1\pm} = M_L^+$. Conditions leading to M_5 during interval I_2 are $D_3^- = c - bN_L^- \geq 0$ and $D_5^+ = a - bN_L^+ + d < \theta$. Conditions leading to M_1 during I_1 are $c - bN^- \geq \theta$, which is implied by $D_3^- \geq \theta$ (due to $N_L^- \geq N^-$) and $D_8^- = d - M_L^- \geq \theta$. Finally, as in case *IL*₁, $w^1 = 1$ implies $D_{10} = a - bN_L^- \geq \theta$ and $a - bM_L^- \geq \theta$. Since $N_L^- \geq M_L^-$ this second condition derives from $D_{10} \geq \theta$ and it can therefore be excluded. Moreover we note that, since $y_A^2 = y_B^2 = 0$, we must have $w^2 = 0$. Thus no other conditions are required.
- *SL* - This state satisfies conditions M_1 during interval I_1 and M_6 during interval I_2 . Given that $w^1 = 1$ we have $s_A^{2\pm} = s_B^{2\pm} = N_L^+$. Condition M_6 requires $D_3^+ = c - bN_L^+ < \theta$ (since it implies $d - bN_L^+ < \theta$). Since $w^2 = 0$ and $y_A^2 = y_B^2 = 0$ we have that $s_A^{1-} = s_B^{1-} = M_L^-$. Condition M_1 requires $D_8^- = d - bM_L^+ \geq \theta$ (since it implies $c - bM_L^+ \geq \theta$). Condition $D_9 = d - bM_L^- \geq \theta$ guarantees that $w^1 = 1$. We note that, since $y_A^2 = y_B^2 = 0$, we must have $w^2 = 0$ with no extra conditions.
- *IDL*₁ - This state satisfies conditions M_2 during the interval I_1 and conditions M_3 during the interval I_2 . Since this state is symmetrical M_2 and M_3 are give equal conditions. Analogously to the case *IL*₁ we have that $s_A^{1-} = s_B^{1-} = N_L^-$. Thus conditions for M_2 are $D_3^- = c - bN_L^- \geq \theta$, $D_7^- = d - bN_L^- < \theta$ and $D_5^- = a - bN_L^- + d \geq \theta$. Condition $w^1 = 1$ leads to $D_{10} = a - bN_L^+ \geq \theta$.
- *IDL*₂ - Analogously to case *IL*₂ we obtain $s_A^{1\pm} = s_B^{1\pm} = N^\pm$ and $s_A^{2\pm} = s_B^{2\pm} = N_L^\pm$. This state (*IDL*₂) satisfies conditions M_2 on interval I_1 and M_3 on interval I_2 . This leads

to $D_3^- = c - bN_L^- \geq \theta$ (which implies $c - bN^- \geq \theta$), $C_7^- = d - bN^- < \theta$ (which implies $d - bN_L^- < \theta$) and $D_5^- = a + d - bN_L^- \geq \theta$ (which implies $d - bN^- < \theta$, hence $y_B^2 = 1$). Similar arguments to the ones shown in case IL_2 lead to $D_{10} < \theta$ and $C_{10} \geq \theta$

- **ASDL₂** - As in case **ASL** we have that $s_A^{2\pm} = s_B^{2\pm} = N_L^\pm$, $s_A^{1-} = N^-$ and $s_B^{1-} = M_L^-$. This state satisfies conditions M_2 on interval I_1 and M_5 on interval I_2 . For the same arguments as case **IDL₂** we must have $D_3^- = c - bN_L^- \geq \theta$. Completing the conditions on I_1 requires $D_8^- = d - bM_L^+ < \theta$ and $D_2^- = a - bM_L^- + d \geq \theta$. Completing the conditions on I_2 requires $D_5^- = a + d - bM_L^- \geq \theta$. As in case **ASL** we also require $D_{10} \geq \theta$.
- **SDL** - Analogously to case **SL** we have $s_A^{2+} = s_B^{2+} = N_L^+$, $s_A^{1-} = s_B^{1-} = M_L^-$ and $D_9 \geq \theta$. This state satisfies conditions M_2 during interval I_1 and M_6 during interval I_2 . As shown in **SL**, conditions M_6 on interval I_2 implies $D_3^+ < \theta$. Instead, conditions M_3 on interval I_1 are $D_4^- = c - bM_L^- \geq \theta$, $D_8^- = d - bM_L^- < \theta$ and $D_2^- = a - bM_L^- + d \geq \theta$.

This concludes the proof of the existence conditions for all the LONG MAIN states shown in Table 8.

11.6. Analysis of 2TR-periodic $LM|SC$, $LC|SC$, $LC|LC$ and $LC|SM$ states. As shown in the Section 6, 2TR-periodic states can be SHORT MAIN (SM), SHORT CONNECT (SC), LONG MAIN (LM) or LONG CONNECT (LC) during each interval I_1 and I_2 . We define $X|Y$ the set of states satisfying condition X during I_1 and Y during I_2 , where $X, Y \in \{SM, SC, LM, LC\}$. In Section 6 we have the existence conditions of all possible states in some of these sets. More precisely:

- The analysis of $SM|SM$ is summarised in Table 1
- The analysis of $SC|SM$, $SM|SC$ and $SC|SC$ is summarized in Table 3
- The analysis of $LM|LM$, $SM|LM$ and $LM|SM$ is summarized in Table 4

In this section we study the remaining combinations of $X|Y$ sets. For all such sets at least one between X and Y are of the LONG type (ie LC or LM). Due to the model's symmetry, we can limit our analysis to the sets where X is LONG, i.e. for LONG states during I_1 ($LC|Z$ and $LM|Z$, where $Z \in \{SM, SC, LM, LC\}$). Indeed, states $Z|LC$ and $Z|LM$ can be obtained respectively from states in $LC|Z$ and $LM|Z$ and by applying the symmetry principles.

The next theorem shows that the matricial form for these states allow us to determining all states that can exist in the parameter space. Indeed the entries of these matrices must satisfy properties (1-6) below.

Theorem 11.4 (Conditions for LONG states in I_1). *Any LONG state in I_1 satisfies:*

1. *If $w^2 = 0 \Rightarrow x_A^2 \leq x_B^1, x_B^2 \leq x_A^1, y_A^2 \leq y_B^1$ and $y_B^2 \leq y_A^1$*
2. *If $w^2 = 0, y_A^2 = y_B^2 = 1 \Rightarrow x_A^1 \geq x_B^1$*
3. *If $w^2 = 1 \Rightarrow x_A^1 \geq x_B^1$*
4. *If $w^2 = 1$ and $x_A^2 = 1$ or $x_B^2 = 1 \Rightarrow x_A^1 \geq x_B^2, x_B^1 \geq x_A^2, y_A^1 \geq y_B^2$ and $y_B^1 \geq y_A^2$*
5. *If $w^2 = 1$ and $x_A^1 = 1$ or $x_B^1 = 1 \Rightarrow x_A^2 \geq x_B^1, x_B^2 \geq x_A^1, y_A^2 \geq y_B^1$ and $y_B^2 \geq y_A^1$*
6. *If V_2 has all zero entries $\Rightarrow x_A^1 \geq x_B^1$*

Proof. Due to Lemma 5.13 for any LONG state in I_1 both units turn are ON at time TD , and turn OFF at time $t^* + D$, for some $t^* \in [0, TD]$. Consequently both delayed synaptic variables exponentially decay during the interval I_2 starting from $t^* + 2D$. This leads to

$s_A^{2-} = s_B^{2-} = e^{-(TR-t^*-2D)/\tau_i}$. We notice that, since $t^* \geq 0$ we have

$$(11.6) \quad s_A^{2-} = s_B^{2-} \geq N_L^-$$

If $w^2 = 0$ (the hypothesis in 1.) the state is SHORT in I_2 (both units turn/are OFF at time TD). This means we can apply identities 6.11 on the interval I_1 and obtain

$$(11.7) \quad s_A^{1-} = s_B^{1-} \leq N^-$$

Inequalities 11.6 and 11.7 thus imply $s_A^{1-} \leq s_B^{2-}$ and $s_B^{1-} \leq s_A^{2-}$. By definition $x_A^1 = H(c - bs_B^{1-})$ and $x_B^2 = H(c - bs_A^{2-})$. Thus we have $x_B^2 \leq x_A^1$ (analogously we have $x_A^2 \leq x_B^1$). Moreover, $y_B^2 = H(ax_A^2 + c - bs_A^{2-}) \leq H(ax_B^1 + c - bs_A^{1-}) = y_A^1$ (and $y_A^2 \leq y_B^1$), proving 1.

One of the hypothesis of 2. is $w^2 = 0$. Thus we can apply identities 6.11 analogously to the previous case. Since $y_A^2 = y_B^2 = 1$, these identities lead to $s_A^{1-} = s_B^{1-} = N^-$. Condition $c \geq d$ guarantees that $x_A^1 = H(c - bN^-) \geq H(d - bN^-) = x_B^1$, thus proving 2.

We proceed by proving 3. Condition $w^2 = 1$ guarantees the corresponding states to be LONG in I_2 . Due to the $2TR$ periodicity we have $s_A^{1-} = s_B^{1-} = e^{-(TR-s^*-2D)/\tau_i}$, for some $s^* \in [0, TD]$. This and $d \leq c$ imply $x_A^1 = H(c - bs_B^{1-}) \geq H(d - bs_A^{1-}) = x_B^1$, which proves 3.

Assuming the hypothesis of 4 (5) at least one unit turns ON at time TD (0). Lemma 5.13 thus implies $s^* = 0$ ($t^* = 0$). Therefore we have that $s_A^{1-} = s_B^{1-} = N_L^-$ ($s_A^{2-} = s_B^{2-} = N_L^-$), which implies $s_A^{1-} \leq s_B^{2-}$ and $s_B^{1-} \leq s_A^{2-}$ ($s_A^{2-} \leq s_B^{1-}$ and $s_B^{2-} \leq s_A^{1-}$). Using a proof similar to 1 we conclude 4 (5).

Assuming the hypothesis of 6. both units are OFF in I_2 . Therefore, both delayed synaptic variables decay monotonically starting from time $t = t^* + 2D$ until time $t = 2TR$. For the $2TR$ periodicity we thus have $s_A^{1-} = s_B^{1-} = e^{-(2TR-t^*-2D)/\tau_i}$. This, $d \leq c$ and the definition of x_A^1 and x_B^1 yield 6. ■

We applied Theorem 11.4 to investigate the possible combinations of states in all remaining sets $LC|Z$ and $LM|Z$, where $Z \in \{SM, SC, LM, LC\}$. We subdivide this analysis in the following cases.

Sets $LM|SC$ and $LM|LC$ - Any state ψ in either of these two sets is LONG and MAIN in I_1 , and CONNECT in I_2 . The LONG condition in I_1 implies that (a) both units are ON at time $\beta = TD$, and (b) $a - bs_A^{1+} \geq \theta$ and $a - bs_B^{1+} \geq \theta$. Condition (a) implies that V_1 must satisfy one of M_{1-3} during the interval I_1 . From (b) we obtain $w^1 = 1$. As shown in the proof of property 5. above, we have that $s_B^{2\pm} = s_A^{2\pm} = N_L^\pm$. The CONNECT condition in I_2 implies that ψ must satisfy one of conditions C_{1-5} . However, since $d \leq c$, we must have $x_A^2 = H(d - bN_L^-) \leq H(c - bN_L^-) \leq x_B^2$ and $z_A^2 = H(a + d - bN_L^-) \leq H(a + c - bN_L^-) \leq z_B^2$. This excluded conditions the states satisfying conditions C_1 and C_4 in I_2 . Property 2. above guarantees that $LM|SC$ states satisfying condition M_3 in I_1 and C_2 or C_5 in I_2 cannot exist. The remaining set of $LM|SC$ states can exist in the parameter space and their name and matricial are given in the first two rows of Table 9. We numerically verified their existence by finding a parameter set for which they are stable using linear programming on their sets of existing conditions and by simulating their dynamics. For states in $LM|LC$ we notice that, since they are LONG in I_2 , they cannot satisfy condition C_3 in this interval (both units would otherwise be OFF at time $TR + TD$). Due to properties 3. and 5. above none of remaining

| $AScIL$ | $ScASL^*$ | $ScIL^*$ | $AScIDL^*$ | $ScASDL^*$ | $ScIDL$ | $ScASDL_2^*$ |
|----------------------|----------------------|----------------------|----------------------|----------------------|----------------------|----------------------|
| 11110010 | 11110000 | 11110010 | 11110010 | 11110000 | 11110010 | 0110000 |
| 11111110 | 11110010 | 11110010 | 01111110 | 01110010 | 01110010 | 1110010 |
| $D_3^- \geq \theta$ | $C_3^- \geq \theta$ | $C_3^- \geq \theta$ | $D_3^- \geq \theta$ | $C_3^- \geq \theta$ | $C_3^- \geq \theta$ | $C_3^- < \theta$ |
| $C_7^- \geq \theta$ | $D_5^+ < \theta$ | $D_5^+ \geq \theta$ | $D_5^- < \theta$ | $D_5^+ < \theta$ | $D_5^+ \geq \theta$ | $C_6^- \geq \theta$ |
| $D_5^- < \theta$ | $D_3^- < \theta$ | $D_3^- < \theta$ | $D_5^+ \geq \theta$ | $D_3^- < \theta$ | $D_3^- < \theta$ | $D_3^+ \geq \theta$ |
| $D_2^+ \geq \theta$ | $D_3^+ \geq \theta$ | $D_3^+ \geq \theta$ | $C_5^- \geq \theta$ | $D_3^+ \geq \theta$ | $D_3^+ \geq \theta$ | $D_5^+ < \theta$ |
| | $D_8^- \geq \theta$ | $D_7^- \geq \theta$ | $D_7^- < \theta$ | $D_8^- < \theta$ | $D_7^- < \theta$ | $D_8^- \geq \theta$ |
| | | | | $D_2^- \geq \theta$ | $C_5^- \geq \theta$ | |
| $D_{10} < \theta$ | $C_{10} \geq \theta$ | $D_{10} < \theta$ | $D_{10} < \theta$ | $C_{10} \geq \theta$ | $D_{10} < \theta$ | $C_{10} \geq \theta$ |
| $C_{10} \geq \theta$ | | $C_{10} \geq \theta$ | $C_{10} \geq \theta$ | | $C_{10} \geq \theta$ | |

Table 9

Matricial form and existence conditions of 2TR-periodic $LM|SC$ states (asymmetrical states in *).

states (the ones satisfying conditions C_2 and C_5) can exist. Therefore, no $LM|LC$ state can exist.

Sets $LC|SC$, $LC|LC$ and $LC|SM$ - Any state in either of these two sets is LONG and CONNECT in I_1 . The LONG condition implies that both units are ON at time $\beta = TD$, thus excluding CONNECT conditions C_3 or C_4 in I_1 . Furthermore, as shown in the case of $LM|LC$ (previous case), this LONG condition also excludes CONNECT conditions C_1 and C_4 for $LC|SC$ and $LC|LC$ states in I_2 , and conditions M_2 and M_4 for $LC|SM$ states in I_2 . For states in $LC|LC$ we notice that, since they are LONG in I_2 , they cannot satisfy condition C_3 in this interval (for an analogue reason of case $LM|LC$). Of the remaining states, the ones described by the following matricial forms cannot exist:

$$\begin{array}{ll} 1111 \ 0000 & 1111 \ 0000 \\ 0011 \ 0010 & \text{and} \\ & 0011 \ 1110 \end{array}$$

Indeed entries $w^1 = 1$ and $y_B^1 = 0$ imply respectively $a - bN^+ \geq \theta$ and $a - M_L^- + d < \theta$. These two conditions imply $d < be^{(D-TR)/\tau_i}(e^{(D-TR)/\tau_i} - 1) < 0$. This is absurd since by hypothesis we must have $TR > D$ and $d \geq 0$. Finally the application of properties 1-6 above reduces the number of possible states. The remaining set of $LM|SC$ states can exist in the parameter space and their name and matricial are given in the first two rows of Table 10.

The last two rows of Tables 9 and 10 show the conditions of existence of the corresponding $LM|SC$, $LC|SC$, $LC|LC$ and $LC|SM$ states. Determining these is straightforward in most cases. Indeed, it requires using formulas 11.3 and 6.11 on the definition of the entries of each matricial form, and application of simplifications, analogously to the previous considered cases, except for $ScASL_2$ and $ZcIL$ (see Table 10). These two need special attention, because they satisfy property C_5 in I_1 , we cannot apply the formulas 11.3 and 6.11. For $ZcIL$ the A unit turns ON before the B units in I_1 ($t^* < s^*$), because both synaptic variables s_A and s_B evolve equally during in this interval (on the fast time scale) and the total input to the A unit is greater than the one to the B unit at time t^* , i.e. $c - bs_B(t^*) \leq d - bs_A(t^*)$. For $ScASL_2$ the

| $ScASDL_3^*$ | $APcIDL^*$ | $ScSDL^*$ | $APcIL$ | $ScASDL_4^*$ | $ScASL_2^*$ | $ZcIL^*$ |
|----------------------|----------------------|---------------------|----------------------|----------------------|-------------|----------|
| 11110010 | 11110010 | 11110000 | 11110011 | 00110000 | 00110000 | 00110010 |
| 00110010 | 00111110 | 00110000 | 00111111 | 11110010 | 00110010 | 00110010 |
| $C_3^- \geq \theta$ | $D_3^- \geq \theta$ | $D_3^+ < \theta$ | $D_3^- \geq \theta$ | $C_6^- < \theta$ | See 11.8 | See 11.9 |
| $D_3^- < \theta$ | $C_5^- < \theta$ | $D_4^- \geq \theta$ | $D_5^- < \theta$ | $D_6^+ \geq \theta$ | | |
| $D_3^+ \geq \theta$ | $D_5^+ \geq \theta$ | $D_2^- < \theta$ | $D_5^+ \geq \theta$ | $D_5^+ < \theta$ | | |
| $D_5^- < \theta$ | | $D_2^+ \geq \theta$ | | $D_8^- \geq \theta$ | | |
| $D_5^+ \geq \theta$ | | | | | | |
| $D_{10} < \theta$ | $D_{10} < \theta$ | $D_9 \geq \theta$ | $D_{10} \geq \theta$ | $C_{10} \geq \theta$ | | |
| $C_{10} \geq \theta$ | $C_{10} \geq \theta$ | | | | | |

Table 10

Matricial form and existence conditions of 2TR-periodic $LC|SC$, $LC|LC$ and $LC|SM$ states (asymmetrical states in *).

two synaptic variables evolve differently on I_1 , which may lead to $t^* < s^*$ or $t^* \geq s^*$. Later we will show that case $t^* \geq s^*$ cannot exist. Lastly there are three degenerate states that exist only under $\tau = 0$, which cannot be numerically simulated. These states conclude all set of existing 2TR-periodic states in the system under the case $TR \leq TD + D$ and $D \geq TD$.

We proceed by describing the existence conditions for $ScASL_2$ for $t^* < s^*$ and state $ZcIL$.

- Case $ScASL_2$ for $t^* < s^*$ - This state satisfies conditions C_5 on I_1 and C_3 on I_2 . Since $y_B^2 = 1$ and $w^2 = 0$ the B unit turns OFF at time $TR + TD$. Due to Lemma 5.13 the synaptic variable $s_B(t)$ exponentially decays starting from time $TR + TD + D$ and due to the 2TR-periodicity we must have $s_B(t) = e^{-(TR+t-TD-D)/\tau_i}$, for $t \in [0, TD]$. From this we obtain $s_B(0) = N^-$ and $s_B(TD) = N^+$. Condition C_5 on I_1 with $t^* < s^*$ requires $C_3^- = c - bN^- < \theta$ and $c - bN^+ \geq \theta$. The turning ON time for the A unit in I_1 is therefore given by

$$t^* = s_B^{-1}((c - \theta)/b) = TR - TD - D - \tau_i \log((c - b)/\theta).$$

From Lemma 5.13 and from $t^* < s^*$ we obtain that both units instantaneously turn OFF at time $t^* - 2D$. Thus the synaptic variable $s_A(t)$ and $s_B(t)$ exponentially decay following the same dynamics on the slow time scale starting from time $t^* + 2D$. This leads to $s_A(t) = s_B(t) = e^{-(t-t^*-2D)/\tau_i}$, for $t \in [TR, TR + TD]$. Moreover, since the A unit is OFF in I_2 and due to the 2TR-periodicity we have $s_A(t) = e^{-(2TR+t-t^*-2D)/\tau_i}$, for $t \in [0, TD]$. These properties yield $s_A^{2+} = s_A(TR + TD) = e^{(D-2TD)/\tau_i}(c - \theta)/b$ and $s_A^{1+} = s_A(TD) = e^{(D-2TD-TR)/\tau_i}(c - \theta)/b$. To complete the conditions C_5 on I_1 we need to guarantee that the B unit turns ON at some time $s^* \geq t^* \in [0, TD]$. These are equivalent to $d - bs_A(t^*) < \theta$ and $a - bs_A^{1+} + d \geq \theta$, which can respectively be rewritten as $d - be^{2(D-TR)/\tau_i} < \theta$ and $a - Lc + d \geq (1 - L)\theta$, where $L = e^{(D-2TD-TR)/\tau_i}$. Condition C_3 on I_2 requires $c - bs_A^{2-} < \theta$ and $c - bs_A^{2+} \geq \theta$. This first of these conditions is not necessary, since it is implied by the already existing condition $C_3^- < \theta$ (since $s_A^{2+} \geq N^-$). The second is equivalent to $(c - \theta)(1 - K) \geq 0$, with $K = e^{(D-2TD)/\tau_i}$, which occurs if and only if $D \leq 2TD$ (since $c \geq \theta$). To complete condition C_3 we need to guarantee that the A unit stays OFF in I_2 , ie that $a - bs_B^{2+} + d < \theta$, which is equivalent to $a - Kc + d < (1 - K)\theta$.

Finally, the last condition derives from $w^1 = 1$ ($w^2 = 0$ is automatically guaranteed since the A is OFF at time $TR + TD$), ie $C_{10} = a - bN^+ \geq \theta$. This guarantees also $a - bs_A^{1+} = a - bM_L^+ \geq \theta$, since $M_L^+ \leq N^+$. Thus in summary the list of conditions for this state is:

$$\begin{aligned}
 (11.8) \quad & C_3^- < \theta \\
 & C_{10} \geq \theta \\
 & D \leq 2TD \\
 & d < \theta - be^{2(D-TR)/\tau_i} \\
 & a - Lc + d \geq (1 - L)\theta \\
 & a - Kc + d < (1 - K)\theta
 \end{aligned}$$

- Case *ZcIL*. This state satisfies conditions C_5 during both intervals I_1 and I_2 . Both units turn OFF at time $TR + TD$. Lemma 5.13 implies that both synaptic variables exponentially decay starting from time $TR + TD + D$ and due to the $2TR$ -periodicity we must have $s_A(t) = s_B(t) = e^{-(TR+t-TD-D)/\tau_i}$, for $t \in [0, TD]$. From the A unit turns ON before the B unit in interval I_1 , precisely at time t^* , and both units turn OFF at time $t^* + D$ for lemma 5.13. Thus the delayed synaptic variables exponentially decay from time $t^* + 2D$ and we have $s_A(t) = s_B(t) = e^{-(t-t^*-2D)/\tau_i}$, for $t \in [TR, TR + TD]$. Thus both variables evolve equally (on the slow time scale) respectively on I_1 and on I_2 . Although condition C_5 on both intervals could lead to potentially 4 cases, we only have one case to consider, the A (B) unit turns ON before the B (A) unit in interval I_1 (I_2). Analogously to the case *ScASL₂*, condition C_5 on I_1 requires $C_3^- = c - bN^- < \theta$ and $c - bN^+ \geq \theta$, and t^* is given by

$$t^* = s_B^{-1}((c - \theta)/b) = TR - TD - D - \tau_i \log((c - b)/\theta).$$

As in case *ScASL₂* condition C_3 on I_2 requires $D \leq 2TD$. To complete the conditions C_5 we require $a - bs_B^{2+} + d \geq \theta$, which is equivalent to $a - Kc + d \geq \theta(1 - K)$. Lastly, we need to guarantee $w^1 = 1$ and $w^2 = 0$, which are equivalent respectively to $C_{10} \geq \theta$ and $a - Kc < \theta(1 - K)$ (ie $a - bs_B^{2+} < \theta$). Thus in summary the list of conditions for this states are:

$$\begin{aligned}
 (11.9) \quad & C_3^- < \theta \\
 & C_{10} \geq \theta \\
 & D \leq 2TD \\
 & a - Kc + d \geq (1 - K)\theta \\
 & a - Kc < (1 - K)\theta
 \end{aligned}$$

Lastly, we show that the following three states may exist only if $\tau = 0$ (degenerate cases). These states complete all the existing states after application of conditions 11.4. This finally concludes the existence conditions for all $2TR$ -periodic states in the system.

$$ScASL_2 = \begin{bmatrix} 0011 & 0000 \\ 0011 & 0010 \end{bmatrix} \text{ for } t^* \geq s^*, ZcIL_2 = \begin{bmatrix} 0011 & 0011 \\ 0011 & 0011 \end{bmatrix} \text{ and } ZcSL = \begin{bmatrix} 0011 & 0000 \\ 0011 & 0000 \end{bmatrix}.$$

We show that these three states cannot exist unless $\tau=0$ (degenerate for the model). Firstly we note that each case satisfies condition C_5 on interval I_1 , so that A turns ON at time t^* and B turns ON at time s^* , for some $t^*, s^* \in [0, TD]$. Next we divide the proof for the three cases above:

1. $ZcSL$ - This state satisfies condition C_5 on interval I_1 . That A turns ON at time t^* and B turns ON at time s^* , for some $t^*, s^* \in I_1$. Since both units turn OFF instantaneously and at the same time in $\mathbb{R}-I$, both synaptic variables evolve equally (on the slow time scale) in I_1 . Therefore we have that $t^* \geq s^*$. Let us rename $t_1 = t^*$. On the fast time scale r the variable $s_A(t)$ converges to 1 at time t_1 following

$$\begin{aligned} s_A(r)' &= (1 - s_A(r)) \\ s_A(0) &= s_A(t_1) \end{aligned}$$

where ' is the derivative with respect to the fast time scale r . The analytic solution is given by $s_A(r) = 1 - (1 - s_A(t_1))e^{-r}$. Therefore, this equation describes the (fast) evolution of the delayed synaptic variable $s_A(t-D)$ at time $t = t_1 + D$. At this time the B unit instantaneously turn OFF, since $j_B(t) = a - bs_A(t-D) \rightarrow a - b < \theta$ for hypothesis (U_2) . We can use the equation for $s_A(r)$ and derive the precise time when u_B turns OFF. Since $a - bs_A(t_1) \geq \theta$ and $a - b < \theta$ there $\exists s^* \in [s_A(t_1), 1]$ for which $a - bs^* = \theta$. Given the evolution of s_A , the time when B unit turns OFF is precisely $r^* = r^*(t_1) = \log((1 - s_A(t_1))/(1 - s^*))$. The latter equality highlights the dependence on t_1 . By adding the delay and returning to the normal time scale the B unit turns OFF at time $t_1 + D + \delta(t_1)$, where $\delta(t_1) = \tau r^*$. Since the dynamics of delayed synaptic variable $s_B(t-D)$ is dictated by the B unit activity, it starts to exponentially decay at time $t_1 + 2D + \delta(t_1)$. Thus it evolves according to $s_B(t-D) = e^{-(t-t_1-2D-\delta(t_1))/\tau_i}$, for $t \in I_3 = [2TR, 2TR+TD]$. A necessary condition for this state to exist is that it satisfies C_5 is that A turns ON within I_3 . This occurs if and only if $c - bs_B(TR-D) < \theta$ and $c - bs_B(TR+TD-D) \geq \theta$. This is equivalent to $\exists t_2 \in I_3^0$ (the open set) such that $c - bs_B(t_2-D) = \theta$. From the analytic solution of $s_B(t_2-D)$ we can solve this equation and obtain $t_2 = t_1 + \delta(t_1) + Q$, where $Q = 2D - \log((c-\theta)/b)$ is a constant. By repeating this process across subsequent the periodic intervals $I_k = [2(k-1)TR, 2(k-1)TR+TD]$ we obtain that the k turning ON time for the A unit is given by the map

$$(11.10) \quad t_{k+1} = t_k + \delta(t_k) + Q.$$

Since we are interested in the limit $\tau \rightarrow 0$ and on TR -periodic solution it must be that $2TR = Q$. However, assuming true this condition and $\tau > 0$ arbitrarily small, this map shows that the A unit turns ON with after a small delay δ across subsequent intervals I_k (ie the map has no fixed point). Therefore, $ZcIL$ cannot exist.

2. $ScASL_2$ for $s^* < t^*$ - The proof is analogous to the case above ($ZcSL$) after swapping the A and B units. Briefly, if the B unit turns ON at time $t_1 \in [0, TD]$ the A unit turns

OFF at time $t_1 + D + \delta(t_1)$, where $\delta(t_1) \sim \tau$. This means that s_A evolves according to $s_A(t-D) = e^{-(t-t_1-2D-\delta(t_1))/\tau_i}$, for $t \in I_3 = [2TR, 2TR+TD]$. The k turning ON time for the B unit is given by the map 11.10, where $Q = 2D - \log((d-\theta)/b)$. As in the previous case, $ScASL_2$ cannot exist because this map has no fixed point unless $\tau = 0$.

3. $ScASL_2$ - This state satisfies condition C_5 in both intervals I_1 and I_2 . Let us call t_1 and s_1 the turning ON times for A and B in I_1 respectively, and t_2 and s_2 the turning ON times for B and A in I_2 respectively. On the slow time scale both (delayed) synaptic variables s_A and s_B evolve equally in I_1 and I_2 , because both units turn OFF instantaneously and at the same time in $\mathbb{R} - I$ for Lemma 5.13. Since $d \leq c$ the total input to A is greater than the one to B for $t \in I_1$, ie $c - bs_B(t-D) \geq d - bs_A(t-D)$, which leads to $t_1 \leq s_1$. Analogous considerations lead to $t_2 \leq s_2$. Moreover, it turns out that $t_1 = t_2 - TR$. Indeed, WLOG suppose that $t_2 - TR > t_1$. Since $c - bs_B(t_1 - D) = \theta$ and due to the monotonic decay of the delayed synaptic variables in I_1 we must have $c - bs_B(t_2 - TR - D) \geq \theta$. Moreover, since $c - bs_A(t_2 - D) = \theta$ we have that $s_B(t_2 - TR - D) < s_A(t_2 - D)$. Since A turns ON at time t_1 the B unit turns OFF at time $t_1 + D + \delta(t_1)$, where $\delta(t_1) \sim \tau$. Thus $s_A(t-D) = e^{-(t-t_1-2D-\delta(t_1))/\tau_i}$, for $t \in I_2$. Similarly, since B turns ON at time t_2 and for the $2TR$ -periodicity we have that $s_B(t-D) = e^{-(2TR+t-t_2-2D-\delta(t_1))/\tau_i}$, for $t \in I_1$. On the slow time scale ($\tau \rightarrow 0$) these identities evaluated at time t_2 imply $s_B(t_2 - TR - D) = e^{(-TR+2D)/\tau_i}$ and $s_A(t_2 - D) = e^{(t_1-t_2+2D)/\tau_i}$. Due to the hypothesis $t_2 - TR > t_1$ the latter lead to $s_B(t_2 - TR - D) \geq s_A(t_2 - D)$, which is absurd. Therefore we have that $t_1 = t_2 - TR$. This in turn leads to $s_B(t-D) = e^{-(t-t_1-TR-2D-\delta(t_1))/\tau_i}$, for $t \in I_3 = [2TR, 2TR+TD]$. Due to the $2TR$ periodicity the second turning ON time for A (after t_1) must be at a time $t_3 = t_1 + 2TR \in I_3$ such that $c - bs_B(t_3 - D) = \theta$. From the analytic solution of $s_B(t_2 - D)$ we obtain $t_3 = t_1 + \delta(t_1) + Q$, where $Q = TR + 2D - \log((c-\theta)/b)$ is a constant. Thus the k turning ON time for the A unit is given by the map 11.10. Due to the dependence on τ , this map has no fixed point unless $\tau = 0$, thus proving that $ScASL_2$ cannot exist.

11.7. $2TR$ -periodic states for $D < TD$ and $TD + D < TR$ and $a + d - b < \theta$.

Theorem 11.5. *Let us now consider $2TR$ -periodic states for $D < TD$, $TD + D < TR$ and $a + d - b < \theta$, and define $L_1 = [0, D]$ and $L_2 = [TR, TR+D]$. The synaptic quantities defining the entries of the matricial form in L_1 and L_2 are given by*

$$(11.11) \quad s_A^{2\pm} = s_B^{1\pm} = N^\pm, \quad s_A^{1\pm} = \begin{cases} R^\pm & \text{if } z_A^2 = 1 \\ M^\pm & \text{otherwise} \end{cases} \quad \text{and} \quad s_B^{2\pm} = \begin{cases} R^\pm & \text{if } z_B^1 = 1 \\ M^\pm & \text{otherwise} \end{cases}$$

Where $R^- = e^{-(TR-2D)/\tau_i}$ and $R^+ = e^{-(TR-D)/\tau_i}$. Quantities M^\pm and N^\pm were defined in equations 6.1.

Proof. Since A (B) is ON in $[0, TD]$ ($[0, TR+TD]$) and turn OFF instantaneously at time TD ($TR+TD$) due to property 7.1. The synaptic variable s_A (s_B) thus exponentially decays on the slow time scale starting from time TD ($TR+TD$) and ending at time TR ($2TR$). Due to this and to the $2TR$ -periodicity the delayed synaptic variable $s_A(t-D)$ ($s_B(t-D)$) evaluated at times TR and $TR+TD$ (0 and TD) are equal to N^\pm , which proves the first identity of the theorem. If $z_A^2 = 1$ the A unit is ON in L_2 and turns OFF instantaneously at time $TR+D$ for

both MAIN or CONNECT states. Thus the synaptic variable s_A slowly decays starting from time $TR+D$ until the A unit turns ON at time $2TR$. This implies $s_A(t-D) = e^{-(t-TR-2D)}$, for $t \in [2TR, 2TR+D]$. The $2TR$ -periodicity leads to $s_A^{1-} = s_A(2TR-D) = e^{-(TR-2D)/\tau_i}$ and $s_A^{1+} = s_A(2TR) = e^{-(TR-D)/\tau_i}$, proving the second identity of the theorem. The proof of the third identity is analogous to the previous one. \blacksquare

11.8. $AScI$ cannot exist for $t^*+D \geq TR$. We now proof that state $AScI$ cannot exist if $t^*+D \geq TR$ and $D < TD$, where $t^* \in [0, D]$ ($t^*+TR \in [TR, TR+D]$) is the turning ON time for the B (A) unit in the interval I_1 (I_2). We need to show that the B (A) unit cannot be OFF for $t < t^*$ ($t < t^*+TR$) and ON for $D \geq t > t^*$ ($D+TR \geq t > t^*+TR$). By absurd suppose the contrary. We now determine the dynamics of the the delayed synaptic variable $s_B(t-D)$ during the interval $[TR, TR+D]$. The B unit turns ON at time $t^* \geq TR-D$ and is ON in I_2 (due to properly 7.1). These properties and the $2TR$ -periodicity of $AScI$ imply that $s_B(t-D)$ evolves according to

$$s_B(t-D) = e^{-(TR+t-TD-D)/\tau_i}, \quad \forall t \in [TR, TR+t^*].$$

Evaluating this equation at time $t_1 = TR$ leads to $s_B(t_1-D) = e^{-(2TR-TD-D)/\tau_i}$. Secondly we have that

$$s_B(t-D) = e^{-(t-2D)/\tau_i}, \quad \forall t \in (2D, TR+D].$$

Evaluating this equation at time $t_2 = TR+D$ leads to $s_B(t_2-D) = e^{-(TR-D)/\tau_i}$. This implies:

$$s_B(t_1-D) \leq s_B(t_2-D).$$

However by hypothesis A is OFF at time $t_1 < t^*+TR$ and ON at time $t_2 > t^*+TR$, i.e. $j_A(t_1) = a + d - bs_B(t_1-D) < \theta$ and $j_A(t_2) = a + d - bs_B(t_2-D) \geq \theta$, which is absurd.